SYNTHESES OF NOVEL OXOMOLYBDENUM(IV) DITHIOLATE COMPLEXES FOR THE STUDY OF MACROMOLECULAR CHELATION

A Doctoral Thesis

by

Mitsuru Kondo

Submitted to

the Faculty of Science, Osaka University

November, 1994

SYNTHESES OF NOVEL OXOMOLYBDENUM(IV) DITHIOLATE COMPLEXES FOR THE STUDY OF MACROMOLECULAR CHELATION

A Doctoral Thesis

by

Mitsuru Kondo

Submitted to

the Faculty of Science, Osaka University

November, 1994

Approval

November, 1994

This thesis is approved as to
style and content by

中村晃

Member-in-chief

蒲池幹治

Member

上山寛一

Member

Acknowledgments

This work has been carried out at Department of Macromolecular Science, Faculty of Science, Osaka University under the direction of Professor Akira Nakamura. The author is greatly indebted to Professor Akira Nakamura for his continuing guidance and encouragement. The author also wishes to express his sincere gratitude to Associate Professor Norikazu Ueyama for his helpful guidance and helpful discussions.

The author acknowledges Professor Mikiharu Kamachi and Dr. Atsushi Kajiwara in this department for the measurements of electron spin resonance spectroscopy. The author also acknowledges Associate Professor Keiichi Fukuyama, Department of Biology, Faculty of Science, Osaka University, and Associate Professor Joyce M. Waters, Eric W. Ainscough, and Professor Andrew M. Brodie in Massey University in New Zealand for the joint research of X-ray analysis studies.

The author thanks to Dr. Wei-Yin Sun for his contribution to the study of the oxomolybdenum-peptide complex in Chapter VI.

The author wishes to thank to Dr. Kenichi Lee, Mr. Mototugu Doi, and Mr. Seiji Adachi for assistance in the NMR spectral measurements. Thanks are extended to all the members of Nakamura Laboratory for their friendship and helpful discussion.

The author also wishes to thank to Professor Susumu Kitagawa in Department of Chemistry, Faculty of Science, Tokyo Metropolitan University for helpful discussion of ^{14}N NMR study in Chapter VII. Finally, the author thanks to all the members of Kitagawa Laboratory for their encouragement.

November, 1994.

近藤 満

Mitsuru Kondo

Contents

Chapter I

General Introduction

1) Unusual Coordination Site Constructed by Polymer Ligand.

The specific and highly catalytic reactivity in metalloenzymes is caused by the unusual coordination of polymer ligand to a metal ion or a metal cluster. For example, molybdenum ion in the molybdoenzymes shows the specific electron-transfer or oxo-transfer reactivities, while molybdenum ion coordinated by simple ligands *e.g.* $Mo(OR)_4$, $Mo(SR)_4$ (R = alkyl) is inert to the catalytic reactions such as oxidation and reduction.[1-4]

The molybdoenzymes are classified by their chemical functions into the two types *i.e.* i) oxomolybdoenzymes such as xanthine oxidase, sulfite oxidase, or nitrate reductase and ii) nitrogenase.[3] The oxo- or dioxomolybdenum(IV or VI) ions in the oxomolybdoenzymes catalytically reduce or oxidize several substrates through the oxo-transfer and electron-transfer reactions. On the other hand, a unique Fe_7Mo cluster at the active site of nitrogenase reduces dinitrogen to two equiv. of ammonia through eight-electron reduction.[3,5]

Recently, the unusual coordination at the active site of nitrogenase, *Azotobacter vinelandii*, was clarified by X-ray crystallographic studies.[6-8] Figure 1 shows the structure of Fe_7Mo cluster in the active site and the stereo view of the coordination circumstance. The Fe_7Mo cluster consists of $[Fe_4S_3]$ and $[Fe_3MoS_3]$ cubane clusters. The terminal Fe1 and Mo atoms are coordinated by the cysteine α275 residue, and histidine α442 and homocitrate, respectively. The results show that the specific peptide environment at the coordination site around the active site causes the unusual reactivity of the Fe_7Mo cluster.

On the other hand, specific high oxo-transfer reactivity of mononuclear oxo- or dioxomolybdenum(IV or VI) ion is attributed to the coordination of dithiolene and one or two cysteine ligands in the active site of the oxomolybdoenzymes. The structural information of the active site has been obtained by EXAFS or ESR spectroscopic studies,

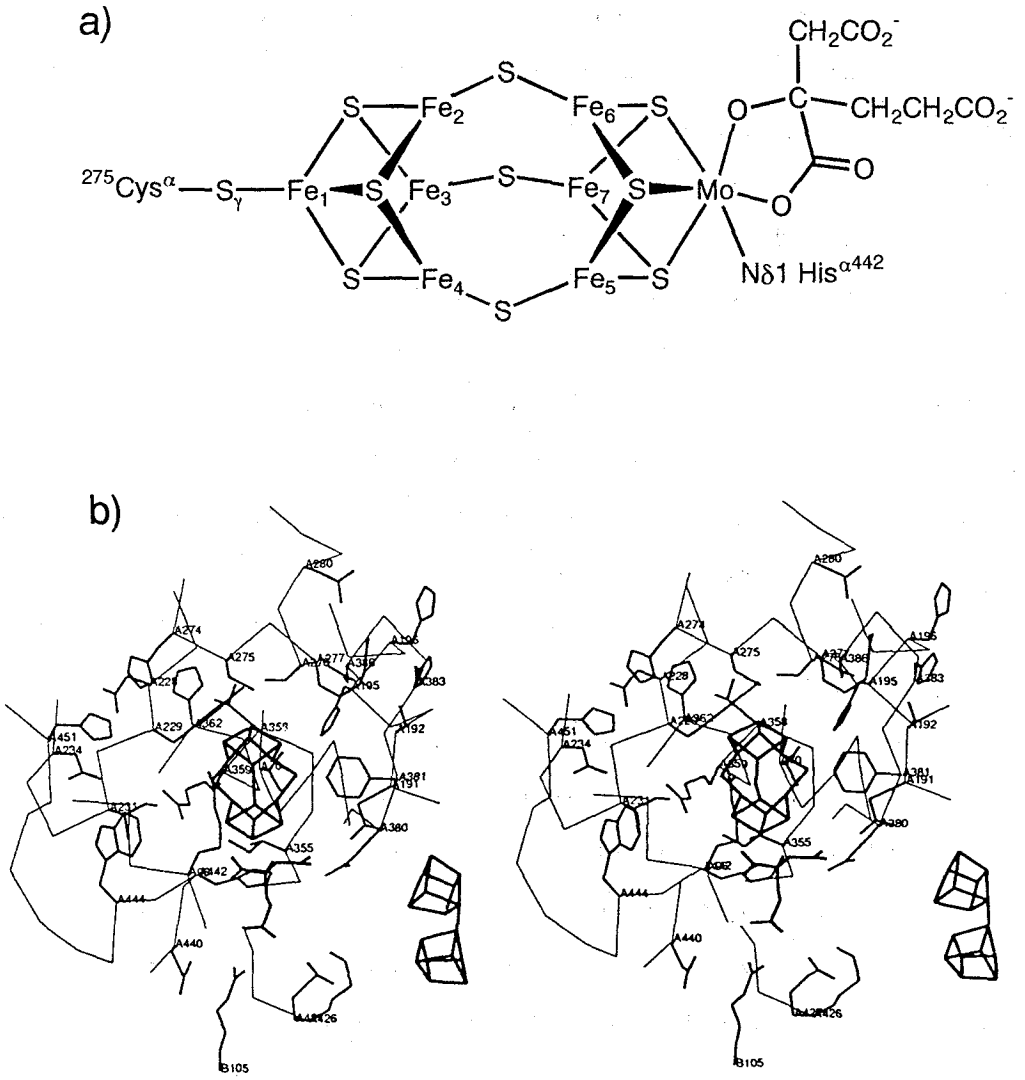

Figure 1. a) The structure of Fe_7Mo cluster of the active site of Nitrogenase, *Azotobacter vinelandii*.[6] b) the stereo view of the coordination circumstance of the Fe_7Mo cluster.

because of the absence of any X-ray crystallographic results.[3,9-13] The proposed coordination environment of the active site of the oxomolybdoenzymes in the oxidized state is shown in Figure 2. Biochemical research has also shown that the pterin derivative connects to the dithiolene ligand.[14] The conjugate system (shown in Figure 2) may be relevant to the activation of molybdenum ion by dithiolene chelation. One or two cysteine ligands are also necessary in the catalytic reaction of the oxomolybdoenzymes.[12]

The molybdenum ion shows the specific high oxo-transfer reactivity to the several inert substrates *e.g.* xanthine, sulfite, aldehyde, or carbon monoxide. The catalytic reaction proceeds by the cycle between Mo(IV) and Mo(VI) states as shown in Figure 3. Thus, the specific high oxo-transfer reactivity of the molybdenum ion is realized by the coordination of these macromolecular arenedithiolate (dithiolene) and alkanethiolate (cysteine residue) ligands.

2) Model Complexes of Oxomolybdoenzymes.

In general, synthetic model complexes for these enzymes have been prepared mainly to simulate the distorted structures from octahedral geometry. However, no successful model complex was synthesized using a simple synthetic ligand such as benzenethiolate. The author intended to synthesize the model complexes containing specific functional groups, which can provide the above specific and catalytic reactivity.

Although a number of dioxo and oxomolybdenum(VI and V) complexes having N, O, or S (thioketone, thioether) ligands have been synthesized as models of the active sites in the oxidized Mo(VI) and resting Mo(V) states, these simple coordinating ligands have not shown the specific high oxo-transfer reactivity.[15-21]

Macromolecular ligands have been considered to contribute to the reactivity. Thus, some model complexes having synthetic macromolecular ligand have been studied. Oguni *et al.* have shown that the cysteine-containing macromolecular ligand, Z-Glu-Cys-OMe, gives the higher reactivity of molybdenum ion than that of the simple low-molecular coordinating ligand.[22] Thus, the oxomolybdenum(V) ion, ($Mo^{V}(O)(\mu$-

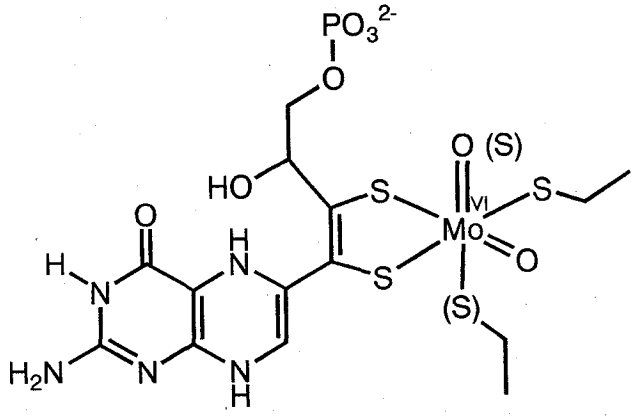

Figure 2. Proposed coordination environment of the active site of the oxomolybdoenzymes in the oxidized state.

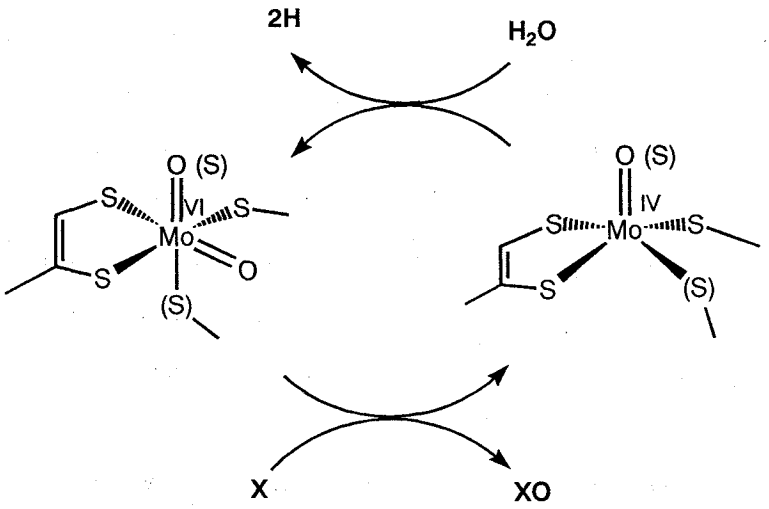

Figure 3. Schematic picture of catalytic reactions of molybdenum ion in the oxomolybdoenzymes.

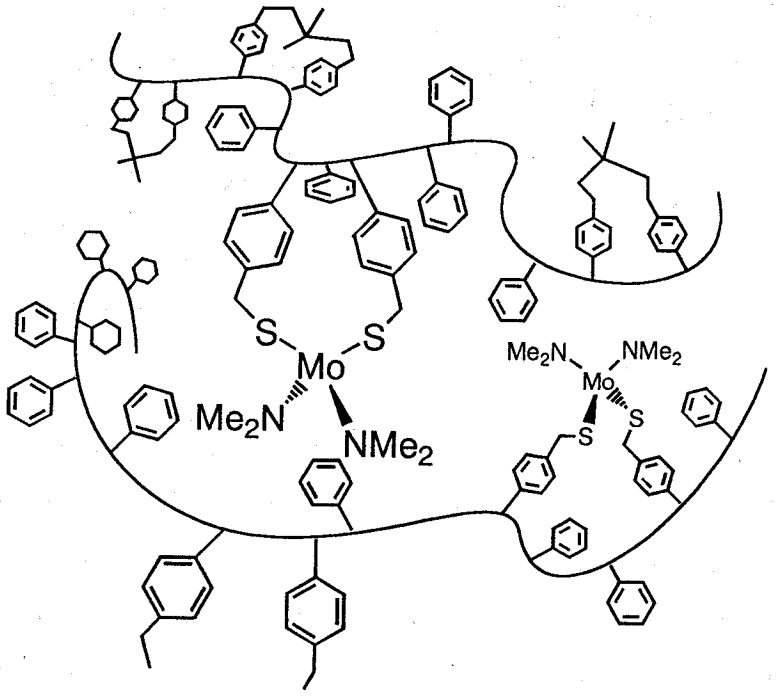

Figure 4. The proposed structure of the polystyrene-supported molybdenum complex.[23]

$S)_2Mo^{V}O)^{2+}$, ligated by the macromolecular ligand showed about 20 times higher reactivity than that of the Mo complex having simple ligands, $[(^{t}Bu\text{-}CH_2\text{-}OCS_2)Mo^{V}(O)(\mu\text{-}S)_2Mo^{V}O(S_2CO\text{-}CH_2\text{-}^{t}Bu)]$, in the catalytic reduction of phenylacetylene or azobenzene. Although the activation of molybdenum ion by the macromolecular ligand was demonstrated, the activation mechanism was unknown because of absence of information about the structure around the metal.

The catalytic reduction of acetylene by molybdenum(IV) thiolate complexes supported by polystyrene was also reported.[23] The molybdenum complex shows the excellent catalytic reactivity for the reduction of acetylene compared with that of the unsupported molybdenum complex with similar structure. The proposed structure of this polystyrene supported molybdenum complex is shown in Figure 4.

Recently, the activation of oxomolybdenum(IV and V) ion by the chelating cysteine thiolates of a macromolecular ligand Z-cys-Pro-Leu-cys-OMe was reported from

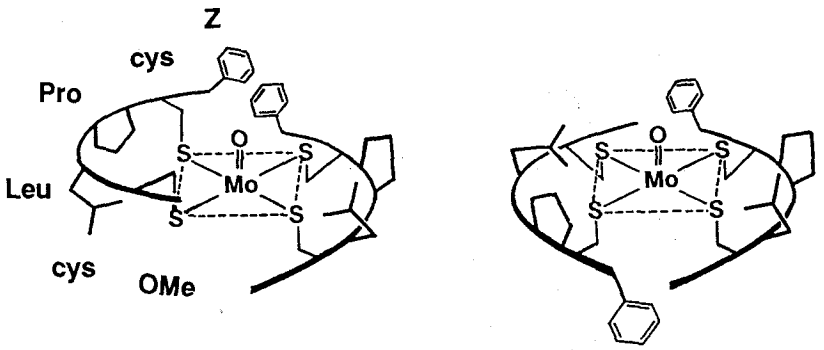

Figure 5. The oxomolybdenum(V) complexes ligated by a chelating peptide having a sequence Z-Cys-Pro-Leu-Cys-OMe.[24]

this laboratory (Figure 5).[24] Thus, the oxomolybdenum(IV) ion having a Z-cys-Pro-Leu-cys-OMe spontaneously removes the oxo ligand to afford the highly reactive molybdenum(IV) ion. The molybdenum(IV) ion shows the reduction activity for several substrates *e.g.* phenylacetylene, benzonitrile, or trimethylsilylazide. By the theoretical energy minimum calculation, the specific O-Mo-S-C torsion angle (ca. 0 or 180°) of the chelating ligand has been expected and considered to be responsible for the occurrence of the high reactivity of molybdenum ion.

Thus, the previous works have suggested that synthetic macromolecular ligands are effective for the occurrence of the specific and catalytic reactivity of the molybdenum ion by the unusual coordination like the active center of metalloenzymes, as shown in Scheme 1. However, the studies using these ligands could not clarify the origins of the reactivity.

Scheme 1

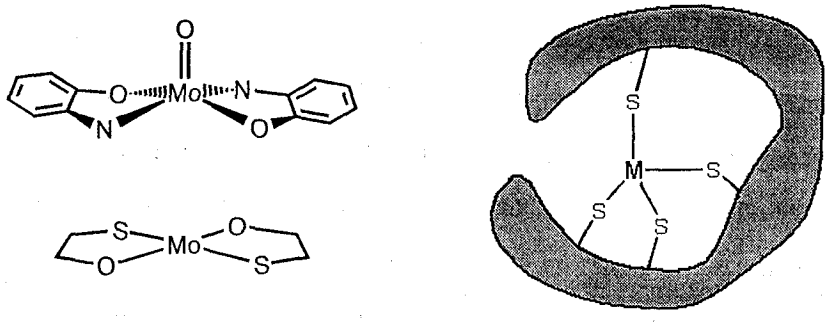

Simple-ligand complex Macromolecular complex

3) Purpose of this Study.

Although a macromolecular ligand causes the high reactivity to the metal ion by unusual coordination, little information on the coordination environments around metal ion having catalytic reactivity has been obtained. The author intends to clarify the relation between the structure and function of the synthetic model complexes containing the specific functional groups. Here, novel oxomolybdenum(IV) complexes having several chelating ligands were systematically synthesized in order to elucidate the activation mechanism of the chelating ligands. The chelating ligands can be considered to serve as one of the specific functions associated with the polymer effects. The molybdenum ion of the oxomolybdoenzymes carries out the oxo-transfer reaction in the cycle between $Mo^{VI}O_2^{2+}$ ($Mo^{VI}OS^{2+}$ in xanthine oxidase, aldehyde oxidase) and $Mo^{IV}O^{2+}$ states. Therefore, study of the oxomolybdenum(IV) complexes with the chelating dithiolate ligands contributes to the elucidation of the chemical reactivity at the active site of oxomolybdoenzymes.

The author developed novel synthetic method for the oxomolybdenum(IV) complexes having several chelating ligands (Figure 6). Only a few oxomolybdenum(IV)

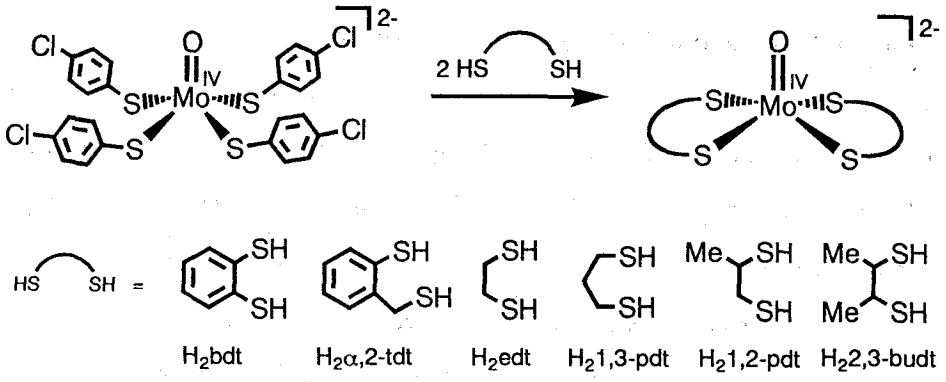

Figure 6. Synthesis of oxomolybdenum(IV) complexes by ligand exchange method.

complexes having thiolate ligands have been synthesized to date because of the limited synthetic method. In general, molybdenum(IV) thiolate complexes are unstable and easily oxidized to give the corresponding oxomolybdenum(V) complex with one-electron oxidation. Actually, it is difficult to synthesize them from the corresponding oxomolybdenum(V) complexes in the mild conditions because of the relatively negative Mo(V)/Mo(IV) redox potential (*ca.* -1 V vs. SCE). The new method readily provides the synthesis of alkanethiolate complexes *e.g.* $[Mo^{IV}O(SCH_2CH_2S)_2]^{2-}$ or $[Mo^{IV}O(SCH_2CH_2CH_2S)_2]^{2-}$. These chelating ligands represent important chemical property of the peptide or native chelating proteins.

4) Effect of Chelating Thiolate on the Reactivity.

Chelating dithiolates, 1,2-benzenedithiolate (bdt^{2-}), α,2-toluenedithiolate (α,2-tdt^{2-}), 1,2-ethanedithiolate (edt^{2-}), 1,3-propanedithiolate (1,3-pdt^{2-}), 1,2-propanedithiolate (1,2-pdt^{2-}), and 2,3-butanedithiolate (2,3-$budt^{2-}$) were employed in this study. These chelating ligands are regarded as the suitable chelating models not only for the several reactive macromolecular ligand, but also for the active site of oxomolybdoenzymes (Scheme 2).

i) Arene- and Alkanethiolate Ligands. Arenethiolate *e.g.* benzenethiolate (SPh^-), 1,2-benzenedithiolate (bdt^{2-}), are simple model ligands for the dithiolene chelation in the active center of oxomolybdoenzymes. The thiolate sulfur has pπ orbitals interacting with dithiolene C=C pπ orbital. The interaction is expected to regulate the chemical function of metal ion.

On the other hand, alkanethiolate ligands serve as models of cysteine residues. The metal-sulfur interaction is stronger than that of arenethiolate in this case. The oxomolybdenum(IV) complexes ligated by alkanedithiolate ligands have the more negative Mo(V)/Mo(IV) redox potential compared with those of arenethiolate complexes, because of the strong electron donating ability.

Scheme 2

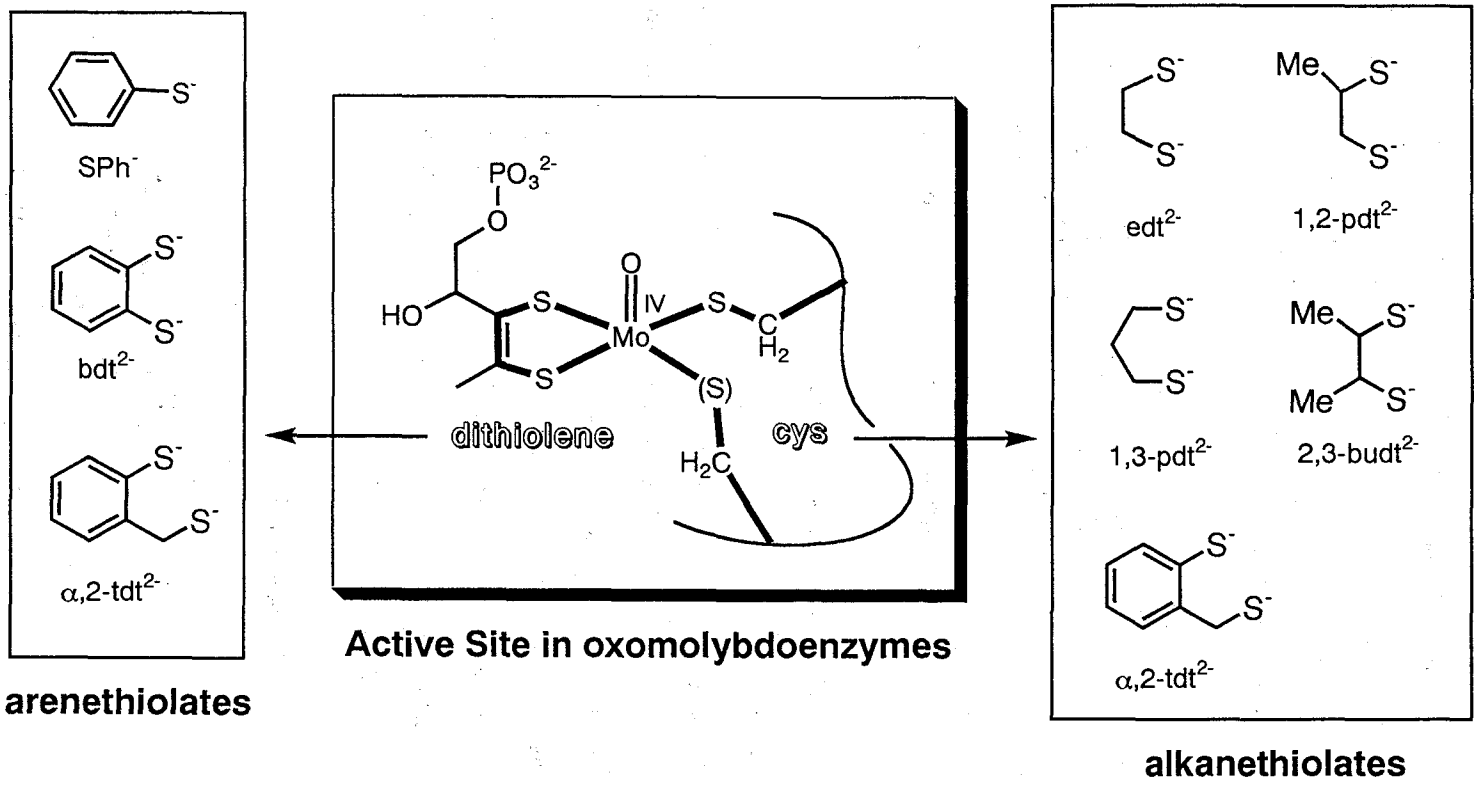
SPh⁻
bdt²⁻
α,2-tdt²⁻
arenethiolates
PO₃²⁻
O
HO
S
O
IV
Mo
S
C
H₂
S
(S)
H₂C
dithiolene
cys
Active Site in oxomolybdoenzymes
edt²⁻
1,2-pdt²⁻
1,3-pdt²⁻
2,3-budt²⁻
α,2-tdt²⁻
alkanethiolates

ii) Effect of Chelating Size. In cys-containing enzymes, the orientation of cys thiolate in peptide chain is known to be responsible to the conformationally restricted folding structure. Chelating dithiolate ligands such as $^{-}SCH_2CH_2S^{-}$ (5-membered) and $^{-}SCH_2CH_2CH_2S^{-}$ (6-membered) are conformationally restricted ligand as shown in Scheme 3. The Mo-S dπ-pπ interaction changes with the Mo-S-C bond angle and the O-Mo-S-C torsion angle.

Scheme 3

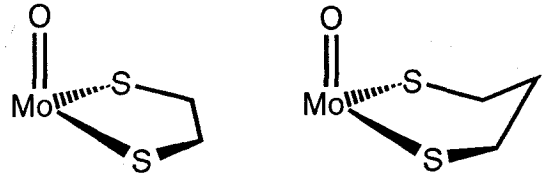

5-membered 6-membered

iii) Steric Effect of Chelating Thiolate on O-Mo-S-C Torsion Angle. The O-Mo-S-C torsion angle is changeable in the conformationally restricted dithiolate chelating ligands. The significance of the O-Mo-S-C torsion angle on the reactivity was suggested by the studies of oxomolybdenum(IV and V) complex chelated by peptide, Z-cys-Pro-Leu-cys-OMe, as mentioned above. In the chelating ligands studied in this thesis, the arene-alkanedithiolate chelating α,2-tdt^{2-} affords the most deviated O-Mo-S-C torsion angle from 90°. (Scheme 4) Thus, the effect of the O-Mo-S-C torsion angle on the reactivity or the physical properties of the oxomolybdenum(IV) ion was studied by using this complex.

Scheme 4

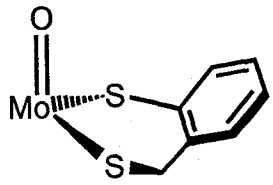

arene- alkane chelation

iv) Binucleation Reaction. In order to understand the effect of the chelating ligands on the oxo-transfer reactivity of oxo- and dioxomolybdenum(IV and VI) ions, the binucleation reactivity was studied.

In general, oxo- and dioxomolybdenum(IV and VI) complexes readily react to give the μ-oxo dimer complex (eq. 1).

$$[Mo^{IV}OL_4] + [Mo^{VI}O_2L_4] \rightleftharpoons [L_4Mo^{V}(O)\text{-}O\text{-}Mo^{V}OL_4] \qquad (1)$$

Since this μ-oxo dimer is quite inert to the oxo-transfer reaction, the formation of this dimer complex during the catalytic reaction deactivates the catalytic reaction. The author shows that the dithiolate chelating controls the binucleation reaction by the limited stereochemical mobility.

v) Effect of Dithiolene Chelating on Nitrido Ligand. The intermediacy of the nitrido complex, $L_nMo{\equiv}N$, has been suggested during the dinitrogen reduction process of the nitrogenase by the studies using dinitrogen-molybdenum(0) complexes (Figure 7).[25-27] Therefore, activation of the nitrido ligand is one of the most important steps for the achievement of the catalytic cycle of ammonia synthesis. However, the reactivity of nitrido in nitridomolybdenum complexes having Cl, P, N, or O ligands is found to be quite low.[28]

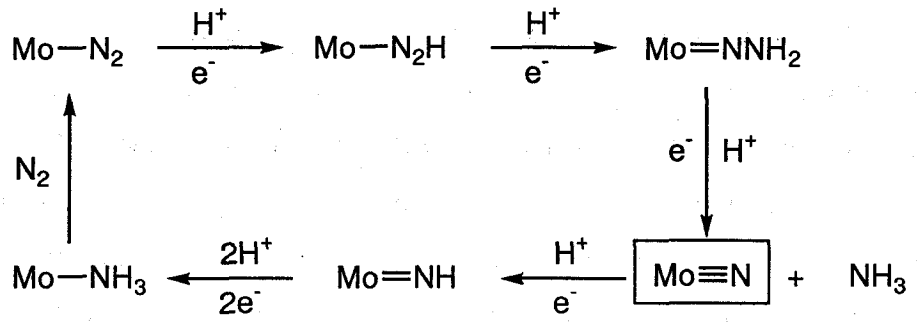

Figure 7. Proposed reduction process of the dinitrogen ligand.

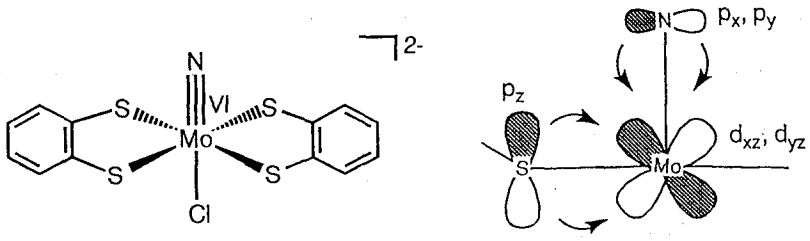

Figure 8. Activation mechanism of the thiolate ligands on the nitrido ligand by competitive pπ donation.

In general, the nitrido and oxo groups have isoelectronic structures, and exist in similar geometries.[29-31] Here, the activation effect of the dithiolate ligand on the reactivity of nitrido ligand will be studied.

The synthesis of nitridomolybdenum(VI) complex having bulky thiolate ligand, $[Mo^{VI}N(S\text{-}^tBu)_4]^-$, has been attempted in this laboratory. Although this complex shows the increased yield of ammonia as compared with $[Mo^{VI}NCl_4]^-$ in the reaction with acids or bases, the activation mechanism by sulfur ligands was not understood because of the difficulties in the isolation .

The author will show that the activation of the nitrido ligand is due to the competitive pπ donation from the thiolate ligand to Mo d_{xy}, d_{xz} (Figure 8).

Scope of this thesis

For understanding of the function of cysteine ligand at the active sites of oxomolybdoenzymes, novel synthetic method was developed for the syntheses of oxomolybdenum(IV) complexes having several alkanedithiolate ligands. Thus, the ligand exchange reaction between oxomolybdenum(IV) complex having monodentate arenethiolate ligand, $[Mo^{IV}O(p\text{-}ClC_6H_4S)_4]^{2-}$ (**1**) and alkanedithiols was carried out. The direct reduction of the oxomolybdenum(V) complexes having alkanethiolate ligands has been impossible, because of the highly negative Mo(IV)/Mo(V) redox couple (> -1.0 V vs SCE), indicating the necessity of the novel synthetic method.

In Chapter II, the synthesis and molecular structure of **1** (Scheme 5) are described. This complex is prepared by the reduction of the corresponding oxomolybdenum(V) complex having a relatively positive Mo(IV)/Mo(V) redox couple (-0.66 V vs SCE) because of the electron withdrawing chloro substituent in the arenethiolate ligand. This complex was useful for the starting material for the syntheses of novel oxomolybdenum(IV) complexes as discussed in Chapter III and IV.

Scheme 5

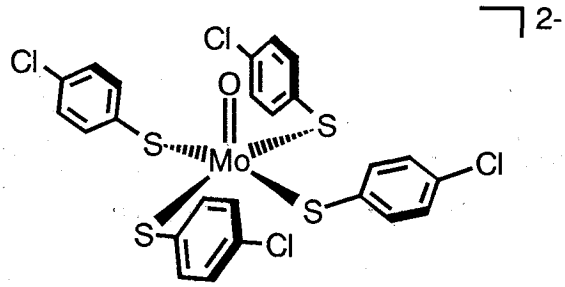

Structure of $[Mo^{IV}O(p\text{-}ClC_6H_4S)_4]^{2-}$

In Chapter III, the synthesis of oxomolybdenum(IV) complex having α,2-toluenedithiolate ligand (Scheme 6) using the ligand exchange method is reported. This complex has both arenethiolate and alkanethiolate ligands, and showed the lower reactivity to the several oxo-transfer reagents such as trimethylamine-*N*-oxide, because of the rigid chelating skelcton.

Scheme 6

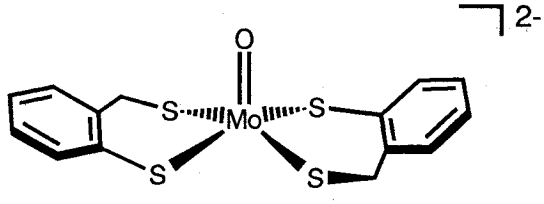

Structure of $[Mo^{IV}O(\alpha,2\text{-}tdt)_2]^{2-}$

In Chapter IV, the syntheses of the series of oxomolybdenum(IV) complexes having several alkanedithiolate ligands, and their molecular structures are described. Thus, the complexes, $[Mo^{IV}O(S_2R)_2]^{2-}$ (S_2R = SCH_2CH_2S, $SCH_2CH_2CH_2S$, $SCH_2CH(\text{-}S)CH_3$, $CH_3\text{-}CH(S)CH(\text{-}S)CH_3$) were synthesized by the ligand exchange method. (Scheme 7) All these complexes have the rigid chelating skeletons, and show the low reactivity with the oxo-donor reagents. The relation between Mo-S-C bond angle and physical properties through the $p\pi$-$d\pi$ interaction was studied.

Scheme 7

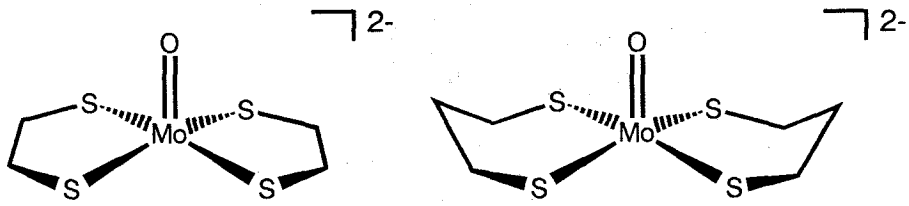

Structure of $[Mo^{IV}O(edt)_2]^{2-}$ (left) and $[Mo^{IV}O(1,3\text{-}pdt)_2]^{2-}$ (right).

In Chapter V, the binucleation reactivity between dioxomolybdenum(VI) complexes and oxomolybdenum(IV) complexes having several different type of ligands is reported. This reactivity depends on the oxo-transfer and accepting reactivities of each starting complexes. The mechanism of the binucleation reaction is discussed. (Scheme 8)

Chapter VI describes the attempted synthesis of oxomolybdenum(IV) complexes chelated by a tetradentate peptide ligand. (Scheme 9) The ligand exchange reaction between $[Mo^{IV}O(p\text{-}ClC_6H_4S)_4]^{2-}$ and the tetradentate peptide ligand does not produce the Mo(IV) complex but a Mo(V) complex. This is due to the strong reducing ability of this Mo(IV) complex produced.

Scheme 8

Simple complex

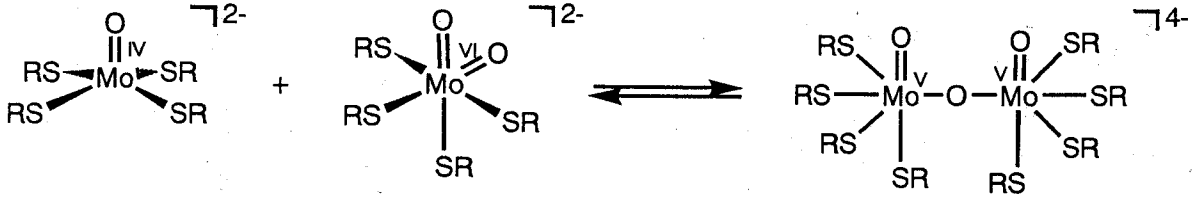

This work

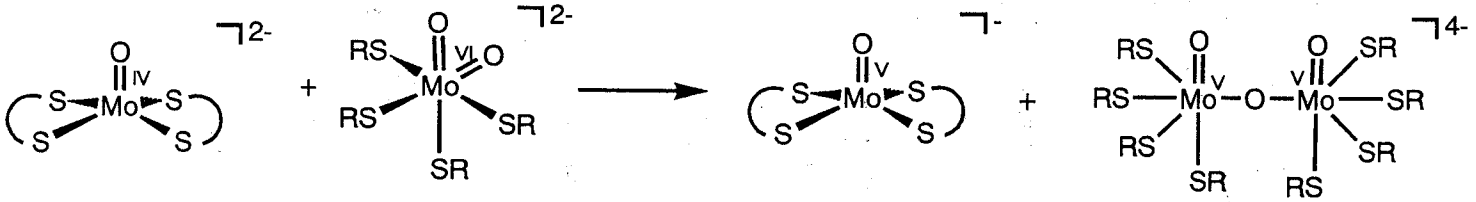

Scheme 9

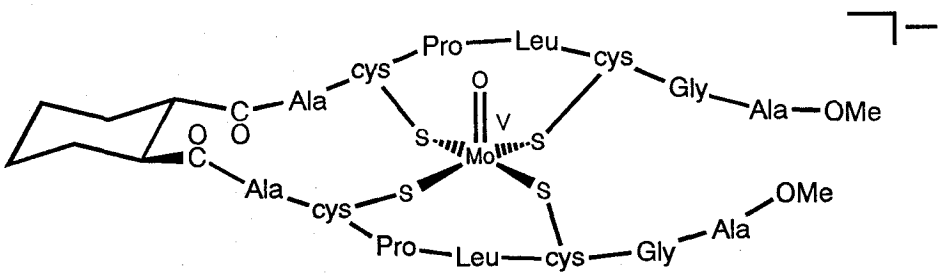

Schematic structure of Mo(V) peptide complex

In Chapter VII, synthesis and physical properties of nitridomolybdenum(VI) complex having bdt ligand are described. This complex has higher electron density on the nitrido ligand compared with nitridomolybdenum(VI) complex having Cl ligands because of the strong competitive pπ donation from the pπ of thiolate ligand to the Mo d_{xy}, d_{yz}. Electronic effect of the thiolate ligand on the activation of the nitrido ligand is discussed.

Scheme 10

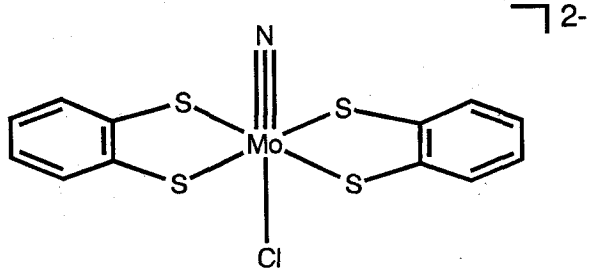

Scheme 10 Structure of $[Mo^{VI}N(bdt)_2Cl]^{2-}$

References

(1) Otsuka, S.; Kamata, M.; Hirotsu, K.; Higuchi, T. *J. Am. Chem. Soc.* **1981**, *103*, 3011.

(2) Bishop, P. T.; Dilworth, J. R.; Hughes, D. L. *J. Chem. Soc., Dalton Trans.* **1988**, 2535.

(3) *Molybdenum Enzymes*; Spiro, T. G., Ed.; John-Wiley: New York, 1985.

(4) Burgmayer, S. J. N.; Stiefel, E. I. *Journal of Chemical Education* **1985**, *62*, 943.

(5) Burgess, B. K. *Chem. Rev.* **1990**, *90*, 1377.

(6) Kim, J.; Rees, D. C. *Science* **1992**, *257*, 1677.

(7) Kim, J.; Rees, D. C. *Nature* **1992**, *360*, 553.

(8) Mortenson, L. E.; Seefeldt, L. C.; Vance, T.; Bolin, J. T. In *Advances in Enzymology and Related Areas of Molecular Biology*; A. Meister, Ed.; Wiley: New York, 1993; Vol. 64; pp 215-290.

(9) Cramer, S. P.; Stiefel, E. I. In *Molybdenum Enzymes*; T. G. Spiro, Ed.; Jphn Wiley: New York, 1985; pp 411-441.

(10) Gardlik, S.; Rajagopalan, K. V. *J. Biol. Chem.* **1990**, *265*, 13047.

(11) Cruber, S.; Kilpatrick, L.; Bastian, N. R.; Rajagopalan, K. V.; Spiro, T. G. *J. Am. Chem. Soc.* **1990**, *112*, 8179-8180.

(12) Barber, M.; Neame, P. J. *J. Biol. Chem.* **1990**, 20912.

(13) Gardlik, S.; Rajagopalan, K. V. *J. Biol. Chem.* **1991**, *266*, 4889.

(14) Rajagopalan, K. V. In *Advances in Enzymology and Related Areas of Molecular Biology*; A. Meister, Ed.; Wiley: New York, 1991; Vol. 64; pp 215-290.

(15) Moore, F. W.; Larson, M. J. *Inorg. Chem.* **1967**, *6*, 998.

(16) Buchanan, I.; Minelli, M.; Ashby, M. T.; King, T. J.; Enemark, J. H.; Garner, C. D. *Inorg. Chem.* **1984**, *23*, 495.

(17) Stiefel, E. I.; Miller, K. F.; Bruce, A. E.; Pariyadath, N.; Heinecke, J.; Corbin, J. L.; Berg, J. M.; Hodgson, K. O. In *Molybdenum Chemistry of Biological*

Significance; W. E. Newton and S. Otsuka, Ed.; Plenum Press: New York and London, 1980; pp 279.

(18) Dowerah, D.; Spence, J. T.; Singh, R.; Wedd, A. G.; Wilson, G. L.; Farchione, F.; Enemark, J. H.; Kristofzski, J.; Bruck, M. *J. Am. Chem. Soc.* **1987**, *109*, 5655.

(19) Roberts, S. A.; Young, C. G.; Kipke, C. A.; Cleland, W. E., Jr.; Yamanouchi, K.; Carducci, M. D.; Enemark, J. H. *Inorg. Chem.* **1990**, *29*, 3650.

(20) Berg, J. M.; Holm, R. H. *J. Am. Chem. Soc* **1985**, *107*, 917.

(21) Berg, J. M.; Holm, R. H. *Inorg. Chem.* **1983**, *22*, 1768.

(22) Oguni, N.; Shimazu, S.; Nakamura, A. *Polymer, J.* **1980**, *12*,

(23) Oguni, N.; Shimazu, S.; Iwamoto, Y.; Nakamura, A. *Polymer J.* **1981**, *13*, 845.

(24) Ueyama, N.; Yoshinaga, N.; Kajiwara, A.; Nakamura, A. *Chem. Lett.* **1990**, 1781.

(25) Chatt, J.; Dilworth, J. R. *J. Chem. Soc., Chem. Commun.* **1975**, 983.

(26) Donovan-Mtunzi, S.; Richards, R. L. *J. Chem. Soc., Dalton Trans.* **1984**, 1329-1332.

(27) Hidai, M. In *Molybdenum enzymes*; T. G. Spiro, Ed.; John-Wiley: New York, 1985; pp 285-341.

(28) Ueyama, N.; Fukase, H.; Zaima, H.; Kishida, S.; Nakamura, A. *J. Mol. Catal.* **1987**, *43*, 141.

(29) Griffith, W. P. *Coord. Chem. Rev.* **1972**, *8*, 369.

(30) Dehnicke, K.; Strähle, J. *Angew. Chem. Int. Ed. Engl* **1981**, *20*, 413-426.

(31) Dehnicke, K.; Strähle, J. *Angew. Chem. Int. Ed. Engl.* **1992**, *31*, 955-978.

Chapter II

Synthesis, Molecular Structure and Physical Properties of an Oxomolybdenum(IV) Complex with *p*-Chlorobenzenethiolate, $[Mo^{IV}O(p\text{-}ClC_6H_4S)_4]^{2-}$, as a Model of Active Sites of Reduced Molybdo-Oxidases

Introduction

A molybdenum ion exists at the center of molybdenum cofactor in the active sites of the oxomolybdoenzymes such as sulfite oxidase, aldehyde oxidase, and xanthine oxidase.[1] Substrates are catalytically oxidized at these sites by a cycle between the oxidation states, Mo(VI) and Mo(IV), via an intermediate Mo(V) state during turnover.[2] EXAFS studies have shown that an $Mo^{IV}(=O)$ center in the reduced state, and $Mo^{VI}(=O)_2$ or $Mo^{VI}(=O)(=S)$ center in the oxidized state is in the active sites. These studies have also shown that two or three sulfur atoms coordinate to the molybdenum ion.[1,3] Chemical analysis of degradation products of the molybdenum cofactor has shown that a dithiolene ligand connected to a pterin derivative coordinates to the molybdenum ions.[4] (see Figure 2 in Chapter I)

A number of dioxomolybdenum(VI) complexes with S(thiolato), N, or S(thioether or thioketone) ligands[5] and oxomolybdenum(V) complexes with S(thiolato) ligands[6,7] have been synthesized as models of active sites of the enzymes. For models of the active sites in reduced states, only a few syntheses of monomeric oxomolybdenum(IV) thiolate complexes have been reported because of the difficulty of the syntheses. We found a convenient synthetic method of an oxomolybdenum(IV) thiolate complex using $(NEt_4)[Mo^{V}O(p\text{-}ClC_6H_4S)_4]$(**2**)[8] as starting material.

In this paper, the synthesis, molecular structure, and physical properties of an oxomolybdenum(IV) complex having *p*-chlorobenzenethiolate, $[Mo^{IV}O(p\text{-}ClC_6H_4S)_4]^{2-}$, are reported. This complex with arenethiolate ligands unconstrained by chelation serves

as fundamental references to other oxomolybdenum(IV) thiolate complexes in consideration for their structures and physical properties.

Experimental Section

All syntheses and physical measurements were carried out under argon atmosphere. 1,2-Dimethoxyethane (DME), MeCN, diethyl ether, and MeCN-d_3 were dried over CaH_2, distilled and deoxygenated before use. *p*-Chlorobenzenethiol, NEt_4I, NEt_4BH_4, and PPh_4Br used were of commercial grade obtained from Tokyo Kasei Co. **2** was prepared by the slight modified method of Boyd *et al.*[6] and Ellis *et al.*[8]

Synthesis of $(NEt_4)_2[Mo^{IV}O(p\text{-}ClC_6H_4S)_4]$ (1a). Complex **2** (3.27 g, 4.00 mmol) and NEt_4BH_4 (0.616 g, 4.25 mmol) were mixed and stirred in DME (100 mL) for 5 h at room temperature. A precipitate obtained was collected with filtration and washed with DME until the filtrate were no longer colored. The green precipitate was dissolved in MeCN (30 mL). The solution was filtered and reduced in a volume to about 10 mL under reduced pressure. A blue microcrystalline product (0.70 g, 19 %) was obtained by the addition of about 10 mL of diethyl ether to the solution, collected by filtration and dried *in vacuo*. Found: C, 50.16; H, 6.10; N, 2.86 %. Calcd for $C_{40}H_{56}N_2OMoS_4Cl_4$: C, 50.74; H, 5.96; N, 2.96 %.

Synthesis of $(PPh_4)_2[Mo^{IV}O(p\text{-}ClC_6H_4S)_4]$ (1b). Complex **1a** (0.163 g, 0.172 mmol) and PPh_4Br (0.176 g, 0.420 mmol) were dissolved in MeCN (14 mL). The solution was stood for overnight at *ca.* 10 °C. Microcrystals obtained were collected by filtration and washed with MeCN (2 mL, three times) and diethyl ether (2 mL), then dried under reduced pressure. Red microcrystals (0.06 g) were obtained in 10% yield. The crystals have MeCN as a crystalline solvent. Found: C, 62.55; H, 4.46; N, 0.98 %. Calcd for $C_{74}H_{59}NOP_2MoS_4Cl_4$: C, 63.20; H, 4.23; N, 1.00 %.

Physical Measurements. Absorption spectra were recorded on a Jasco Ubest-30 spectrometer in MeCN solution with 1 mm matched silica cells. Raman spectra were obtained on a Jasco R-800 spectrometer in solid state with 514.5 nm excitation. The

cyclic voltammograms were taken on a Yanaco P-1100 polarographic analyzer in MeCN solution (2 mM) with a glassy carbon electrode working and $(n\text{-Bu})_4NClO_4$ (100 mM) as a supporting electrolyte. ^1H NMR spectra were measured on a Jeol JNH-GSX 270 spectrometer in MeCN-d_3 at 30 °C.

X-Ray Structure Determination. A single crystal of **1b** was sealed in a glass capillary under argon atmosphere for X-ray measurements. Diffraction experiment was performed with a Rigaku four-circle diffractometer using Ni-filtered CuKα radiation. Cell constants were determined by a least squares method based on setting angles of 24 reflections. Crystal data and experimental details are summarized in Table I. Three intense reflections were recollected every 100 reflections and showed only 1.3 % of decay of the intensities through data collections. Lorentz and polarization correction were applied, but no absorption correction was made. The structure was solved by using *SHELX 86*,[9] and refined by the block-diagonal least squares method.[10] All of the non-hydrogen atoms were refined with anisotropic temperature factors. Except the three hydrogen atoms of MeCN all hydrogen atoms were placed in idealized positions (C-H distance 1.08 Å) and added to the structure factor calculation, but their positions were not refined.

High R and R_W values and relatively large standard deviations of interatomic distances and angles are due to the poor quality of the crystal.

EHMO Calculation. As a simple model of **1b**, $[MoO(SH)_4]^{2-}$ in ideal C_{4v} symmetry was adopted for the calculations. The geometrical parameters used are: 1.690 Å for one Mo-O, 2.415 Å for four Mo-S, 1.08 Å for four S-H, 107.7° for O-Mo-S angle, 116.24° for Mo-S-H angle on the basis of the crystal structure of **1b**. The EHMO parameters for Mo were taken from a reported work[11], and those for S, O, and H are the standard ones.

Table I. Crystal and Refinement Data for $(PPh_4)_2[Mo^{IV}O(p\text{-}ClC_6H_4S)_4]$ (**1b**).

Formula	$C_{74}H_{59}NOP_2MoS_4Cl_4$
Formula weight	1406.25
Crystal system	triclinic
a, Å	21.131(18)
b, Å	13.690(3)
c, Å	13.490(5)
α, °	100.96(3)
β, °	117.62(3)
γ, °	78.77(5)
V, Å^3	3369(3)
Z	2
Space group	$P\bar{1}$
t, C°	20±1
Dcalcd	1.39
Radiation	CuKα
$2\theta_{max}$, °	120
Scan mode	2θ-ω
No. of reflections measured	8207
No. of observns I>3σ(I)	7725
R[a)]	0.094
R_W[b)]	0.104

a) $R = \Sigma||Fo|-|Fc||/\Sigma|Fo|$. b) $R_W = [\Sigma w(|Fo|-|Fc|)^2/\Sigma w|Fo|)^2]^{1/2}$; $w = 1/[\sigma^2(|Fo|)+0.34|Fo|+0.0048|Fo|^2]$.

Results and Discussion

Synthesis. The air-sensitive, diamagnetic oxomolybdenum(IV) complex with monodentate thiolato ligands, **1a**, was synthesized by reduction of **2** with NEt_4BH_4. A DME solution was useful for this reaction because the product obtained gradually precipitates. Although, diamagnetic yellow byproducts are produced in this reaction process, these can be removed by washing with DME. Blue microcrystals were obtained by reprecipitation from MeCN/diethyl ether.

Only a few papers are found on the syntheses of monomeric oxomolybdenum(IV) complexes with thiolate ligands, since synthetic methods of these complexes were limited. Mitchell and Pygall reported the syntheses of $K_2[Mo^{IV}O(edt)_2]$, (edt = 1,2-ethanedithiolato), $K_2[Mo^{IV}O(tdt)_2]$, (tdt = 3,4-toluenedithiolato), and $[Mo^{IV}O(dtc)_2]$, (dtc = diethyldithiocarbamato) by the reaction of $K_4[Mo^{IV}O_2(CN)_4]$ with 2 eq. of the corresponding ligands in H_2O,[12] and Boyde *et al.* synthesized $(NEt_4)_2[Mo^{IV}O(bdt)_2]$ (bdt = 1,2-benzenedithiolato) by their modified method.[13] Ellis *et al.* prepared $(NHEt_3)_2[Mo^{IV}O(SC_6F_5)_4]$ by the reaction of $[Mo^{IV}OCl_2(PPh_2Me)_3]$ with pentafluorobenzenethiol and NEt_3 in CH_2Cl_2.[10] However, this method could not be applied to other thiols. Coucouvanis *et al.* obtained $[Mo^{IV}O(S_2C_2(CO_2Me)_2)_2]^{2-}$ from the reaction between $[Mo^{IV}O(S_4)_2]^{2-}$ and dicarbomethoxyacetylene.[14]

The use of NR_4BH_4 for the reductant is convenient for the syntheses of oxomolybdenum(IV) complexes from the corresponding oxomolybdenum(VI or V) complexes. Subramanian *et al.* reported the synthesis of an oxomolybdenum(IV) complex having bulky ligands, $[Mo^{IV}O(3\text{-}t\text{-Bu-hbeH}_2)]$, (3-*t*-Bu-hbeH$_4$ = N,N'-bis(2-hydroxy-3-*t*-butylbenzyl)-1,2-diaminoethane) by the reduction of $[Mo^{VI}O_2(3\text{-}t\text{-Bu-hbeH}_2)]$ with excess $(n\text{-Bu})_4NBH_4$ in MeOH.[15] The synthesis of homoleptic molybdenum(VI) thiolate complexes is difficult when the direct reaction of Mo(VI) ions with free thiols is attempted because Mo(VI) ions are readily reduced to Mo(IV) or Mo(V) states by free thiols.[16] Recently the successful synthesis of dioxomolybdenum(VI) complex with two conjugated dithiolate ligands, $(NEt_4)_2[Mo^{VI}O_2(bdt)_2]$, by the O-atom

transfer oxidation of $(NEt_4)_2[Mo^{IV}O(bdt)_2]$ with Me_3NO was reported by Yoshinaga *et al.*[17]

Many oxomolybdenum(V) complexes with thiolate ligands were synthesized to date.[6,7] However, the reduction of oxomolybdenum(V) complexes with NR_4BH_4 is very difficult in most cases because of their negative Mo(V)/Mo(IV) redox potentials. Actually, it was difficult to complete the reduction of $(NEt_4)[Mo^{V}O(SC_6H_5)_4]$ to Mo(IV) state by NEt_4BH_4. Ellis *et al.* showed that the redox potential of $[Mo^{V}O(SAr)_4]^-$ complexes (Ar = aryl) shifted to the positive side by electron-withdrawing substituents on the benzenethiolate ligands.[8] The redox potential (-0.72 V vs. SCE) of $(NEt_4)[Mo^{V}O(SC_6H_5)_4]$ is more negative to the value of -0.66 V (vs. SCE) of **2**. Thus **2** is more readily reduced to the Mo(IV) state with NEt_4BH_4. Recently, Ueyama *et al.* reported the synthesis of an oxomolybdenum(IV) complex with monodentate thiolate ligands, $(NEt_4)_2[Mo^{IV}O(o\text{-}RCONHC_6H_4S)_4]$, by the NEt_4BH_4 reduction of the corresponding oxomolybdenum(V) complexes[18] which have a positive-shifted Mo(V)/Mo(IV) redox potentials (-0.2 V ~ -0.5 V) by the effect of NH-S hydrogen bond.

Description of Structure. The molecular structure of **1b** which was prepared by the cation exchange reaction of **1a** with PPh_4Br in MeCN was determined by a single-crystal X-ray analysis. This complex crystallizes in the space group $P\bar{1}$ and contains four cations, two anion, and two MeCN molecules in an asymmetric unit. This MeCN molecule does not coordinate to the molybdenum(IV) ion. Perspective view of the anion of **1b** is shown in Figure 1. The selected bond distances and bond angles are presented in Table II.[19] The geometry of $MoOS_4$ core of **1b** is based on a square pyramid with C_{4v} symmetry, and this molecular structure is similar to that of $[Mo^{V}O(SPh)_4]^-$ reported by Bradbury *et al.*[20] In **1b** Mo atom lies 0.73 (2) Å above a plane formed by four sulfur atoms. The Mo=O distance of 1.690 (9) Å is in the range of the distances observed in oxomolybdenum(IV) thiolate complexes reported to date. For example, Mo=O bond distances of $[Mo^{IV}O(bdt)_2]^{2-}$, $[Mo^{IV}O(S_2C_2(CO_2Me)_2)_2]^{2-}$, and $(NEt_4)_2[Mo^{IV}O(S\text{-}o\text{-}CH_3CONH\text{-}C_6H_4)_4]$ are 1.699 (6) Å,[13] 1.686 (6) Å,[14] and 1.689 (5) Å,[18] respectively. The average Mo-S distance (2.415 Å) of **1b** is nearly the same with the distance of

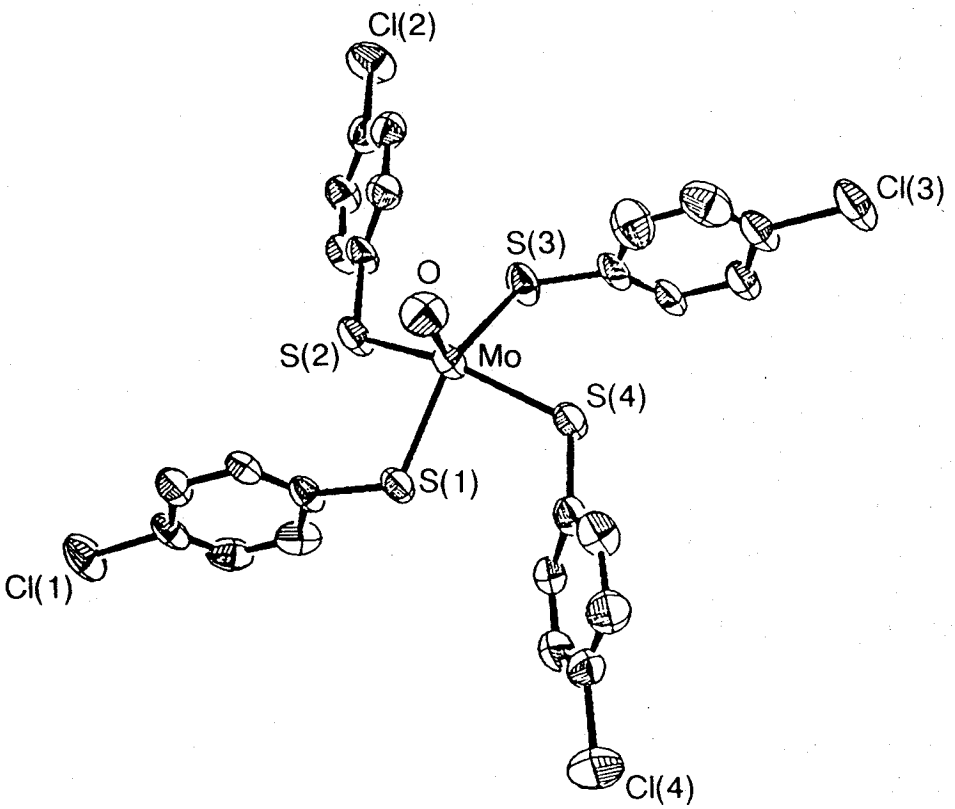

Figure 1. Perspective view of the structure of the anion part of $(PPh_4)_2[Mo^{IV}O(p\text{-}ClC_6H_4S)_4]$ (**1b**). The atoms are drawn as 50% probability ellipsoids. Hydrogen atoms are omitted for clarity.

Table II. Selected Bond Distances, Bond Angles, Torsion Angles, and Dihedral Angles of $(PPh_4)_2[Mo^{IV}O(p\text{-}ClC_6H_4S)_4]$ (**1b**).

Bond Distances/Å			
Mo-O	1.690(9)	S(1)-C(111)	1.78(1)
Mo-S(1)	2.395(3)	S(2)-C(121)	1.78(1)
Mo-S(2)	2.418(4)	S(3)-C(131)	1.77(1)
Mo-S(3)	2.416(4)	S(4)-C(141)	1.77(1)
Mo-S(4)	2.431(3)		
mean Mo-S	2.415		
Bond Angles/°			
S(1)-Mo-S(2)	85.0(1)	Mo-S(1)-C(111)	116.9(4)
S(2)-Mo-S(3)	84.7(1)	Mo-S(2)-C(121)	116.3(4)
S(3)-Mo-S(4)	83.1(1)	Mo-S(3)-C(131)	114.1(5)
S(4)-Mo-S(1)	86.3(1)	Mo-S(4)-C(141)	117.7(4)
S(1)-Mo-S(3)	140.6(1)		
S(2)-Mo-S(4)	148.5(2)		
O-Mo-S(1)	109.3(3)		
O-Mo-S(2)	105.6(3)		
O-Mo-S(3)	110.1(3)		
O-Mo-S(4)	105.8(3)		
Torsion Angles/°			
O-Mo-S(1)-C(111)	86.9(6)		
O-Mo-S(2)-C(121)	81.3(6)		
O-Mo-S(3)-C(131)	74.6(6)		
O-Mo-S(4)-C(141)	90.9(6)		
Dihedral Angles/°			
Mo-S(1)-C(111) and the phenyl ring	64.6(4)		
Mo-S(2)-C(121) and the phenyl ring	35.0(4)		
Mo-S(3)-C(131) and the phenyl ring	70.9(5)		
Mo-S(4)-C(141) and the phenyl ring	69.9(4)		

$(PPh_4)_2[Mo^{IV}O(S\text{-}o\text{-}CH_3CONH\text{-}C_6H_4)_4]$ (av. 2.408 (8) Å)[18] and is longer than that of $[Mo^{IV}O(bdt)_2]^{2-}$ (av. 2.388 (2) Å)[13] and $[Mo^{IV}O(S_2C_2(CO_2Me)_2)_2]^{2-}$ (av. 2.380 (2) Å)[14]. The results show that the present monodentate benzenethiolate ligands more weakly coordinate to Mo(IV) ions than bdt or dithiolene chelate ligands. Although $[Mo^{IV}O(S_2CNPr_2)_2]$ has chelate ligands, the Mo-S distances are somewhat longer (av. 2.414 (2) Å)[21], because of formal thioketone character of one of the two sulfur ligands, and a somewhat small metal-ligand overlap caused by narrow S-Mo-S bite angles (av. 72.4°) of the four-membered Mo-S-C-S ring.[22]

The O-Mo-S-C torsion angles of **1b** range from 74° to 91°. EHMO calculation of $[Mo^{IV}O(SH)_4]^{2-}$ showed that **1b** has a relatively stable structure in the torsion angles which are near 90°. (*vide infra*) The Mo-S-C bond angles (av. 116.2°) show that these sulfur atoms have a strong sp^2 character. However, the torsion angles between Mo-S-C plane and phenyl ring are far apart from 0° because of the steric effect among four phenyl rings. (Table II) The O-Mo-S-C torsion angles in $[Mo^{V}O(SPh)_4]^-$ range from *ca.* -33° to -45°.[20]

The geometry around Mo(V) may reflect the d-electronic state, which has a singly occupied d_{xy} orbital. Then the repulsion between this d_{xy} orbital and pπ of sulfur atom is smaller than that of **1b** with a fully-occupied d_{xy} orbital. Actually the torsion angles of $[Mo^{V}O(SPh)_4]^-$ are far apart from 90°. This complex has a structure in which conjugation between Mo-S-C plane and phenyl ring is larger than **1b**.

Cleland *et al.* showed that $[LMo^{V}O(SPh)_2]$ (L = hydrotris(3,5-dimethyl-1-pyrazolyl)borate) has two quite different O-Mo-S-C torsion angles in solid state (-34° and -110°) and that the O-Mo-S bond angles depend on this torsion angle due to the dπ-pπ repulsion between (Mo-O) and S atoms.[23] The O-Mo-S bond angles of **1b** does not depend on O-Mo-S-C torsion angles.

In order to elucidate the structure of **1b**, the EHMO calculations of $[Mo^{IV}O(SH)_4]^{2-}$ as a model (Figure 2 a) was carried out. In these calculations the O-Mo-S-C torsion angle (θ) was defined as Figure 2 b. The total energy of $[Mo^{IV}O(SH)_4]^{2-}$ has a minimum at θ = 90° and has two maxima at θ = 0° and 180°. (Figure 3) This is

explicable by orbital interactions. Thus, overlap of the anti-bonding orbital on d_{xy} of Mo with pπ of sulfur atom in HOMO maximizes at θ = 0° and 180° and minimizes at θ = 90°.(Figure 4)

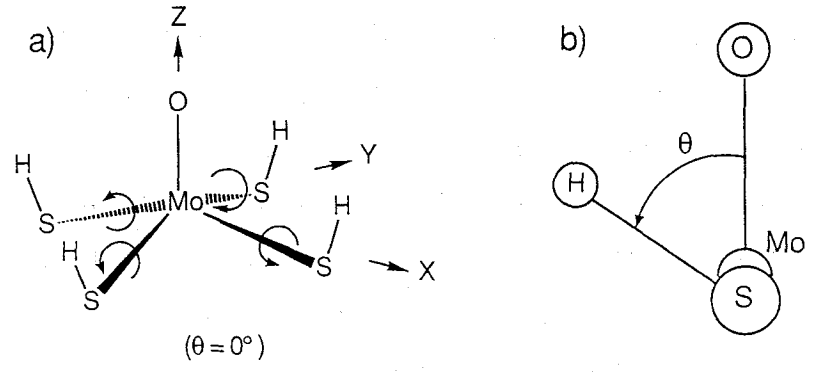

Figure 2. a) Model used in EHMO calculation. b) The O-Mo-S-C torsion angle which was defined in these calculations.

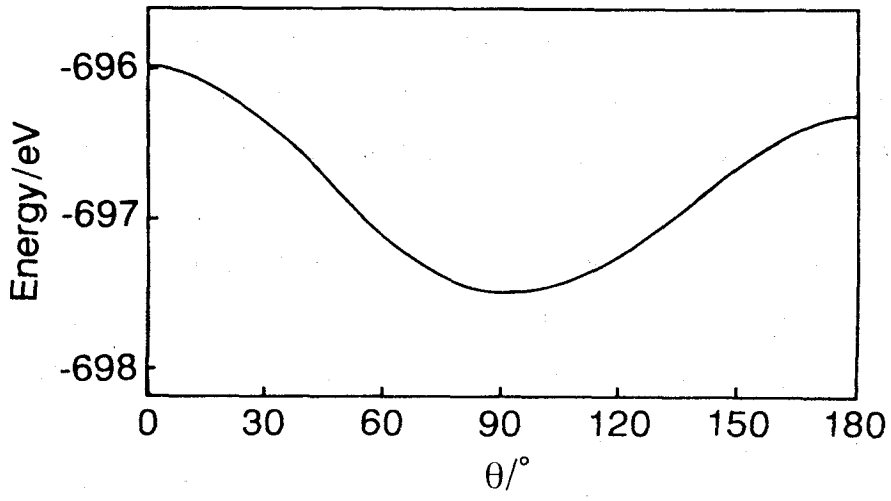

Figure 3. Variation of the total energy of $[MoO(SH)_4]^{2-}$ with change in all O-Mo-S-H (θ) torsion angles.

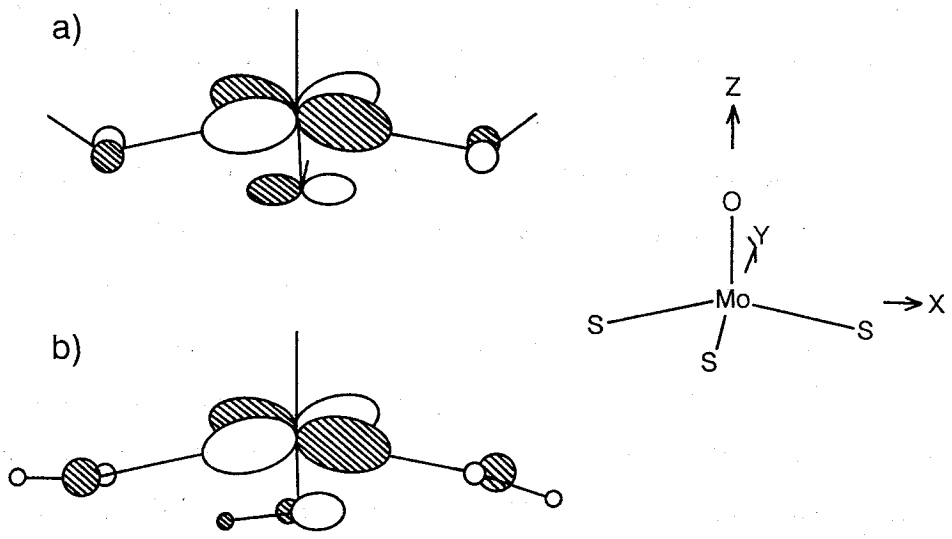

Figure 4. Molecular orbitals of $[MoO(SH)_4]^{2-}$ a) at $\theta = 0°$ and b) $\theta = 90°$ in HOMO.

Physical Properties. The cyclic voltammograms (CV) of **1a** displayed a quasi-reversible Mo(V)/Mo(IV) redox couple at -0.65 V vs. SCE and irreversible oxidation to Mo(VI) at 0.54 V in MeCN. These redox potentials of **1a** were the same as those of **2** which showed a quasi-reversible Mo(V)/Mo(IV) couple at -0.65 V and irreversible oxidation to Mo(VI) at 0.54 V. The CV of **2** was remeasured to compare with **1** in the same condition. The i_{pa}/i_{pc} value of **1a** and **2** were 1.0 and 0.83 respectively.

The absorption spectra of **1a** and **2** in MeCN are shown in Figure 5. The distinct absorption maxima of **1a** appeared at 265 nm (51,000 $M^{-1}cm^{-1}$), 313 nm (30,000) and 588 nm (480). **2** shows absorption maxima at 250 nm (55,000), 290 nm (sh 25,000), 330 nm (sh 16,500), and 604 nm (6,950). Generally monooxomolybdenum(V) complexes have a *d-d* transition in low-energy region and CT transition in high-energy region. For example, $[Mo^{V}OCl_4]^-$ has a weak *d-d* transition at 604 nm.[24] Soft ligands such as thiolate shift the CT transition to lower-energy region.[24,25] Hanson *et al.* reported that $[Mo^{V}O(SC_6H_5)_4]^-$ have a strong absorption band at 598 nm. They assigned this band to an LMCT transition from sulfur ligands to Mo(V) ions from the following features : i) large extinction; ii) lower energy shift by electron-donating substituents on benzenethiolate ligand; iii) qualitative agreement with Jørgensen's theory.[26] A weak *d-d* transition in the oxomolybdenum(V) complexes, $[Mo^{V}O(S\text{-}aryl)_4]^-$ is masked by the strong LMCT transition. Ellis *et al.* proposed that one-electron reduction of those oxomolybdenum(V) thiolato complexes causes a blue shift of the LMCT band to appear at the *d-d* transition region.[12] The weak band at 588 nm near the LMCT region (604 nm) of **2** is thus assignable to a d_{xy}-d_{xz}, or d_{yz} transition.

Raman spectra of **1a** and **2** showed ν(Mo=O) at 932 cm^{-1} and 942 cm^{-1}, respectively. The difference (10 cm^{-1}) in ν(Mo=O) is not due to the structural change but due to the decrease of π-donation of O-pπ to Mo-dπ. Similar shift was observed between oxomolybdenum(IV and V) complexes having bdt or SC_6F_5 ligands. Thus, $[Mo^{IV}O(bdt)_2]^{2-}$ and $[Mo^{V}O(bdt)_2]^-$ show ν(Mo=O) stretching at 905 cm^{-1} and 944 cm^{-1} respectively.

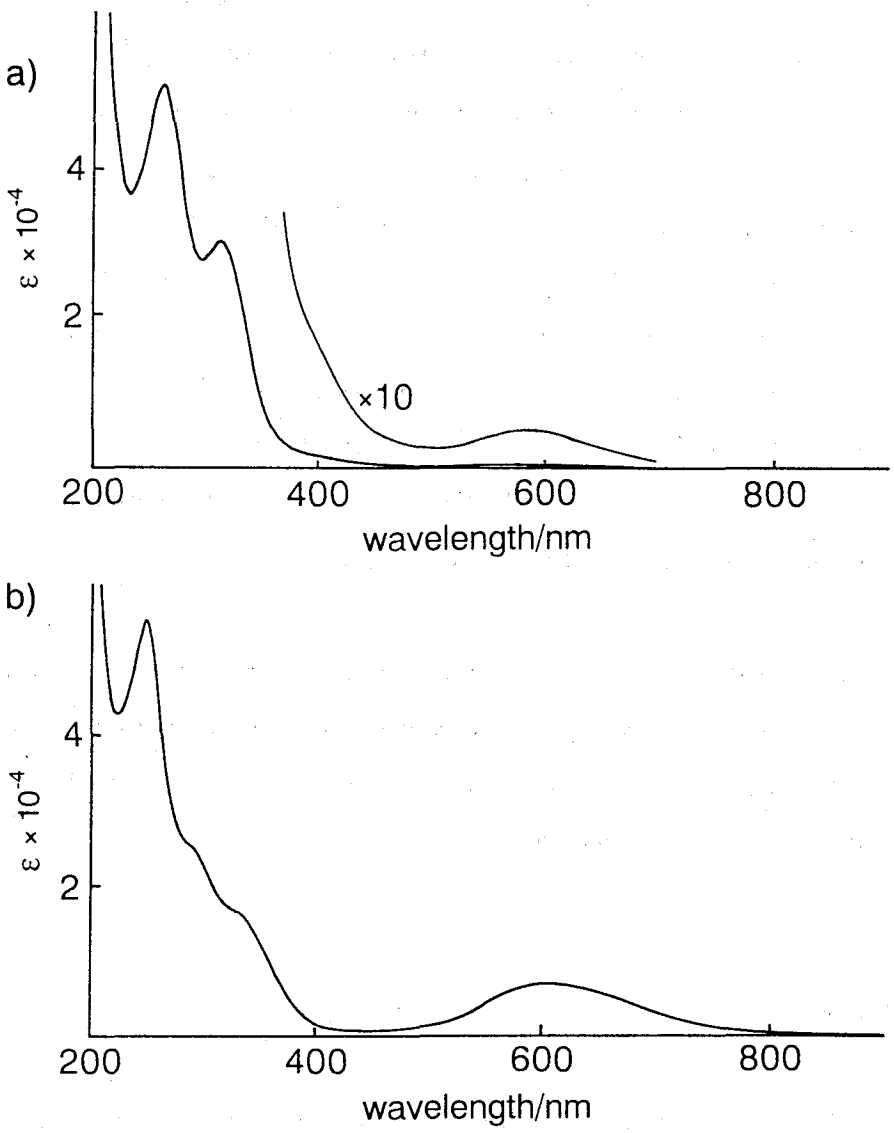

Figure 5. Absorption spectra in MeCN of a) $(NEt_4)_2[Mo^{IV}O(p\text{-}ClC_6H_4S)_4]$ and b) $(NEt_4)[Mo^{V}O(p\text{-}ClC_6H_4S)_4]$.

^{1}H NMR (270 MHz) spectrum of **1** indicated diamagnetic d^2 configuration in MeCN-d_3. The proton signals of the benzene rings were observed as two doublets at 7.3 and 6.9 ppm (J = 8.3 Hz), and the proton signals of counter cation, NEt_4^+, appeared at 3.1 (CH_2, q) and 1.1 ppm (CH_3, m). These proton chemical shifts of the *p*-chlorobenzenethiolate ligands were nearly the same with sodium *p*-chlorobenzenethiolate which has two doublets at 7.1 and 6.8 ppm.

1a (or **1b**) was found to be a useful starting material to produce various oxomolybdenum(IV) dithiolate complexes by a ligand exchange reaction because this complex was coordinated by only monodentate thiolate ligands. Similar methods have been developed for the syntheses of oxomolybdenum(V) dithiolate complexes, $[Mo^VO(bdt)_2]^-$,[13] $[Mo^VO(edt)_2]^-$,[7] and $[Mo^VO(\alpha\text{-tdt})_2]^-$ (α-tdt = α-toluenedithiolato)[27] by a ligand exchange reaction between $[Mo^VO(SPh)_4]^-$ and the corresponding dithiols. The details of these syntheses will be published elsewhere.

Acknowledgment. We are grateful to Professor Yukiteru Katsube and Dr. Mamoru Sato for their kind help in installing *SHELX 86* in a PC9801 computer, and to the staffs of Research Center of Protein Engineering, Institute for Protein Research, Osaka University for using X-ray equipment.

References

(1) Hille, R. and Massey, V. In *Molybdenum Enzymes*; Spiro, T. G., Ed.; John-Wiley: New York, 1985; Chap.9, pp 443-518.

(2) George, G. N. and Bray, R. C. *Biochemistry*, **1988**, *27*, 3603.

(3) Cramer, S. P. and Hille, R. *J. Am. Chem. Soc.* **1985**, *107*, 8164.

(4) Cramer, S. P. and Stiefel, E. I. In *Molybdenum Enzymes*; Spiro, T. G., Ed.; John-Wiley: New York, 1985, Chap.8, pp 411-441.

(5) a) Berg, J. M. and Holm, R. H. *J. Am. Chem. Soc.* **1985**, *107*, 917. b) Moore, F. W. and Larson, M. J. *Inorg. Chem.* **1967**, *6*, 998. c) Buchanan, I.; Minelli,M.; Ashby, M. T.; King, T. J.; Enemark, J. H. and Garner, C. D. *Inorg. Chem.* **1984**, *23*, 495. d) Stiefel, E. I.; Miller, K. F.; Bruce, A. E.; Pariyadath, N.; Heinecke, J.; Corbin, J.; Berg, J. M. and Hodgson, K. O. In *Molybdenum Chemistry of Biological Significance*; Newton, W. E. and Otsuka, S., Ed.; New York, 1980, pp 279-294. e) Dowerah, D.; Spence, J. T.; Singh, R.; Wedd, A. G.; Wilson, G. L.; Farchione, F.; Enemark, J. H.; Kristofzski, J. and Bruck, M. *J. Am. Chem. Soc.* **1989**, *109*, 5655. f) Roberts, S. A.; Young, C. G.; Kipke, C. A.; Cleland, W. E. Jr.; Yamanouchi, K.; Carducci, M. D. and Enemark, J. H. *Inorg. Chem.* **1990**, *29*, 3650.

(6) Boyd, I. W. ; Dance, I. G.; Murray, K. S. and Wedd, A. G. *Aust. J. Chem.* **1978**, *31*, 279.

(7) Ellis, S. R.; Collison, D.; Garner, C. D. and Clegg, W. *J. Chem. Soc., Chem. Commun.* **1986**, 1483.

(8) Ellis, S. R.; Collison, D. and Garner, C. D. *J. Chem. Soc., Dalton Trans.*, **1989**, *413*.

(9) Sheldrick, G. M. SHELX 86 In Crystallographic Computing 3, Sheldrick, G. M.; Krüger, C. and Goddard, R. Ed., Oxford University Press, 1985; pp 175-189.

(10) Ashida, T. HBLS-V, The Universal Crystallographic Computing System, 1973, The Computation Center, Osaka University, pp 55.

(11) Kamata, M.; Hirotsu, K.; Higuchi, T.; Tatsumi, K.; Hoffmann, R.; Yoshida, T. and Otsuka, S. *J. Am. Chem. Soc.* **1981**, *103*, 5772.

(12) Mitchell, P. C. H. and Pygall, C. F. *Inorg. Chim. Acta* **1979**, *33*, L109.

(13) Boyde, S.; Ellis, S. R.; Garner, C. D. and Clegg, W. *J. Chem. Soc., Chem. Commun.* **1986**, 1541.

(14) Coucouvanis, D.; Hadjikyriacou, A.; Toupadakis, A.; Koo, S. M.; Ileperuma, O.; Draganjac, M. and Salifoglou, A. *Inorg. Chem.* **1991**. *30*, 754.

(15) Subramanian, P.; Spence, J. T.; Ortega, R. and Enemark, J. H. *Inorg. Chem.* **1984**, 23, 2564.

(16) Berg, J. M.; Hodgson, K. O.; Cramer, S. P.; Corbin, J. L.; Elsberry, A.; Pariyadath, N. and Stiefel, E. I. *J. Am. Chem. Soc.* **1979**, *101*, 2774.

(17) Yoshinaga, N.; Ueyama, N.; Okamura, T. and Nakamura, A. *Chem. Lett.*, **1990**, 1655.

(18) Ueyama, N.; Okamura, T. and Nakamura, A. *J. Am Chem. Soc.* **1992**, *114*, 8129.

(19) The Fo-Fc table, the coordinates of hydrogen, anisotropic thermal parameters of non-hydrogen atoms, and remained bond lengths and angles are deposited as Document No. at the Office of the Editor of Bull. Chem. Soc. Jpn.

(20) Bradbury, J. R.; Mackay, M. F. and Wedd, A. G. *Aust. J. Chem.* **1978**, 31, 2423.

(21) Ricard, L.; Estienne, J.; Karagiannidis, P.; Toledano, P.; Fischer, J.; Mitschler, A. and Weiss, R. *J. Coord. Chem.* **1974**, *3*, 277.

(22) Chatt, J.; Dilworth, J. R.; Schmutz, J. A. and Zubieta, J. A. *J. Chem. Soc., Dalton Trans.* **1979**, 1595.

(23) Cleland, W. E. Jr.; Barnhart, K. M.; Yamanouchi, K.; Collison, D.; Mabbs, F. E.; Ortega, R. B. and Enemark, J. H. *Inorg. Chem.* **1978**, *26*, 1017.

(24) Collison, D. *J. Chem. Soc., Dalton Trans.* **1990**, 2999.

(25) Deeth, R. J. *J. Chem. Soc., Dalton Trans.* **1991**, 1895.

(26) Hanson, G. R.; Brunette, A. A.; McDonell, A. C.; Murray, K. S. and Wedd, A. G. *J. Am. Chem. Soc.* **1981**, *103*, 1953.

(27) Ueyama, N.; Yoshinaga, N.; Kajiwara, A.; Nakamura, A. and Kusunoki, M. *Bull. Chem. Soc. Jpn.* **1991**, *64*, 2458.

Chapter III

Structure and Properties of $(NEt_4)_2[Mo^{IV}O(\alpha,2\text{-toluenedithiolato})_2]$. Absence of Direct Oxo-Transfer Reaction from Trimethylamine-*N*-Oxide

Introduction

Molybdenum is an essential component of a number of enzymes catalyzing two-electron redox reactions.[1] The molybdenum center of sulfite oxidase, trimethylamine-*N*-oxide reductase and dimethylsulfoxide reductase has been considered to be bound to a bidentate dithiolene ligand connecting pterin and phosphate groups.[2-4] The EXAFS analysis of the reduced states has indicated that the molybdenum center has one or more Cys thiolate ligands besides the dithiolene ligand.[5] The chemical properties of Mo(IV) thiolate complexes as a model of the reduced enzymes is still equivocal.

A simple thiolate complex, $[Mo^{V}O(SPh)_4]^-$,[6] has been studied in detail. Some monooxomolybdenum(IV) complexes having symmetrical dithiolate chelating ligands have been reported as the precursor model complexes for the reduced species of the active site of molybdoenzyme, e.g. $[Mo^{IV}O(SCH_2CH_2S)_2]^{2-}$,[7] $[Mo^{IV}O(bdt)_2]^{2-}$ (bdt = 1,2-benzenedithiolato),[8] $[Mo^{IV}O(S_2C_2(CO_2Me)_2)_2]^{2-}$,[9] $[Mo^{IV}O(SC_6H_4\text{-}p\text{-}Cl)_4]^{2-}$ [10]. Novel model monooxomolybdenum(IV) complexes have been studied using a tridentate chelating ligand, e.g. sterically bulky tridentate monooxomolybdenum(IV) complexes,[11-13] and hydrotris(3,5-dimethyl-1-pyrazolyl)borate.[14,15]

The active center of sulfite oxidase and dimethylsulfoxide reductase has Mo(IV) species containing two or three thiolate ligands in the reduced state.[5] If the metal center has three thiolate ligands, one Cys thiolate is probably involved besides one dithiolene ligand. Complexation of two dithiolene-like ligands and two alkanethiolate to $(MoO)^{2+}$ ion in unsymmetrical dithiolate, α,2-toluenedithiolate (α,2-tdt), seems to furnish one of the relevant model complexes. Scheme 1 shows the structure of α,2-tdt ligand.

Scheme 1

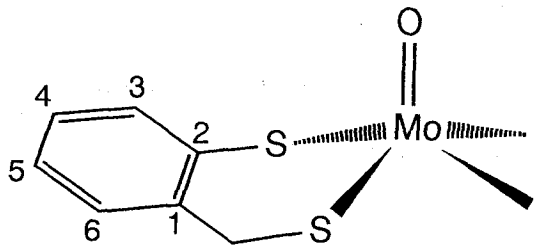

α, 2 - tdt

Furthermore, the detailed structural comparison between Mo(V) and Mo(IV) complexes is of interest to get information on ligand addition process on tetragonal pyramidal complexes to octahedral complexes associated with increasing number of thiolate ligands. The role of thiolate ligand on the process is also of interest since its biochemical relevance has been established.

Experimental Section

All syntheses and physical measurements were performed under argon atmosphere. 1,2-Dimethoxyethane (DME), acetonitrile, *N,N*-dimethylformamide (DMF) and diethyl ether were purified by distillation over calcium hydride under argon atmosphere before use.

α,2-Toluenedithiol (α,2-tol-H_2) was prepared by the literature method.[16,17]

Synthesis of $(NEt_4)_2[Mo^{IV}O(\alpha,2\text{-tdt})_2]$. The complex was synthesized by the novel ligand exchange method with $(NEt_4)_2[Mo^{IV}O(SC_6H_4\text{-}p\text{-}Cl)_4]$.[10]

A mixture of $(NEt_4)_2[Mo^{IV}O(SC_6H_4\text{-}p\text{-}Cl)_4]$ (1.1 g, 1.2 mmol) and α,2-toluenedithiol (0.37 g, 2.4 mmol) were stirred in 50 mL of DME for 4 days at room temperature. A yellow-orange precipitate was collected with filtration and washed three times with 20 mL of diethyl ether to remove free thiols, and dried *in vacuo* and dissolved in 35 mL of acetonitrile. The solution was filtered and concentrated to 6 mL volume under reduced pressure. Deep brown microcrystals were obtained by addition of 10 mL

of diethyl ether to the solution. The crude complex was recrystallized from acetonitrile/diethyl ether. Yield, 0.65 g (81 %). Anal. Calcd for $C_{30}H_{52}N_2OMoS_4$: C, 52.92; H, 7.70; N, 4.11. Found: C, 53.23; H, 8.02; N, 4.59.

Reaction of $(NEt_4)_2[Mo^{IV}O(\alpha,2\text{-tdt})_2]$ with dioxygen or trimethylamine-*N*-oxide. To an acetonitrile solution (3 mL) of $(NEt_4)_2[Mo^{IV}O(\alpha,2\text{-tdt})_2]$ (0.057 g, 0.084 mmol) was added to trimethylamine-*N*-oxide (8.7 mg, 0.11 mmol) with stirring vigorously at room temperature. The ^1H NMR spectrum of the above mixture in acetonitrile-d_3 indicated that no reaction proceeded at 30 °C.

The reaction with dioxygen was carried out by bubbling dioxygen gas (27 μL, 0.0012 mmol) into an acetonitrile solution (0.6 mL) of $(NEt_4)_2[Mo^{IV}O(\alpha,2\text{-tdt})_2]$ (0.0012 mmol). The reaction occurred immediately as evidenced by the color change from yellow-green to blue which was monitored by the characteristic absorption maxima of $(NEt_4)[Mo^{V}O(\alpha,2\text{-tdt})_2]$ using an electronic spectrophotometer.

Physical measurements. Visible spectra were recorded in an acetonitrile solution of $(NEt_4)_2[Mo^{IV}O(\alpha,2\text{-tdt})_2]$ on a Jasco Ubest-30 spectrophotometer. Phase-sensitive 2D NOESY ^1H NMR spectra were measured on a Jeol JNH-GSX 400 spectrometer with 3.0 s mixing time in acetonitrile-d_3 at 30 °C. A total of 8 FID's were recorded with the sweep width of 3333.3 Hz and the time domain of 512 data points. Raman spectrum was obtained on a Jasco R-800 spectrophotometer equipped with a HTV-R649 photomultiplier. A KBr disk sample sealed in a capillary was irradiated with a 514.5 nm argon laser excitation line. The frequency calibration of the spectrometer was carried out with indene as a standard. Electrochemical measurements were carried out using a Yanaco P-1100 instrument in acetonitrile solution that contained 0.1 M tetrabutylammonium perchlorate as a supporting electrolyte. $E_{1/2}$ value, determined as $(E_{p,a} + E_{p,c})/2$, was referenced to the SCE electrode at room temperature and a value uncorrected with junction potential was obtained. ESR spectra in DMF/acetonitrile (1/4 v/v) were recorded on a Jeol JES-FE1X spectrometer at room temperature and at ca. 80 K.

X-ray structure and determination. A single crystal of $(NEt_4)_2[Mo^{IV}O(\alpha,2\text{-tdt})_2]$ was sealed in a glass capillary under argon atmosphere for the X-ray measurement. X-ray measurement was performed at 23 °C on a Rigaku AFC5R diffractometer with graphite monochromated MoKα radiation and a 12 kW rotating anode generator. An empirical absorption correction, based on azimuthal scans of several reflections, was applied which in transmission factors ranging from 0.87 to 1.00. The data were corrected for Lorentz and polarization effects. The basic crystallographic parameters for $(NEt_4)_2[Mo^{IV}O(\alpha,2\text{-tdt})_2]$ are listed in Table I. Unit cell dimensions were refined with 25 reflections. Three standard reflections were chosen and monitored with every 100 reflections and did not show any significant change. The structures were solved by the direct method using a TEXAN crystallographic software package. The non-hydrogen atoms were refined anisotropically. Hydrogen atoms were placed on the calculated positions. The final refinement was carried out using full-matrix least-squares techniques with non-hydrogen atoms. The refinement with anisotropic thermal parameters converged at $R = 0.044$. Atom scattering factors and dispersion corrections were taken from the International Table.[18]

Table I. Crystallographic Data for $(NEt_4)_2[Mo^{IV}O(\alpha,2\text{-tdt})_2]\ Et_2O$.

Chemical formula		$C_{34}H_{62}N_2O_2MoS_4$
Fw		755.08
Crystal system		monoclinic
a		15.429(3)Å
b		16.618(2)Å
c		15.079(3)Å
β		99.38(2)°
V		3815(2)Å^3
Z		4
Space group		*C*c
t		23°C
D_{calcd}		1.315 gcm^{-3}
μ		5.67 cm^{-1}
Radiation		MoKα
$2\theta_{max}$		60.2°
Scan type		ω-2θ
No. of reflections measured	Total	5975
	Unique	5780
No. of observns with I>3σ(I)		3853
R[a]		0.044
R_w[b]		0.052

a $R = \sum||Fo|-|Fc||/\sum|Fo|$.

b $R_w = [\sum w(|Fo|-|Fc|)^2/\sum w|Fo|^2]^{1/2}$; $w = 1/\sigma^2(|Fo|)$.

Results and Discussion

Synthesis. Only a few monooxomolybdenum(IV) thiolate complexes have been reported since the direct synthesis is still limited. For example, $K_2[Mo^{IV}O(edt)_2]$ (edt = 1,2-ethanedithiolato), $K_2[Mo^{IV}O(tdt)_2]$ (tdt = 3,4-toluenedithiolato) and $[Mo^{IV}O(diethyldithiocarbamato)_2]$ were synthesized from the reaction between $K_4[Mo^{IV}O_2(CN)_4]$ and the corresponding ligands.[7] $(NEt_4)_2[Mo^{IV}O(bdt)_2]$ (bdt = 1,2-benzenedithiolato) was also prepared by the above modified method.[8] Novel methods were adopted for the synthesis for $(NHEt_3)_2[Mo^{IV}O(SC_6F_5)_4]$[8] derived from $[Mo^{IV}OCl_2(PPh_2Me)_3]$ and $[Mo^{IV}O\{S_2C_2(CO_2Me)_2\}_2]^{2-}$ obtained from $[Mo^{IV}O(S_4)_2]^{2-}$.[9] Recently, $(NEt_4)_2[Mo^{IV}O(SC_6H_4\text{-}p\text{-}Cl)_4]$ has been isolated from $(NEt_4)[Mo^{V}O(SC_6H_4\text{-}p\text{-}Cl)_4]$ with a mild reductant, NEt_4BH_4, since the Mo(V) complex has a relatively positive-shifted redox potential due to the electron-withdrawing thiolate ligand.[19,10]

$(NEt_4)_2[Mo^{IV}O(\alpha,2\text{-}tdt)_2]$ was synthesized from $(NEt_4)_2[Mo^{IV}O(SC_6H_4\text{-}p\text{-}Cl)_4]$ by the following ligand exchange method (equation 1).

$$(NEt_4)_2[Mo^{IV}O(SC_6H_4\text{-}p\text{-}Cl)_4] + 2\cdot\alpha,2\text{-}tdt\text{-}H_2 \longrightarrow (NEt_4)_2[Mo^{IV}O(\alpha,2\text{-}tdt)_2] + 4\cdot HSC_6H_4\text{-}p\text{-}Cl \quad (1)$$

A direct synthesis of $(NEt_4)_2[Mo^{IV}O(\alpha,2\text{-}tdt)_2]$ from $(NEt_4)[Mo^{V}O(\alpha,2\text{-}tdt)_2]$ is unsuccessful since the Mo(V) complex has too negative Mo(IV)/Mo(V) redox potential (-0.73 V vs SCE in acetonitrile)[20] to be reduced by a convenient reductant such as NEt_4BH_4. The present successful synthesis was accomplished by the lower solubility of the product than that of the starting material during the ligand exchange reaction. From the above reaction only the trans isomer was obtained using unsymmetrical dithiolate ligands as that of $(NEt_4)[Mo^{V}O(\alpha,2\text{-}tdt)_2]$.[20] The present Mo(IV) complex is thermally stable but extremely air sensitive.

Crystal structure. The complex crystallizes in the space group *Cc* and contains four independent $[Mo^{IV}O(\alpha,2\text{-tdt})_2]^{2-}$ anions, eight cations and four diethyl ether molecules in an unit cell. The perspective view of the $[Mo^{IV}O(\alpha,2\text{-tdt})_2]^{2-}$ anion having trans configuration for the two unsymmetrical dithiolate ligands is shown in Figure 1. Selected bond distances and angles are listed in Table II. The complex has an intermediate geometry between square-pyramidal and trigonal-bipyramidal with C_{2v} local symmetry. The ordinary Mo^{IV}=O distance (1.686 (4) Å) in $[Mo^{IV}O(\alpha,2\text{-tdt})_2]^{2-}$ is observed. The Mo^{IV}-S (alkanethiolate) distance is 2.366 Å (mean) similar to a mean distance (2.366 Å) for the Mo-S distance of $[Mo^{IV}O(SCH_2CH_2PPh_2)_2]$,[21] while the Mo^{IV}-S (arenethiolate) distance (2.430 Å) is longer than those of other conventional Mo(IV) complexes.

The Mo=O distance of the Mo(IV) complex is similar to that of the corresponding Mo(V) complex, $(NEt_4)[Mo^{V}O(\alpha,2\text{-toluenedithiolato})_2]$, reported previously.[20] The same constancy of Mo(V)=O and Mo(IV)=O distances is also observed in $(NEt_4)[Mo^{V}O(S\text{-}o\text{-acetylamido-}C_6H_4)_4]$ and $(NEt_4)_2[Mo^{IV}O(S\text{-}o\text{-acetylamido-}C_6H_4)_4]$,[22] although the exceptional difference in the M=O bond distances between $(NEt_4)[Mo^{V}O(bdt)_2]$ and $(NEt_4)_2[Mo^{IV}O(bdt)_2]$ has been reported.[8,23] Thus, upon one-electron reduction the Mo=O bonding does not change largely since the d_{xy} orbital accommodating the added electron is not influenced by the $p\pi$-orbital of the O atom. The Mo-S bond distances of $[Mo^{IV}O(\alpha,2\text{-tdt})_2]^{2-}$ are longer than those of $[Mo^{V}O(\alpha,2\text{-tdt})_2]^{-}$. The reduction to Mo(IV) results in elongation of the Mo-S bonds due to an antibonding HOMO between Mo(IV) d_{xy} and sulfur $p\pi$ orbitals. The Mo-S (arenethiolato) bond distance is longer than that of Mo-S (alkanethiolato) indicative of the stronger Mo-S (alkanethiolato) bonding. The conjugation of sulfur $p\pi$ and phenyl ring $p\pi$ orbitals weakens the π-interaction between Mo(IV) and sulfur. The angles, S(2) (alkanethiolato)-Mo-S(4) (alkanethiolato), is 135.46 (7)° which is slightly smaller than 136.15 (23)° in $[Mo^{V}O(\alpha,2\text{-tdt})_2]^{-}$. The large deviation from 180° reflects a strong π-bonding of Mo-S as reported previously for $[Mo^{V}O(\alpha,2\text{-tdt})_2]^{-}$. The angles, S(1) (arenethiolato)-Mo-S(3) (arenethiolato), is 150.28 (7)° which is similar to 150.10 (24)° in $[Mo^{V}O(\alpha,2\text{-tdt})_2]^{-}$.

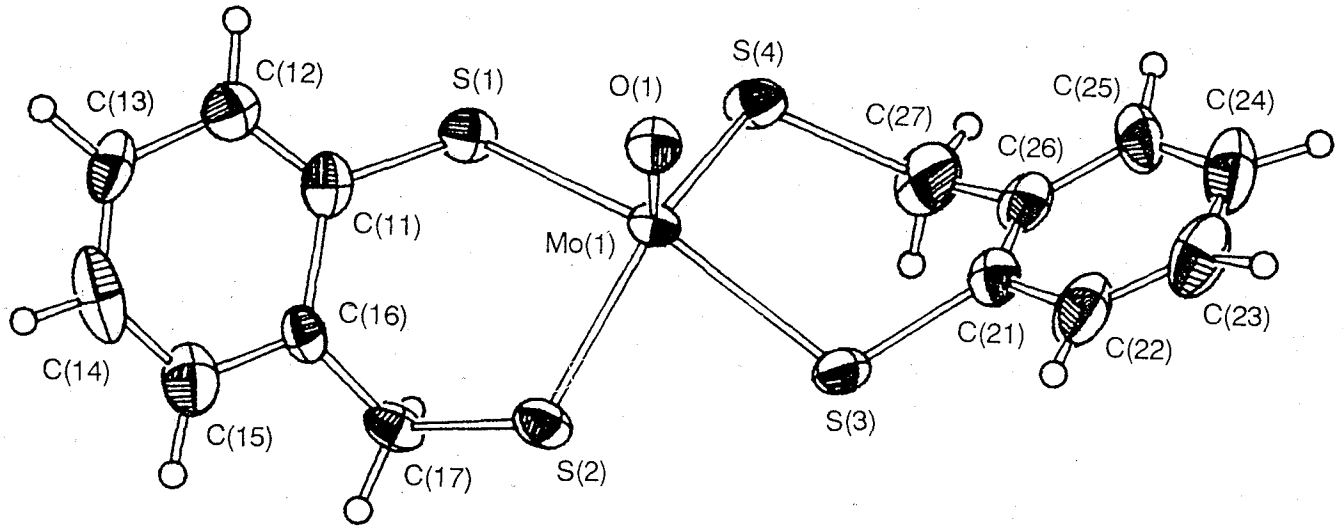

Figure 1. Perspective view of $[Mo^{IV}O(\alpha,2\text{-tdt})_2]^{2-}$ anion showing the partial atom-labeling scheme

Table II. Selected intramolecular distances (Å) and angles (deg) for $(NEt_4)_2[Mo^{IV}O(\alpha,2\text{-tdt})_2]\cdot Et_2O$ compared with those of $(NEt_4)[Mo^{V}O(\alpha,2\text{-tdt})_2]$.

	$(NEt_4)_2[Mo^{IV}O(\alpha,2\text{-tdt})_2]\cdot Et_2O$	$(NEt_4)[Mo^{V}O(\alpha,2\text{-tdt})_2]$.
Distances		
Mo=O	1.686(4)	1.688(18)
Mo-S(1) (arenethiolato)	2.426(2)	2.406(7)
Mo-S(2) (alkanethiolato)	2.362(2)	2.368(7)
Mo-S(3) (arenethiolato)	2.433(2)	2.431(7)
Mo-S(4) (alkanethiolato)	2.369(2)	2.366(7)
mean Mo-S (arenethiolato)	2.430	2.418
mean Mo-S (alkanethiolato)	2.366	2.368
S(1)-C(11)	1.699(9)	1.771(23)
S(2)-C(17)	1.750(8)	1.881(27)
S(3)-C(21)	1.857(9)	1.811(26)
S(4)-C(27)	1.98(1)	1.881(24)
Angles		
S(1)-Mo-S(2)	88.10(7)	89.93(23)
S(2)-Mo-S(3)	81.37(7)	79.74(23)
S(3)-Mo-S(4)	90.29(7)	89.28(23)
S(4)-Mo-S(1)	77.91(7)	78.75(23)
S(1)-Mo-S(3)	150.28(7)	150.10(24)
S(2)-Mo-S(4)	135.47(8)	136.15(23)
O-Mo-S(1)	103.9(4)	105.(34)
O-Mo-S(2)	112.3(5)	112.92(64)
O-Mo-S(3)	105.8(4)	104.53(64)
O-Mo-S(4)	112.1(5)	110.92(64)
Mo-S(1)-C(11)	110.3(3)	

Mo-S(2)-C(17)	114.9(2)
Mo-S(3)-C(21)	110.4(2)
Mo-S(4)-C(27)	108.6(3)
Torsion angles	
O-Mo-S(1)-C(11)	-69.9(6)
O-Mo-S(2)-C(17)	109.5(5)
O-Mo-S(3)-C(21)	-72.2(6)
O-Mo-S(4)-C(27)	105.4(6)
C(15)-C(16)-C(17)-H(5)	120.9
C(15)-C(16)-C(17)-H(6)	2.1
C(11)-C(16)-C(17)-H(5)	-52.5
C(11)-C(16)-C(17)-H(6)	-171.4
C(25)-C(26)-C(27)-H(11)	123.3
C(25)-C(26)-C(27)-H(12)	8.7
C(21)-C(26)-C(27)-H(11)	-58.4
C(21)-C(26)-C(27)-H(12)	-173.0
Displacement of Mo	
from S_4 plane	0.752

Actually, $[Mo^{IV}O(SC_6H_4\text{-}p\text{-}Cl)_4]^{2-}$ has two wide S-Mo-S angles (S(1)-Mo-S(3) 140.6(1)°, S(2)-Mo-S(4) 148.5(2)°) due to sole presence of arenethiolate ligands.[10]

Distortion in the Mo(IV) state similar to the above case has been found for $[Mo^{IV}O(SCH_2CH_2PPh_2)_2]$ [24] and $(NEt_4)_2[Mo^{IV}O(S\text{-}o\text{-acetylamido-}C_6H_4)_4]$.[22] In the case of dithiocarbamate complex, e.g., $[Mo^{IV}O(S_2CNPr^n{}_2)_2]$ exhibits a local square-pyramidal structure having longer Mo-S bonds. The long Mo-S bond has been considered to be due in part to structural trans influence produced by trans terminal oxo- or bridging oxo-groups and to the steric reasons of a small bite angle by the four membered chelate rings in the dithiocarbamate Mo(IV) complexes.[24] However, our results indicate that the long Mo-S (arenethiolato) bond distance of $[Mo^{IV}O(\alpha,2\text{-tdt})_2]^{2-}$ similar to those (2.45 Å ~ 2.55 Å) of the dithiocarbamate Mo(IV) complexes[25] is ascribed to the weakening of Mo-S π-bonding by the π-conjugation between sulfur and benzene ring.

The observed short Mo-S (alkanethiolate) bond distance (mean 2.366 Å) is a reasonable bond distance for the Mo-S (alkanethiolato) distance (mean 2.360 Å) as reported for $[Mo^{IV}O(SCH_2CH_2PPh_2)_2]$.[24] The short Mo-S (alkanethiolato) bond is due to the strong π-interaction between Mo and sulfur atoms although the doubly-occupied HOMO is antibonding with Mo d_{xy} and sulfur $p\pi$-orbitals.

Electronic spectrum of $(NEt_4)_2[Mo^{IV}O(\alpha,2\text{-tdt})_2]$. Figure 2 shows the UV-visible absorption spectra of $(NEt_4)_2[Mo^{IV}O(\alpha,2\text{-tdt})_2]$ and, for the comparison, that of $(NEt_4)[Mo^{V}O(\alpha,2\text{-tdt})_2]$ in acetonitrile. Four distinct absorption maxima were observed at 250 nm (37,700 $M^{-1}cm^{-1}$), 287 nm (20,700), 384 nm (5,520), and 590 nm (370) in $(NEt_4)_2[Mo^{IV}O(\alpha,2\text{-tdt})_2]$. The weak maximum at 590 nm is assignable to *d-d* transition as those at 552 nm for $(NEt_4)_2[Mo^{IV}O(S\text{-}o\text{-acetylamido-}C_6H_4)_4]$ in acetonitrile.[22] The presence of the weak *d-d* transition band overlapping with a strong LMCT band at this region has been predicted by the detailed analysis of the electronic spectra of various Mo(V) benzenethiolate complexes. Furthermore, the presence of only weak *d-d* band of the Mo(IV) complex at 590 nm confirms that the four intense visible

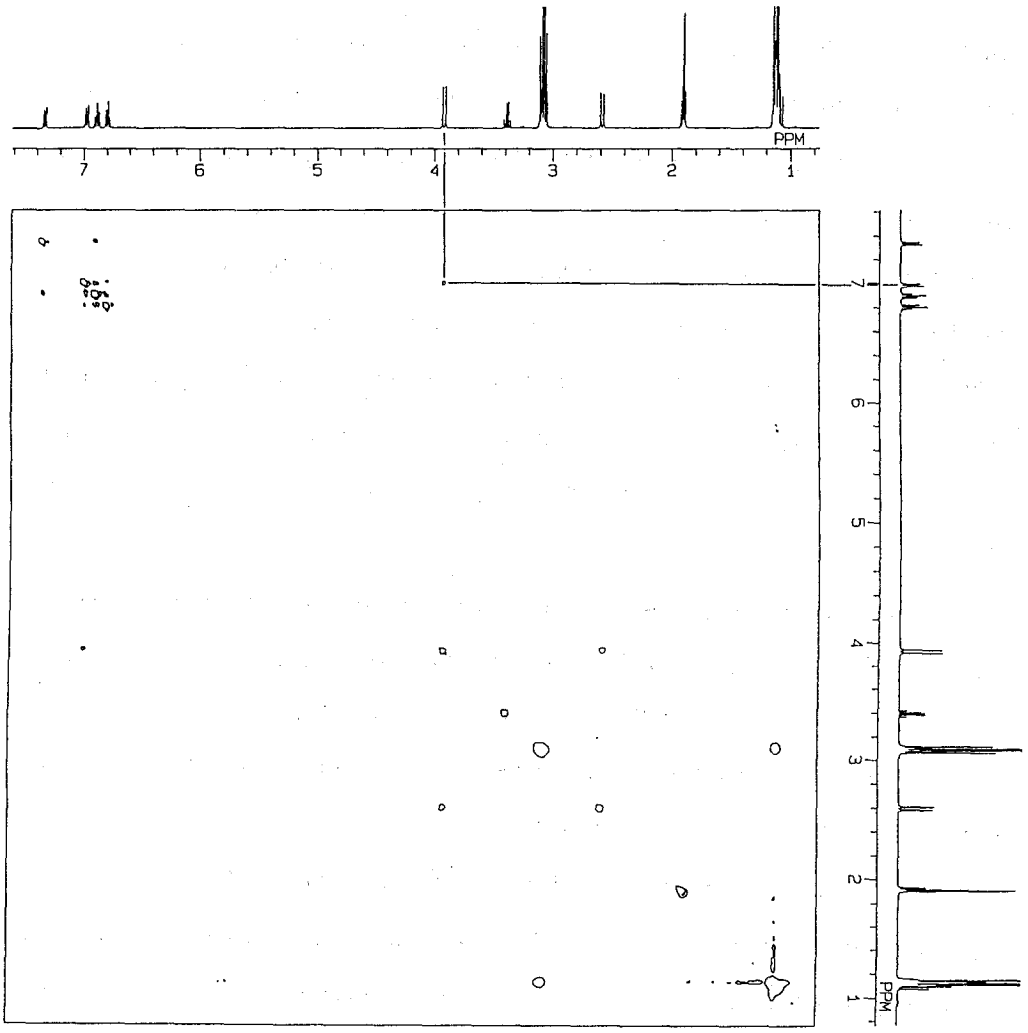

Figure 2. ^{1}H-^{1}H-NOESY spectrum of $(NEt_4)_2[Mo^{IV}O(\alpha,2\text{-tdt})_2]$ in acetonitrile-d_3.

maxima of $(NEt_4)[Mo^{V}O(\alpha,2\text{-tdt})_2]$ observed at 454, 520, 600, and 720 nm are ascribed to LMCT bands from sulfur p to Mo d_{xy},d_{yz}.

Solution structure of $(NEt_4)_2[Mo^{IV}O(\alpha,2\text{-tdt})_2]$ determined by ^1H NMR spectrum. The ^1H NMR signals of methylene protons, CH_AH_B, in $(NEt_4)_2[Mo^{IV}O(\alpha,2\text{-tdt})_2]$ were observed separately with a set of doublets at 2.59 and 3.92 ppm (J_{gem} = 10.8 Hz) in acetonitrile-d_3 and Figure 3 shows the ^1H-^1H-NOESY spectrum. These well-resolved spectra were obtained only after the addition of tetraethylammonium borohydride (1 %) to remove a small amount of paramagnetic $[Mo^{V}O(\alpha,2\text{-tdt})_2]^-$ species which is responsible for the broadness of ^1H signals with fast electron exchange between the Mo(V) and Mo(IV) complexes. All of the assignable benzene ring protons are observed at 7.33 ppm (d) for 3-position, 6.80 ppm (t) for 4-position, 6.89 ppm (t) for 5-position and 6.98 ppm (d) for 6-position.

Two possible explanations are considered for the origin of the difference in the chemical shift between H_A and H_B. One is the different shielding for them by the Mo=O group which influences the protons by anisotropic shielding just like the ketonic double bonding or the alkyne triple bonding as has been recently discussed.[22] The other is the shielding from the benzene ring of α,2-tol ligand. The results of NOE between 6-position H and CH_B (3.92 ppm) support the significance of the shielding of CH_A (2.59 ppm) by the benzene ring as shown in the Scheme 2.

Scheme 2

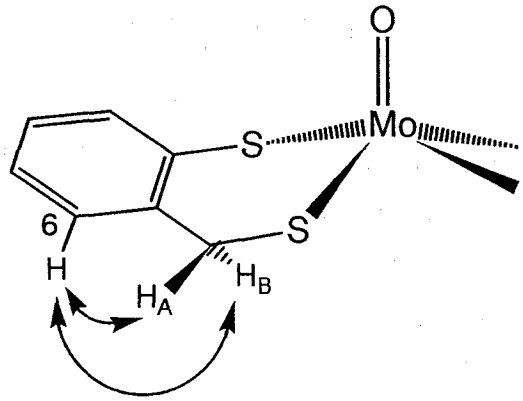

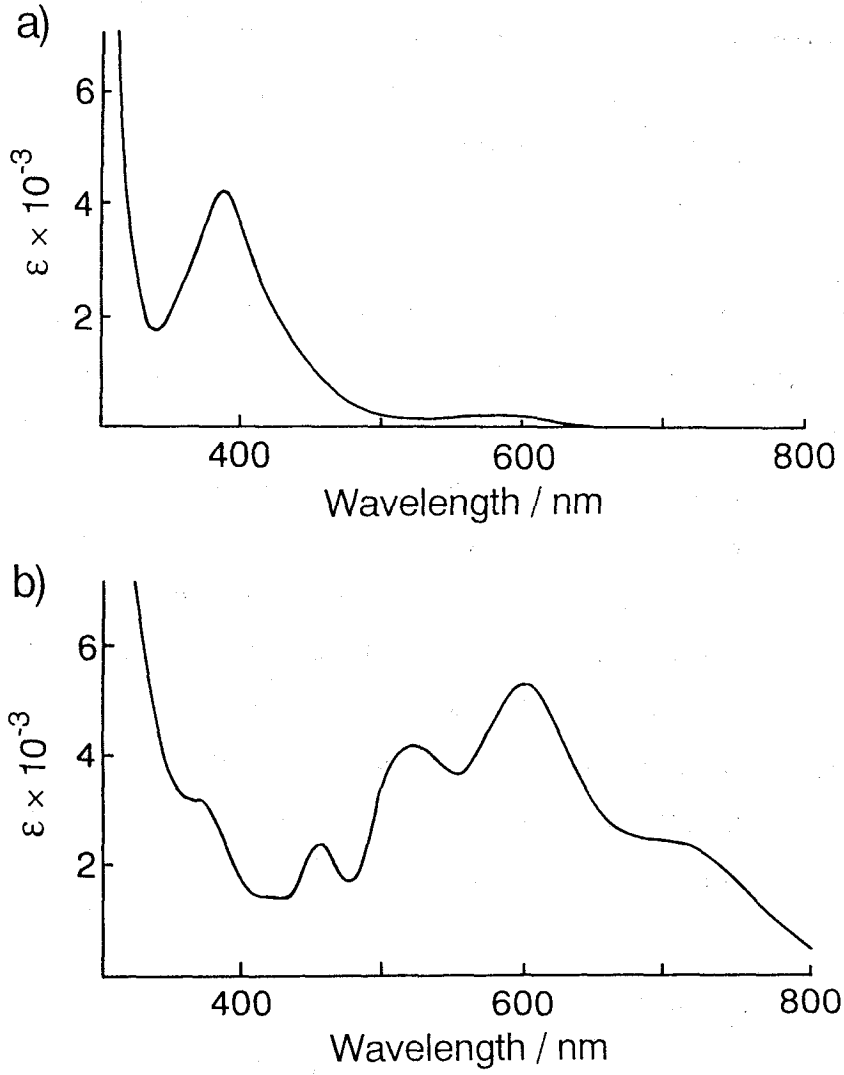

Figure 3. UV-visible absorption spectra of a) $(NEt_4)_2[Mo^{IV}O(\alpha,2\text{-tdt})_2]$ and b) $(NEt_4)[Mo^{V}O(\alpha,2\text{-tdt})_2]$ in acetonitrile at 23 °C. Conditions; concentration, 1.0 mM.

Temperature dependence was not observed in the range of -40°C ~ 40°C, indicative of a rigid structure of the six-membered chelating ring in $(NEt_4)_2[Mo^{IV}O(\alpha,2\text{-}tdt)_2]$. Actually, the crystallographic data of the complex in solid state show the different environments for the two protons as one proton locates at torsion angle, 52.5° or 58.4°, from the benzene plane and then another proton locates at 2.1° or 8.7° from the benzene plane. By the X-ray analysis of the complex in a solid state, the H-H distances between 6-position H and CH_A(2.59 ppm) and CH_B(3.92 ppm) were determined to be approximately 3.4 Å and 2.3 Å, respectively.

Raman spectrum of $(NEt_4)_2[Mo^{IV}O(\alpha,2\text{-}tdt)_2]$ in solid state. Figure 4 shows the Raman spectrum of $(NEt_4)_2[Mo^{IV}O(\alpha,2\text{-}tdt)_2]$ in solid state which is compared with that of $(NEt_4)[Mo^{V}O(\alpha,2\text{-}tdt)_2]$. The ν(Mo=O) stretching (940 cm^{-1}) of Mo(V) complex shifts to 922 cm^{-1} in the Mo(IV) complex. The relatively large shift (18 cm^{-1}) is similar to the reported IR shift (39 cm^{-1}) of ν(Mo=O) bands (905 cm^{-1} and 944 cm^{-1}) for $(NEt_4)_2[Mo^{IV}O(bdt)_2]$ and $(PPh_4)[Mo^{V}O(bdt)_2]$, respectively.[8] On the contrary, no shift between $(NEt_4)_2[Mo^{IV}O(S\text{-}o\text{-}acetylamido\text{-}C_6H_4)_4]$ and $(NEt_4)[Mo^{V}O(S\text{-}o\text{-}acetylamido\text{-}C_6H_4)_4]$ was observed as shown in the previous paper.[22] The Raman results of the Mo(IV) and Mo(V) complexes in solid state indicate that the large shift (18 cm^{-1}) of ν(Mo=O) is observed in spite of the same Mo=O bond distances of both complexes as shown by the crystallographic data. Almost identical structural feature for the both Mo(IV) and Mo(V) complexes indicates that the shift of ν(Mo=O) is caused by the change of Mo=O bond character rather than the geometry of $MoOS_4$ core. The observed trend is definitely different from those for a Mo(V)-Mo(IV) pair, $(NEt_4)[Mo^{V}O(bdt)_2]$ and $(NEt_4)_2[Mo^{IV}O(bdt)_2]$.[8]

Electrochemical property. Figure 5 shows the cyclic voltammogram of $(NEt_4)_2[Mo^{IV}O(\alpha,2\text{-}tdt)_2]$ which exhibits a quasi-reversible redox couple of Mo(V)/Mo(IV) at -0.74 V vs SCE (i_{pa}/i_{pc} = 0.98) in acetonitrile. The redox potential is almost the same as that (-0.73 V vs SCE) of the corresponding $(NEt_4)[Mo^{V}O(\alpha,2\text{-}tdt)_2]$ in acetonitrile[20] and is approximately middle between the values (-0.35 V vs SCE and

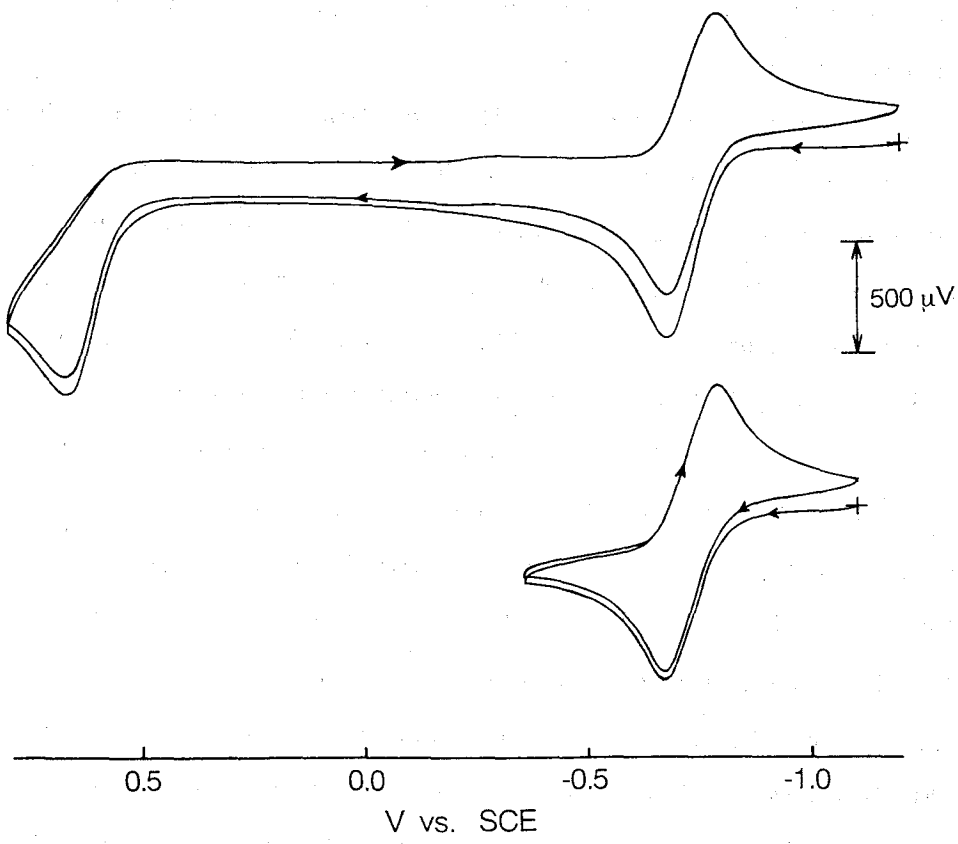

Figure 4. Cyclic voltammogram of $(NEt_4)_2[Mo^{IV}O(\alpha,2\text{-tdt})_2]$ in acetonitrile at 23 °C. Conditions: concentration, [Mo(IV)], 2.0 mM; $[(n\text{-}Bu)_4NClO_4]$, 100 mM; scanning rate, 100 mV/sec.

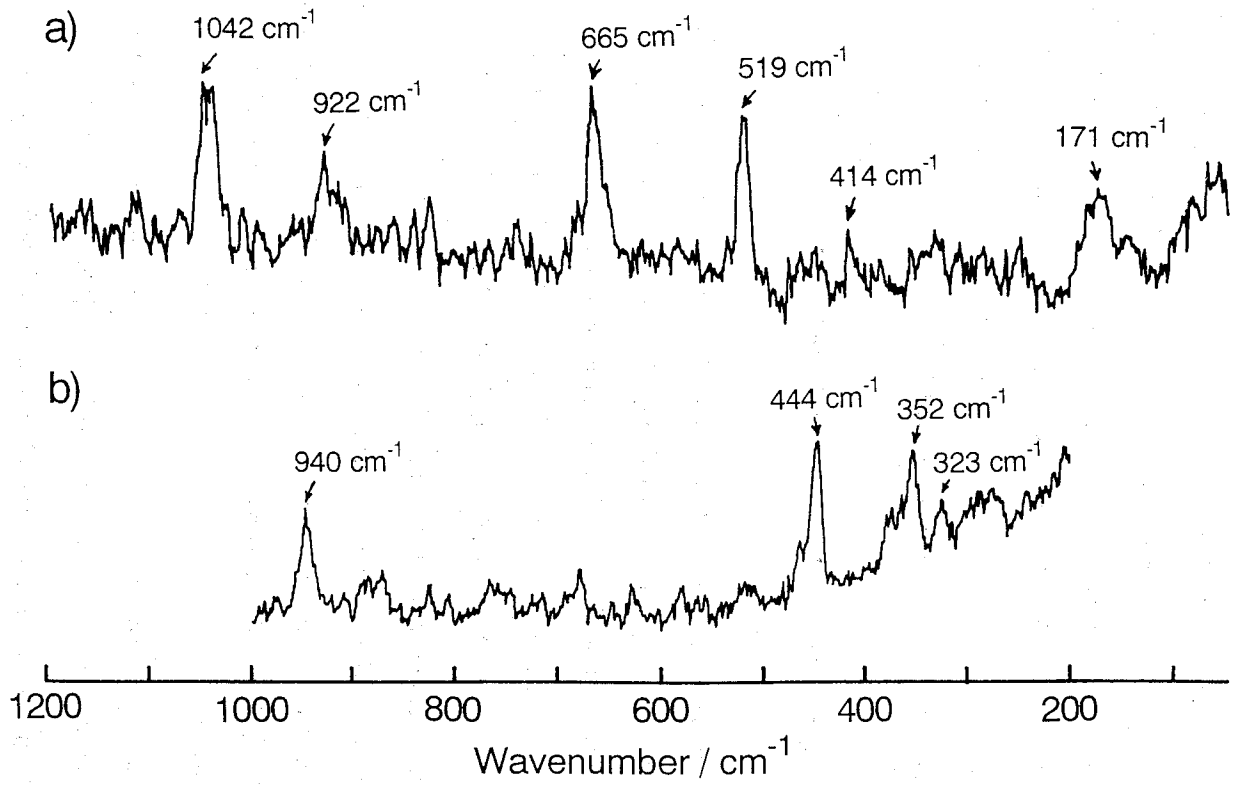

Figure 5. Resonance Raman spectra of a) $(NEt_4)_2[Mo^{IV}O(\alpha,2\text{-tdt})_2]$ and b) $(NEt_4)[Mo^{V}O(\alpha,2\text{-tdt})_2]$ in solid state.

-1.18 V vs SCE) of $(NEt_4)[Mo^{V}O(bdt)_2]$ in DMF[8] and $(NEt_4)[Mo^{V}O(SCH_2CH_2CH_2S)_2]$ in acetonitrile,[26] respectively.

Chemical reactivity. The Mo(IV) complex in acetonitrile solution readily reacts with dioxygen and gives a dark blue solution. The product was identified as $(NEt_4)[Mo^{V}O(\alpha,2\text{-tdt})_2]$ by the observations of four intense visible maxima at 454, 520, 600, and 720 nm and of an ESR signal at $g_1 = 2.035$, $g_2 = 1.980$, and $g_3 = 1.976$ in acetonitrile/DMF (4/1 v/v) at 80 K which are the same as those reported for $(NEt_4)[Mo^{V}O(\alpha,2\text{-tdt})_2]$.[20] One-electron transfer thus occurs between $[Mo^{IV}O(\alpha,2\text{-tdt})_2]^{2-}$ and dioxygen to produce superoxide anion as shown in the equation 2 because the complex has a suitable redox couple at -0.74 V vs SCE.

$$[Mo^{IV}O(\alpha,2\text{-tdt})_2]^{2-} + O_2 \longrightarrow [Mo^{V}O(\alpha,2\text{-tdt})_2]^{-} + O_2^{-} \qquad (2)$$

This reaction commonly occurs for the Mo(IV) complex having many thiolate ligands, e.g. $K_2[Mo^{IV}O(SCH_2CH_2S)_2]$,[7] $[Mo^{IV}O(S_2CNEt_2)_2]$,[7,27] $(NEt_4)_2[Mo^{IV}O(bdt)_2]$.[8]

Interestingly, $(NEt_4)_2[Mo^{IV}O(\alpha,2\text{-tdt})_2]$ is inert to trimethylamine-*N*-oxide in acetonitrile at 30 °C, although the oxidant reacts slowly with $(NEt_4)_2[Mo^{IV}O(bdt)_2]$ to give a dioxomolybdenum(VI) complex, $(NEt_4)_2[Mo^{VI}O_2(bdt)_2]$.[28] In general, monooxomolybdenum(IV) complexes having (S,N), (S,S(thioketone)), (N,N) or (S,O) ligand reacts readily with various amine-N-oxides to give the corresponding dioxomolybdenum(VI) complexes because of its negative redox potential. $[Mo^{IV}O(S_2CNEt_2)_2]$ also easily reacts with the oxidant and gives oxo-transfer product, $[Mo^{VI}O_2(S_2CNEt_2)_2]$.

The inertness is attributed to the following two possibilities. One is the absence of the coordination of amine-*N*-oxide to the position of $[Mo^{IV}O(\alpha,2\text{-tdt})_2]^{2-}$ trans to Mo=O due to the narrow S (alkanethiolato)-Mo-S (alkanethiolato) angle as shown in Scheme 3a. The other is the slow trans-cis rearrangement after coordination of amine-*N*-oxide to the trans position. The two strong Mo-S (alkanethiolate) bonds in $(NEt_4)_2[Mo^{IV}O(\alpha,2\text{-tdt})_2]$ prevent the complex from the trans-cis interconversion of

trans since the reformation of the *Oh* structure requires dissociation of Mo-S bond in the Mo(IV) complex having chelating ligands as shown in the Scheme 3b. In contrast to the non-dissociative nature of α,2-tdt ligand, oxomolybdenum complexes such as $(NEt_4)_2[Mo^{VI}O_2(bdt)_2]$ and $[Mo^{IV}O(S_2CNEt_2)_2]$ have weak, dissociative Mo-S bonds with π-conjugation between sulfur and benzene ring as described above.

Scheme 3a

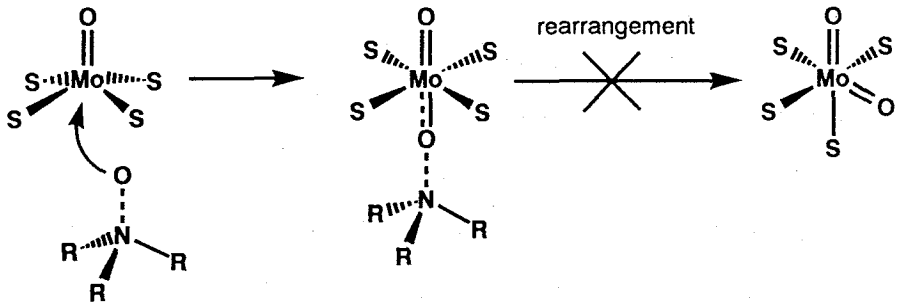

Scheme 3b

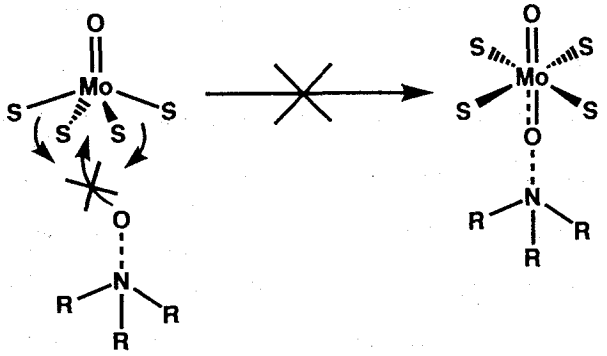

Thus, although $(NEt_4)_2[Mo^{IV}O(\alpha,2\text{-tdt})_2]$ has an ordinary square-pyramidal structure and a relatively negative redox potential in acetonitrile, it is not oxidized by trimethylamine-*N*-oxide. A small amount of $[Mo^{V}O(\alpha,2\text{-tdt})_2]^-$ species is obtained in the reaction with dioxygen just as some other monooxomolybdenum(IV) complexes.

Holm *et al.* have studied the reaction of a five-coordinate Mo(IV) complex, $[Mo^{IV}O(LNS_2)]$ (LNS_2 = 2,6-bis(2,2-diphenyl-2-mercaptoethyl)pyridine(2-)) having a vacant coordination site for a substrate, e.g. dimethylsulfoxide or nitrate ion and proposed the existence of a complex of Mo(IV) and substrate as an intermediate.[29,30] On the other hand, Enemark *et al.* have reported a dissociation mechanism for the reaction of an octahedral Mo(IV) complex, $Mo^{IV}O[HB(Me_2pz)_3][S_2P(OEt)_2]$ with dimethylsulfoxide.[31] The *Oh* structure of the complex has no accessible site for the coordination of substrate.

The unexpected inertness of $(NEt_4)_2[Mo^{IV}O(\alpha,2\text{-tdt})_2]$ against oxo-transfer reaction seems peculiar from the high reductive reactivity by its negative redox potential. Furthermore, the formation of $(NEt_4)_2[Mo^{VI}O_2(bdt)_2]$ from the oxidation of $(NEt_4)_2[Mo^{IV}O(bdt)_2]$ by trimethylamine-*N*-oxide has suggested the addition of an oxo ligand trans to Mo=O in the square-pyramidal Mo(IV) complex.[28] Thus, it is likely that the narrow S-Mo-S angle prevents the coordination of relatively-strong oxo-donors such as trimethylamine-*N*-oxide.

The active site of Mo(IV) in Mo-oxidases has at least three thiolate ligands including a dithiolene ligand. Our results suggest that, if the third thiolate comes from a cysteine thiolate, this type of complex containing many thiolate ligands is disadvantageous to trans-cis rearrangement for the substrate coordination. Therefore, our results support the necessity of a cis coordination of substrate, e.g. amine-*N*-oxide or dimethylsulfoxide, in the dithiolene Mo(IV) center of Mo-oxidases. Holm and his coworkers have pointed out that a vacant site at the cis position of Mo=O group of their elegant model complexes is crucial for the facile oxo-transfer oxidation by the above substrates.[11-13]

On the other hand, a fast reaction between $[Mo^{IV}O(S_2CNEt_2)_2]$ and pyridine-*N*-oxide still suggests a possibility of the trans-cis rearrangement mechanism for the oxo-transfer oxidation by trimethylamine-*N*-oxide and dimethylsulfoxide in biological systems.[11-13] The rearrangement following the trans coordination of amine-*N*-oxide to the Mo=O group of $[Mo^{IV}O(S_2CNEt_2)_2]$ is caused by the two mobile dithiocarbamate ligands with a small S-Mo-S bite angle (ca 72°) or by the dissociative thioketo groups of the ligand. The other amino acid side chain ligands besides dithiolene ligands in Mo-oxidases can serve for the facile cis-trans rearrangement. Further study on oxo-transfer reaction of Mo(IV) complexes with other thiolate chelating ligands is in progress.

References

(1) Holm, R. H. *Chem. Rev.* **1987**, *87*, 1401.

(2) Bray, R. C. *Quart. Rev. Biophys.* **1988**, *21*, 299.

(3) Yamamoto, J.; Okubo, N.; Ishimoto, M. *J. Biochem.* **1986**, *99*, 1773.

(4) Johnson, J. L.; Bastian, N. R.; Rajagopalan, K. V. *Proc. Natl. Acad. Sci. USA* **1990**, *87*, 3190.

(5) Cramer, S. P.; Wahl, R.; Rajagopalan, K. V. *J. Am. Chem. Soc.* **1981**, *103*, 7721.

(6) Hanson, G. R.; Brunette, A. A.; McDonell, A. C.; Murray, K. S.; Wedd, A. G. *J. Am. Chem. Soc.* **1981**, *103*, 1953.

(7) Mitchell, P. C. H.; Pygall, C. F. *Inorg. Chim. Acta* **1979**, *33*, L109.

(8) Boyde, S.; Ellis, S. R.; Garner, C. D.; Clegg, W. *J. Chem. Soc., Chem. Commun.* **1986**, 1541.

(9) Coucouvanis, D.; Hadjikyriacou, A.; Toupadakis, A.; Koo, S.; Ileperuma, O.; Draganjac, M.; Salifoglou, A. *Inorg. Chem.* **1991**, *30*, 754.

(10) Kondo, M.; Ueyama, N.; Fukuyama, K.; Nakamura, A. *Bull. Chem. Soc. Jpn* **1992**,

(11) Berg, J. M.; Holm, R. H. *J. Am. Chem. Soc* **1985**, *107*, 917.

(12) Harlan, E. W.; Berg, J. M.; Holm, R. H. *J. Am. Chem. Soc.* **1986**, *108*, 6992.

(13) Craig, J. A.; Harlan, E. W.; Snyder, B. S.; Whitener, M. A.; Holm, R. H. *Inorg. Chem.* **1989**, *28*, 2082.

(14) Scullane, M. I.; Tylor, R. D.; Minelli, M.; Spence, J. T.; Yamanouchi, K.; Enemark, J. H.; Chasteen, N. D. *Inorg. Chem.* **1979**, *18*, 3213.

(15) Young, C. G.; Roberts, S. A.; Ortega, R. B.; Enemark, J. H. *J. Am. Chem. Soc.* **1987**, *109*, 2938.

(16) Klingsberg, E.; Scheiber, A. M. *J. Am. Chem. Soc.* **1962**, *84*, 2941.

(17) Hortmann, A. G.; Aron, A. J.; Bhattacharya, A. K. *J. Org. Chem.* **1978**, *43*, 3374.

(18) Cromer, D. T.; Waber, J. T. *International Tables for X-ray Crystallography*; Kynoch Press: Birmingham, 1974; Vol. IV, pp Table 2.

(19) Ellis, S. R.; Collison, D.; Garner, C. D. *J. Chem. Soc., Dalton Trans.* **1989**, 413.

(20) Ueyama, N.; Yoshinaga, N.; Kajiwara, A.; Nakamura, A.; Kusunoki, M. *Bull. Chem. Soc. Jpn.* **1991**, *64*, 2458.

(21) Chatt, J.; Dilworth, J. R.; Schumutz, J. A.; Zubieta, J. A. *J. Chem. Soc., Dalton Trans* **1979**, 1595.

(22) Ueyama, N.; Okamura, T.; Nakamura, A. *J. Am. Chem. Soc.* **1992**, *114*, 8129.

(23) Ellis, S. R.; Collison, D.; Garner, C. D. *J. Chem. Soc., Chem. Commun.* **1986**, 1483.

(24) Chatt, J.; Dilworth, J. R.; Schumutz, J. A.; Zubieta, J. A. *J. Chem. Soc., Dalton Trans* **1979**, 1595.

(25) Spivak, B.; Dori, Z. *Co-ordination Chem. Rev.* **1975**, *17*, 99.

(26) Bishop, P. T.; Dilworth, J. R.; Hutchinson, J.; Zubieta, J. A. *J. Chem. Soc., Chem. Commun.* **1982**, 1052.

(27) Ueyama, N.; Yoshinaga, N.; Nakamura, A. *J. Chem. Soc., Dalton Trans.* **1990**, 387.

(28) Yoshinaga, N.; Ueyama, N.; Okamura, T.; Nakamura, A. *Chem. Lett.* **1990**, 1655.

(29) Caradonna, J. P.; Reddy, P. R.; Holm, R. H. *J. Am. Chem. Soc.* **1988**, *110*, 2139.

(30) Craig, J. A.; Holm, R. H. *J. Am. Chem. soc.* **1989**, *111*, 2111.

(31) Roberts, S. A.; Young, C. G.; W. E. Cleland, J.; Ortega, R. B.; Enemark, J. H. *Inorg. Chem.* **1988**, *27*, 3044.

Chapter IV

Syntheses and Structures of Oxomolybdenum(IV) Complexes Having Alkanedithiolate Ligands. Effect of the Chelating Ring Size on the Physical Properties

Introduction

A molybdenum ion exists at the active sites which is called molybdenum cofactor in oxomolybdoenzymes such as sulfite oxidase, aldehyde oxidase, xanthine oxidase, and nitrate reductase.[1] The molybdenum center carries out the oxo transfer reaction by a shuttle between Mo(IV) and Mo(VI) states through two-electron redox reaction. EXAFS studies have shown that a $(Mo^{IV}O)^{2+}$ center is present in the reduced state, and that one or more cysteines coordinate to the molybdenum ion. Actually, Barber *et al.* showed that a cysteine residue is necessary in reconstitution of apo-nitrate reductase.[2] A dithiolene ligand connecting a pterin derivative has been shown to coordinate to the molybdenum ion.[1,3]

Scheme 1

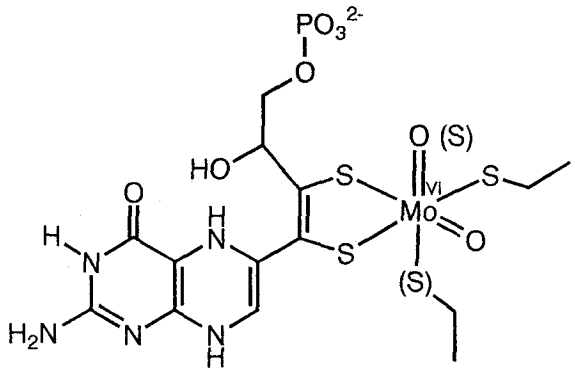

For models of the active sites in the reduced state of the enzymes, only a limited number of monomeric oxomolybdenum(IV) thiolate complexes have been reported because of difficulty of the syntheses. Especially, the synthesis of oxomolybdenum(IV) complexes having alkanethiolate ligands is difficult because of the extremely negative Mo(V)/Mo(IV) redox couple (ca. -1 V vs. SCE). Recently, we reported a novel synthetic method of oxomolybdenum(IV) dithiolate complexes using $[Mo^{IV}O(S\text{-}p\text{-}C_6H_4Cl)_4]^{2-}$ (S-*p*-C_6H_4Cl = *p*-chlorobenzenethiolato) as a starting material.[4] Thus, $(NEt_4)_2[Mo^{IV}O(\alpha,2\text{-tdt})_2]$ (α,2-tdt = α,2-toluenedithiolato) was synthesized in good yield by the ligand exchange reaction between $[Mo^{IV}O(S\text{-}p\text{-}C_6H_4Cl)_4]^{2-}$ and 2 equiv. of α,2-toluenedithiol.[5]

As models of the cysteine ligation to the molybdenum ion in the active sites of oxomolybdoenzymes, we report here the syntheses of oxomolybdenum(IV) complexes having alkanedithiolate ligands, $[Mo^{IV}O(S_2R)_2]^{2-}$,where S_2R is 1,2-ethanedithiolato (1,2-edt) (**1**), 1,2-propanedithiolato (1,2-pdt) (**2**), 2,3-butanedithiolato (2,3-budt) (**3**), or 1,3-propanedithiolato (1,3-pdt) (**4**), by the same or a modified ligand exchange method. Physical properties, chemical reactivities to the oxo-donor reagents, and molecular structures of tetraphenylphosphonium salts of **1** and **4** were studied. All these alkanedithiolate complexes are highly air-sensitive, because of the negative Mo(V)/Mo(IV) redox couple (ca. -0.8 V ~ -1.0 V vs. SCE) compared with the known chelating arenedithiolate complexes, *e.g.* $(NEt_4)_2[Mo^{IV}O(bdt)_2]$[6] (-0.37 V).

The effect of the ligand geometry of the oxomolybdenum(V) complexes on their physical properties has been studied for a variety of oxomolybdenum(V) complexes. For example, Chang *et al.* suggested that the redox potentials and absorption peak positions of $[\{BH(pyMe)_3\}Mo^{V}O(X_2R)]$ ($BH(pyMe)_3$ = hydrotris(3,5-dimethyl-1-pyrazolyl)borate), (X_2R = dithiolato or diolato ligands) change according to the kinds of the ligands, and proposed that the changes are due to the effect of O-Mo-S-C torsion angle.[7] Ueyama *et al.* also reported the synthesis of an oxomolybdenum(V) complex having a peptide ligand, $(NEt_4)[Mo^{V}O(Z\text{-}cys\text{-Pro-Leu-}cys\text{-OMe})_2]$, and showed that this complex has two structural isomers, *i.e.* parallel and anti-parallel conformer.[8] These

isomers showed the unique difference in redox potential, Raman and absorption spectra. It was then postulated that the differences of those physical properties are due to the differences of the O-Mo-S-C torsion angles. In the present paper, we describe the effect of five- and six-membered chelate ring size of alkanedithiolate ligands on absorption and Raman spectra and redox properties of oxomolybdenum(IV) ion of the complexes $[Mo^{IV}O(S_2R)_2]^{2-}$ (S_2R = chelating alkane dithiolato ligands). Our studies show that the change of the chelate ring size mainly affects the Mo-S-C bond angle and intra-ligand S-Mo-S bite angle.

Experimental Section

Materials. All syntheses and physical measurements were carried out under argon atmosphere. Tetrahydrofuran (THF), 1,2-dimethoxyethane (DME) and diethyl ether were distilled from sodium benzophenone ketyl prior to use. Acetonitrile (MeCN), *n*-propanol, methanol (MeOH), acetonitrile-d_3 (MeCN-d_3), and methanol-$d4$ (MeOH-d_4) were dried over calcium hydride, distilled under argon before use. 1,2-Propanedithiol, tetraethylammonium borohydride (NEt_4BH_4), sodium borohydride ($NaBH_4$), and tetraethylammonium chloride (NEt_4Cl) used were of commercial grade obtained from Tokyo Kasei Co. 1,2-Ethanedithiol, 1,3-propanedithiol, 2,3-butanedithiol, and tetraphenylphosphonium chloride (PPh_4Cl) were purchased from Aldrich Co. Disodium 1,3-propanedithiolate was prepared by the usual reaction between sodium metal and the dithiol in THF. The complex $(NEt_4)_2[Mo^{IV}O(S\text{-}p\text{-}C_6H_4Cl)_4]$ and $(PPh_4)_2[Mo^{IV}O(S\text{-}p\text{-}C_6H_4Cl)_4]$ were prepared by the reported method.[4]

Synthesis of $(NEt_4)_2[Mo^{IV}O(edt)_2]$ (1a). A mixture of $(NEt_4)_2[Mo^{IV}O(S\text{-}p\text{-}C_6H_4Cl)_4]$ (1.0 g, 1.1 mmol) and 1,2-ethanedithiol (0.25 g, 2.7 mmol) was stirred in 50 mL of DME for 4 days at room temperature. A pink precipitate was collected with filtration and washed three times with 10 mL of DME to remove free thiols, and dried *in vacuo*, and dissolved in 20 mL of MeCN. The solution was filtered, reduced in volume to about 5 mL under reduced pressure. Brownish red microcrystals

were obtained by addition of 5 mL of diethyl ether to the solution, and were dried in vacuum. Yield, 0.45 g (74.2 %). Anal. Calcd for $C_{20}H_{48}N_2OMoS_4$: C, 43.14; H, 8.69; N, 5.03. Found: C, 42.57; H, 8.76; N, 5.21.

Synthesis of $(PPh_4)_2[Mo^{IV}O(edt)_2]$ (1b). A mixture of $(PPh_4)_2[Mo^{IV}O(S\text{-}p\text{-}C_6H_4Cl)_4]$ (0.15 g, 0.11 mmol) and 1,2-ethanedithiol (0.02 g, 0.20 mmol) was stirred in 18 mL of DME for 9 days at room temperature. A yellow precipitate was collected with filtration and washed three times with 10 mL of DME to remove free thiols, and dried *in vacuo*. The powder obtained was dissolved in 20 mL of MeCN. The solution was filtered, and reduced in volume to about 5 mL under reduced pressure. Pink-purple microcrystals were obtained by addition of 10 mL of diethyl ether, and were dried in vacuum. The crystals have MeCN as a crystalline solvent. Yield, 0.03 g (30 %). Anal. Calcd for $C_{54}H_{51}NOP_2MoS_4$: C, 63.83; H, 5.06; N, 1.38. Found: C, 63.20; H, 4.98; N, 1.17.

Synthesis of $(NEt_4)_2[Mo^{IV}O(1,2\text{-}pdt)_2]$(2) and $(NEt_4)_2[Mo^{IV}O(2,3\text{-}budt)_2]$(3). **2** and **3** were synthesized by the same method used for the preparation of **1a**. Both complexes were obtained as yellow-orange powder. These complexes showed the low crystallizability, and showed the high air-sensitivity in the state of fine powder. Low carbon analysis values are inevitable for these complexes.

2; Yield, (38 %). Anal. Calcd for $C_{22}H_{52}N_2OMoS_4$: C,45.18; H,8.96; N,4.79. Found: C,42.01 ;H,8.73; N,4.26.

3; Yield, (19 %). Anal. Calcd for $C_{24}H_{56}N_2OMoS_4$: C,47.03; H,9.21; N,4.57. Found: C,43.36 ;H,8.67; N,4.34.

Synthesis of $Na_2[Mo^{IV}O(1,3\text{-}pdt)_2]$(4a). A mixture of $(NEt_4)_2[Mo^{IV}O(S\text{-}p\text{-}C_6H_4Cl)_4]$ (1.9 g, 2.0 mmol) and disodium 1,3-propanedithiolate (1.2 g, 7.9 mmol) was stirred in 20 mL of DME for 30 h at room temperature. A pink precipitate was collected with filtration and washed three times with 20 mL of DME and two times with 10 mL of MeCN, and dried *in vacuo*. The pink powder obtained was dissolved in 40 mL of *n*-propanol. The solution was filtered and evaporated in vacuum. The crude product was recrystallized from MeOH / diethyl ether to give pink cubic

crystals. Elemental analysis and 1H NMR spectrum showed that the cation of this complex consists of about 80 % of sodium cation, Na^+ and 20 % of tetraethylammonium cation, $(NEt_4)^+$. Yield, 0.44 g (55 %) Anal. Calcd for $C_{9.2}H_{20}ON_{0.4}Na_{1.6}MoS_4$: C,26.74; H,4.88; N,1.36. Found: C,27.04; H, 5.39; N,1.57.

Synthesis of $(NEt_4)_2[Mo^{IV}O(1,3\text{-pdt})_2]$(4b). **4a** (0.22 g, 0.53 mmol) and NEt_4Cl (0.17 g, 1.0 mmol) were stirred in 20 mL of MeOH for 20 min. The red-purple solution was evaporated *in vacuo*, to give orange powder. This powder was dissolved in 30 mL of MeCN. The solution was filtered and the filtrate was reduced in volume to about 3 mL in vacuum. A pink precipitate was obtained by addition of 5 mL of diethyl ether, and dried under reduced pressure. Pink crystals were obtained by recrystallization from MeOH / diethyl ether. Yield, 0.13 g (42 %). Anal. Calcd for $C_{22}H_{52}N_2OMoS_4$: C,45.18; H,8.96; N,4.79. Found: C,43.96; H, 9.36; N,4.89.

Synthesis of $(PPh_4)_2[Mo^{IV}O(1,3\text{-pdt})_2]$(4c). **4a** (0.15 g, 0,41 mmol) and PPh_4Cl (0.31 g, 0.83 mmol) were stirred in 20 mL of MeOH for 30 min. A red purple powder was obtained by evaporation, and dissolved in 30 mL of MeCN. This solution was stirred overnight at room temperature. The solution was filtered and concentrated in volume to about 4 mL. Black microcrystals obtained were collected with filtration, and dried under reduced pressure. Yield, 0.10 g (24%). Anal. Calcd for $C_{54}H_{52}OP_2MoS_4$: C, 64.66; H, 5.22. Found: C, 64.22; H, 5.35.

Physical Measurements. Absorption spectra were recorded on a Jasco Ubest-30 spectrometer in MeCN solution with 1 mm matched silica cells. Raman spectra were obtained on a Jasco R-800 spectrometer in solid state with 514.5 nm excitation. The cyclic voltammograms were taken on a Yanaco P-1100 polarographic analyzer in MeCN solution (2 mM) with a glassy carbon electrode and $(n\text{-Bu})_4NClO_4$ (100 mM) as a supporting electrolyte. ^1H and ^{13}C NMR spectra were measured on Jeol JNM EX-270, JNM GSX-400, and JNM GX-500 spectrometers. The spectra were internally referenced to the residual CHD_2CN ($\delta \equiv 1.90$) or CD_3CN ($\delta \equiv 118.2$) signals. The measurements were carried out in MeCN-d_3 for **1a**, D_2O for **4a**, and MeCN-d_3/MeOH-d_4 (9/1) for other complexes in the presence of about 0.1 equiv. of NEt_4BH_4 (or $NaBH_4$

for **4a**) at 30 °C. 2D NOESY and COSY NMR spectra were collected on a Jeol JNM GSX-400 or a JNM GX-500 NMR spectrometer. The phase-sensitive 2D NOESY 1H NMR spectra were obtained with 1.0 s mixing time at 30 °C. A total of 8 FID's were recorded with sweep width of 2000.0 Hz and a time domain of 1024 data points.

X-Ray Structure Determination. Single crystals of **1b** and **4c** were sealed in a glass capillary under argon atmosphere for X-ray measurements. All measurements were made on a Rigaku AFC5R diffractometer with graphite monochromated Mo Kα radiation and a 12 kW rotating anode generator. For each compound, unit cell constants were obtained from a least-squares refinement using the setting angles of 25 carefully centered reflections in the range $22.81 < 2\theta < 26.64°$. Crystal data and experimental details are listed in Table I. Three intense reflections were chosen and measured after every 100 reflections through data collections, and did not show any significant change in both measurements. Lorentz, polarization, and absorption corrections based on azimuthal scans, were applied. The structures were solved by direct method and refined by the block-diagonal least squares method. For **1b** all non-hydrogen atoms, and for **4b** the non-hydrogen atoms of the anion and P atoms of the cations were refined anisotropically, and other non-hydrogen atoms were refined isotropically. All hydrogen atoms were placed in idealized positions. The final refinements were carried out using full-matrix least-squares techniques with non-hydrogen atoms. All calculations were performed using the TEXSAN crystallographic software package of Molecular Structure Corporation.

EHMO Calculation. As a simple model of oxomolybdenum(IV) thiolate complexes having square pyramidal structure, a simplified molecule $[Mo^{IV}O(SH)_4]^{2-}$ in ideal *C*4 symmetry was adopted for the EHMO calculation. The basal geometrical parameters used are: 1.690 Å for one Mo-O, 2.415 Å for four Mo-S, 1.08 Å for four S-H, 107.7° for O-Mo-S angle, 116.24° for Mo-S-H angle on the basis of the crystal structure of $[Mo^{IV}O(S\text{-}p\text{-}C_6H_4Cl)_4]^{2-}$ having no-constrained structure. The EHMO parameters for Mo were taken from a reported work,[9] and those for S, O, and H are the standard ones.

Table I. Crystal and Refinement Data for $(PPh_4)_2[Mo^{IV}O(cdt)_2]\cdot MeCN$ (**1b**) and $(PPh_4)_2[Mo^{IV}O(1,3\text{-pdt})_2]$ (**4c**).

	1b	**4c**
Formula	$C_{54}H_{51}NOP_2MoS_4$	$C_{54}H_{52}NOP_2MoS_4$
Formula weight	1016.13	1003.13
Crystal system	orthorhombic	monoclinic
a, Å	10.230(3)	11.132(4)
b, Å	24.421(4)	15.650(6)
c, Å	19.958(4)	27.836(4)
β, °		92.46(2)
V, Å^3	4986(4)	4845(2)
Z	4	4
Space group	*P*bcn	*P*21
t, C°	23±1	23±1
Dcalcd, g/cm^3	1.353	1.375
Radiation	MoKa	MoKa
2θmax, °	55.1	55.1
Scan mode	ω	ω
No. of reflections measured		
Total	6393	12195
Unique	6393	11609 (Rint = 0.069)
No. of observns I>3σ(I)	1801	4078
No. of variables	279	637
R[a)]	0.049	0.057
*R*w[b)]	0.051	0.053

a) $R = \Sigma||Fo|-|Fc||/S|Fo|$.

b) $Rw = [\Sigma w(|Fo|-|Fc|)^2/\Sigma w|Fo|)^2]^{1/2}$; $w = 1/[\sigma^2(|Fo|)+0.34|Fo|+0.0048|Fo|^2]$.

Results and Discussion

Syntheses. Oxomolybdenum(IV) complexes having alkanedithiolate ligands were synthesized by the ligand exchange methods (method A and B) as equations (1) and (2).

Method A; $(NEt_4)_2[Mo^{IV}O(S\text{-}p\text{-}C_6H_4Cl)_4]$ + alkanedithiol

$\longrightarrow (NEt_4)_2[Mo^{IV}O(\text{alkanedithiolato})_2]$ + 4 HS-p-C_6H_4Cl (1)

Method B; $(NEt_4)_2[Mo^{IV}O(S\text{-}p\text{-}C_6H_4Cl)_4]$ + 2 Na_2-alkanedithiolate

$\longrightarrow Na_2[Mo^{IV}O(\text{alkanedithiolato})_2]$ + 2 $(NEt_4)(S\text{-}p\text{-}C_6H_4Cl)$

+ 2 $Na(S\text{-}p\text{-}C_6H_4Cl)$ (2)

It has been considered that these ligand exchange reactions proceed by (i) the chelate effect of the dithiolate ligands, and (ii) lower solubility of the product than that of the starting material. Although solubilities of **2** and **3** are higher than that of the starting material, these complexes and **1a** were synthesized by the method A. The complex $[Mo^{IV}O(1,3\text{-pdt})_2]^{2-}$ (**4**) was not synthesized by the method A, because of the weak nucleophilicity of sulfur atom of the 1,3-propanedithiol, and the higher solubility of **4**. This chelate complex was synthesized by the method B successfully, using disodium 1,3-propanedithiolate having the high nucleophilicity of the sulfur atom. **4a** produced in method B has the lower solubility than that of the starting complex. **4b** and **4c** were obtained by the exchange of the Na^+ cation to $(NEt_4)^+$ or $(PPh_4)^+$ cations, respectively (eq. 3).

$Na_2[Mo^{IV}O(1,3\text{-pdt})_2]$ + 2 ACl $\longrightarrow A_2[Mo^{IV}O(1,3\text{-pdt})_2]$ + 2 NaCl

(ACl = NEt_4Cl, PPh_4Cl) (3)

Since synthetic methods were limited, only a few reports of the monomeric oxomolybdenum(IV) complexes with alkanethiolate ligands exist. For example, as the complex having alkanedithiolate ligand, an ethanedithiolate complex $K_2[Mo^{IV}O(edt)_2]$ was reported to be synthesized by the reaction of $K_4[Mo^{IV}O_2(CN)_4]$ with 2 equiv. of the corresponding ligands in aqueous solution.[10] As the complexes containing alkanethiolate ligands, the oxomolybdenum(IV) complex having alkanethiolate and phosphorus ligands $[Mo^{IV}O(SCH_2CH_2PPh_2)_2]$ has been synthesized by the reaction between $[Mo^{VI}O_2(acac)_2]$ (acac = pentane-2,4-dionate) and excess $Ph_2PCH_2CH_2SH$ in methanol or toluene.[11] The oxomolybdenum(IV) complex having bulky ligand $[Mo^{IV}O(L\text{-}NS_2)]$ ($L\text{-}NS_2$ = 2,6-bis(2,2-diphenyl-2-mercaptoethyl)pyridine(2-))[12,13] and $[Mo^{IV}O(t\text{BuL-NS})]$ (*t*BuL-NS = bis(4-*tert*-butylphenyl)-2-pyridylmethanethiolato)[14,15] were synthesized by the reduction of the dioxomolybdenum(VI) complexes with PPh_3.

Recently, we reported the synthesis of $(NEt_4)_2[Mo^{IV}O(S\text{-}p\text{-}C_6H_4Cl)_4]$ by reduction of the corresponding oxomolybdenum(V) complex with NEt_4BH_4,[4] and showed that this complex is a convenient starting material for the syntheses of novel oxomolybdenum(IV) dithiolate complexes. Thus, $(NEt_4)_2[Mo^{IV}O(\alpha,2\text{-tdt})_2]$ was synthesized successfully in good yield by the ligand exchange reaction between $(NEt_4)_2[Mo^{IV}O(S\text{-}p\text{-}C_6H_4Cl)_4]$ and 2 equiv. of α,2-toluenedithiol in DME.[5]

1-4 were synthesized by the same or modified ligand exchange reaction. These complexes are not obtained by the direct reaction from the corresponding Mo(V) complexes with a convenient reductant, NEt_4BH_4, because of the negative Mo(V)/(IV) redox potentials.

Description of Structure of $(PPh_4)_2[Mo^{IV}O(edt)_2]$ (1b) and $(PPh_4)_2[Mo^{IV}O(1,3\text{-pdt})_2]$ (4c). Perspective views of anions of **1b** and **4c** are shown in Figure 1 and 2, respectively with numbering scheme. The selected bond distances, bond angles and torsion angles are presented in Table II.

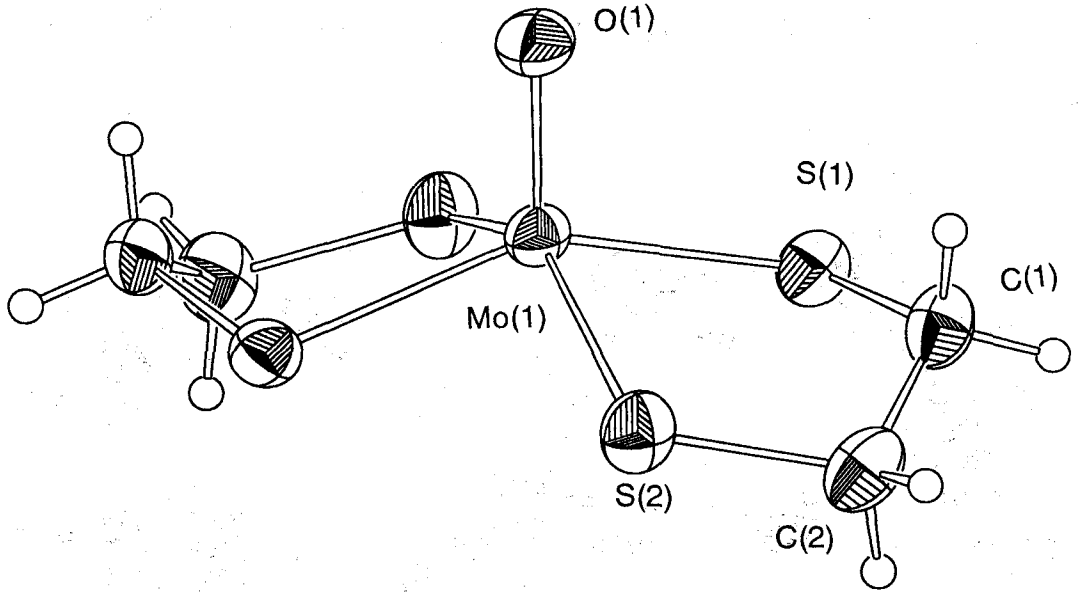

Figure 1. ORTEP drawing of anion part in $(PPh_4)_2[Mo^{IV}O(edt)_2]$ (**1b**) with 30 % probability ellipsoids.

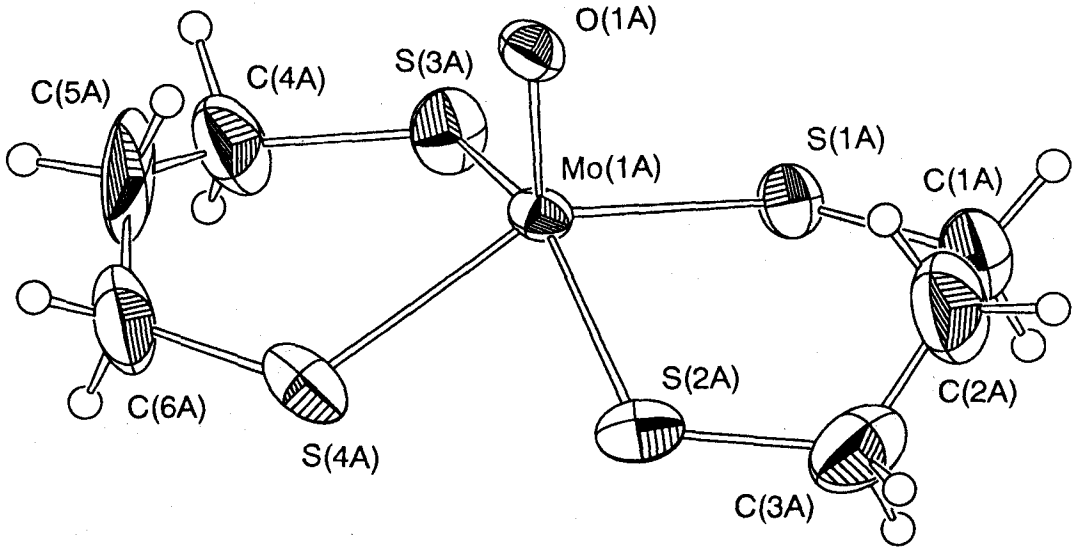

Figure 2. ORTEP drawing of anion part in $(PPh_4)_2[Mo^{IV}O(1,3\text{-pdt})_2]$ (**4c**) with 30 % probability ellipsoids.

Table II. Selected Bond Distances, Bond Angles, Torsion Angles, and Dihedral Angles of $(PPh_4)_2[Mo^{IV}O(edt)_2]\cdot MeCN$ (**1b**) and $(PPh_4)_2[Mo^{IV}O(1,3\text{-}pdt)_2]$ (**4c**).

	1b	**4c** (A)	**4c** (B)
	Bond Distances/Å		
Mo-O	1.693(7)	1.68(1)	1.69(1)
Mo-S(1)	2.400(3)	2.409(5)	2.413(5)
Mo-S(2)	2.377(1)	2.381(5)	2.390(5)
Mo-S(3)		2.400(6)	2.397(6)
Mo-S(4)		2.400(5)	2.399(5)
mean Mo-S	2.389	2.398	2.400
S(1)-C(1)	1.810(9)	1.78(2)	1.80(3)
S(2)-C(2)	1.85(1)	1.78(3)	1.84(2)
S(3)-C(3)		1.81(3)	1.77(3)
S(4)-C(4)		1.80(3)	1.80(3)
mean S-C	1.83	1.79	1.80
	Bond Angles/°		
S(1)-Mo-S(2)	86.04(7)	91.8(2)	91.9(2)
S(1)-Mo-S(3)	109.11(8)	77.5(2)	77.7(2)
S(2)-Mo-S(4)	86.04(7)	77.1(2)	77.4(2)
S(3)-Mo-S(4)	86.04(7)	91.1(2)	91.0(2)
S(1)-Mo-S(4)	148.0(1)	140.7(2)	144.8(2)
S(2)-Mo-S(3)	141.8(2)	146.4(2)	143.2(2)
O-Mo-S(1)	106.02(7)	107.9(4)	108.4(4)
O-Mo-S(2)	109.11(8)	106.8(4)	108.3(4)

O-Mo-S(3)	—	106.8(4)	105.4(4)
O-Mo-S(4)		111.3(4)	106.4(4)
mean O-Mo-S	107.57	108.2	107.1
Mo-S(1)-C(1)	102.3(3)	117.9(8)	114.0(8)
Mo-S(2)-C(2)	107.8(3)	114.6(9)	114.9(7)
Mo-S(3)-C(3)		116(1)	114.7(9)
Mo-S(4)-C(4)		115.7(9)	115.3(9)
mean Mo-S-C	105.1	116.1	114.7
	Torsion angles/°		
O-Mo-S(1)-C(1)	80.8(3)	72.2(9)	-77(1)
O-Mo-S(2)-C(2)	-98.7(4)	-89(1)	84(1)
O-Mo-S(3)-C(3)		-89(1)	83(1)
O-Mo-S(4)-C(4)		80(1)	-78(1)
deviation from 90° (mean)	9.0	7.5	9.5
distance of Mo			
from S4 plane	0.711	0.753	0.741

The complex molecule of **1b** has a crystallographic 2-fold rotational axis in the unit cell. The *C*2 axis lies through the Mo=O bond of anion and the terminal carbon atom of the acetonitrile molecule which is involved as crystalline solvent. Positions of the other two atoms of acctonitrile were solved as each atoms have 50 % occupancy.

There are two independent anions in the unit cell of **4c**, which have similar structures. Distinction between both anions in **4c** is made by the use of designation "A" and "B".

The geometry of $MoOS_4$ cores of **1b** and **4c** is based on a square pyramid with *C*4v symmetry as seen in other monomeric oxomolybdenum(V and IV) complexes having thiolate ligands. The two carbon atoms of edt ligands in **1b** have the sterically stable staggered conformation. The three carbon atoms of 1,3-pdt ligands in **4c** adopt boat-like conformation as seen in one of the conformers of cyclohexane.

The Mo=O bond distances of the complexes **1b** and **4c** are normal (1.693 (7) Å in **1b**, 1.68 (1) and 1.69 (1) Å in **4c**). These Mo^{IV}=O distances are longer than the Mo^{V}=O distances of the corresponding oxomolybdenum(V) complexes. It has been reported that the Mo^{V}=O distances of $(PPh_4)_2[Mo^{V}O(edt)_2]$[16] and $(PPh_4)_2[Mo^{V}O(1,3\text{-}pdt)_2]$[17] are 1.678 (5) and 1.667 (8) Å, respectively. The lengthening of Mo=O bond by reduction is shown in $[Mo^{IV/V}O(bdt)_2]^{2-/-}$ complexes[6] (1.699 (6) and 1.668 (3) Å), but not in $[Mo^{IV/V}O(\alpha,2\text{-}tdt)_2]^{2-/-}$ complexes (1.686 (4) and 1.688 (18) Å).[5,18].

The Mo-S bond distances of **1b** (av. 2.389 Å) and **4c** (av. 2.398 (A) and 2.400 (B) Å) are longer than those of the corresponding oxomolybdenum(V) complexes (av. 2.372 (3)[16] and 2.389 Å[17], respectively), because the HOMO orbital which is singly occupied in oxomolybdenum(V) and fully occupied in oxomolybdenum(IV) complexes is anti-bonding between *d*xy of Mo and *p*π of S atoms.[4,19] This tendency is consistent with the results of previous studies of oxomolybdenum(IV and V) complexes having bdt,[6] α,2-tdt,[5,18] and *o*-acylaminobenzenethiolate[20] ligands. The Mo-S bond distances of **1b** and **4c** are shorter than that of $(PPh_4)_2[Mo^{IV}O(S\text{-}p\text{-}C_6H_4Cl)_4]$ (av. 2.415 Å),[4] because of the strong *p*π donation and chelate effects of alkanedithiolate ligands.

1b has two types of Mo-S bonds as shown in Scheme 2. One of the Mo-S bonds, Mo-S(1) (2.400 (3) Å) is longer than the other Mo-S(2) (2.377 (3) Å). The longer Mo-S(1) bond has a shorter S(1)-C(1) bond (1.810 (9) Å vs. 1.85 (1) Å) and a smaller Mo-S(1)-C(1) bond angle (102.3 (3)°) compared with the other (107.8 (3)°).

Scheme 2

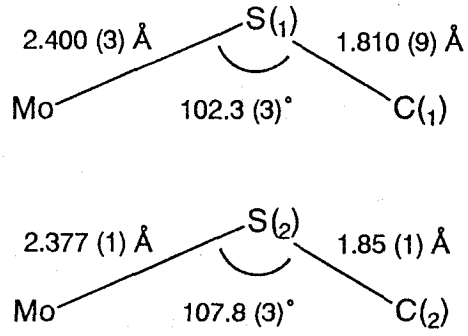

Previously, the relation between the M-S (Se) bond distance and M-S-C bond angle has been discussed by Ueyama et al. in the $[M^{II}(XPh)_4]^{2-}$ (M = Zn, Cd; X = S, Se) complexes.[21] They showed that the complexes with larger M-S-C bond angles have shorter (*i.e.* higher covalent) M-S bonds because of the stronger donation of $p\pi$ electron of S (Se) atoms to the metal ions. Similar results are found for the two Mo-S bonds of an anion in **1b**.

The intraligand S-Mo-S bond angles of **4c** (av. 91.5°, each A and B) are larger than those of **1b** (86.04 (7)°) or $(PPh_4)_2[Mo^{IV}O(S\text{-}p\text{-}C_6H_4Cl)_4]$ (av. 84.8°). This is a characteristic of 1,3-propanedithiolate ligand which forms a six-membered ring as compared with a five-membered ring of edt ligand or non-chelate ligand, $(S\text{-}p\text{-}C_6H_4Cl)^-$. Similarly, the intraligand S-Mo-S angle of $(NEt_4)_2[Mo^{IV}O(\alpha,2\text{-tdt})_2]$ with a six-membered chelate ring is also relatively large (av. 89.20°).[5]

In addition, **4c** has the relatively larger Mo-S-C bond angles (av. 116.1° (A), 114.7° (B)) compared with those of **1b** (av. 105.1°). Similar large Mo-S-C bond angles were also reported in $(NEt_4)_2[Mo^{IV}O(\alpha,2\text{-tdt})_2]$ (av. 111.1 °) or an oxomolybdenum(IV)

complex having no-chelating thiolate ligands; $(PPh_4)_2[Mo^{IV}O(S\text{-}p\text{-}C_6H_4Cl)_4]$ (av. 116.3°).

The O-Mo-S-C torsion angles of **1b** are 80.8 (3)° and -98.7 (4)° and of **4c** are in the range from (+ or -) 72° to 89°. The deviation from 90° of the torsion angles of **1c** (av. 9.0°) is similar to those of **4c** (av. 7.5° (A), 9.5° (B)). These deviations of the torsion angles from 90° of **1b** and **4c** are not large, since the mean value of $(PPh_4)_2[Mo^{IV}O(S\text{-}p\text{-}C_6H_4Cl)_4]$ is 6.6°, which has a non-constrained structure because of the coordination of monodentate thiolate. Our EHMO calculation showed that the O-Mo-S-C torsion angle is energetically the most stable at 90°. On the other hand the torsion angles of $(NEt_4)_2[Mo^{IV}O(\alpha,2\text{-tdt})_2]$ which has an asymmetric chelate ligand are -71.1° and 107.5°, and deviate considerably from 90° (av. 18.2°).[5]

Absorption Spectra. All the oxomolybdenum(IV) dithiolate complexes show a *d-d* transition band at 450 nm ~ 600 nm and a ligand to metal charge transfer (LMCT) band at 300 nm ~ 390 nm. The absorption spectrum of **4b** in MeCN is shown in Figure 3, and the numerical data of the other oxomolybdenum(IV) thiolate complexes are summarized in Table III. These *d-d* bands are assigned as a transition from *d*xy (HOMO) to degenerated orbitals, d_{xz} or d_{yz} (LUMO), so that the *d-d* transition energy reflects the energy gap between HOMO and LUMO orbitals.

The *d-d* transition bands of **1-3** appear in a similar region (478 ~ 480 nm). These results indicate that the energy gap is little affected by the electronic effect of the ligand. In contrast, **4b** shows a lower energy *d-d* transition band (528 nm) compared with those of **1-3**, indicating the energy gap between HOMO and LUMO of **4b** is smaller than those of **1-3**. The smaller energy gap of **4b** is thought to be not due to the electronic effect but to the steric effect of the 1,3-pdt ligand.

Our EHMO calculation suggests that the energy levels of HOMO and LUMO dynamically change according to the variation of O-Mo-S-C torsion angle, and showed that the energy gap is the largest at 90° of O-Mo-S-C torsion angle. Actually, the extremely high energy *d-d* transition band (457 nm) of $(NEt_4)_2[Mo^{IV}O(bdt)_2]$[6] is found at the O-Mo-S-C torsion angles of ca. 90°. The X-ray analysis results show that the

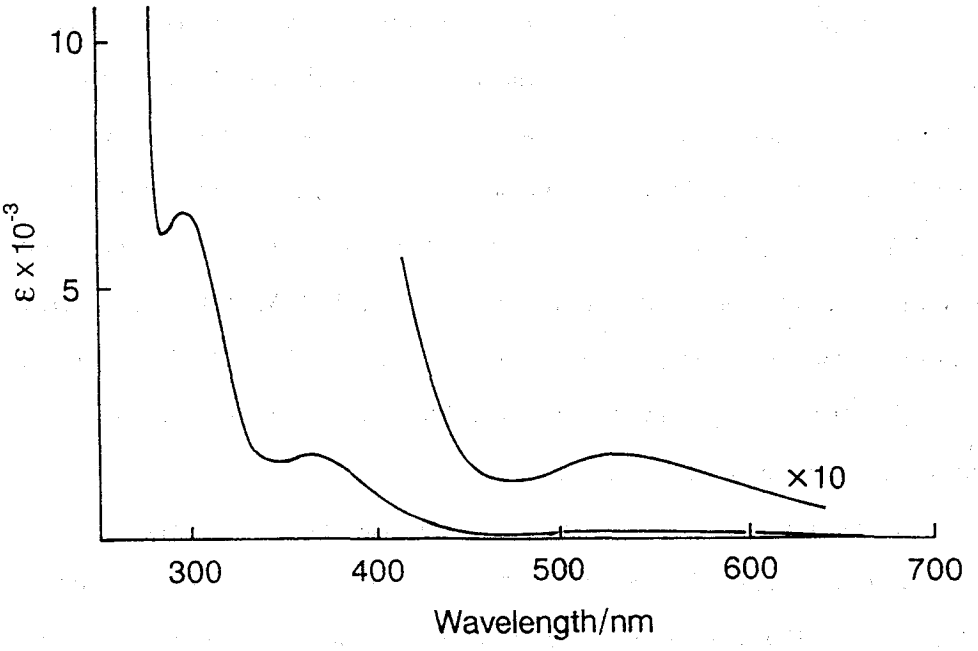

Figure 3. Absorption spectrum of $(PPh_4)_2[Mo^{IV}O(1,3\text{-pdt})_2]$ (**4b**) in MeCN solution (2 mM).

deviation from 90° of the O-Mo-S-C torsion angles is similar in **1b** and **4c**. As another factor explaining for the difference of HOMO-LUMO energy gap, we suggest the effect of Mo-S-C angle based on the EHMO calculation results. The calculation suggests that the energy gap decreases as the Mo-S-C bond angle changes from 105° to 115° (*vide infra*). Thus, the lower energy *d-d* transition band of **4** is expected to be caused by larger Mo-S-C bond angle (*ca.* 115°) compared with **1** (*ca.* 105°).

The complex $(NEt_4)_2[Mo^{IV}O(\alpha,2\text{-tdt})_2]$ shows the lower energy *d-d* transition band (588 nm) compared with $(NEt_4)_2[Mo^{IV}O(bdt)_2]$ (457 nm) or $(NEt_4)_2[Mo^{IV}O(edt)_2]$ (480 nm). This lower energy *d-d* transition is due to both the effects of O-Mo-S-C torsion angle and the relatively large Mo-S-C bond angles (av. 111.1°). The torsion angle of $(NEt_4)_2[Mo^{IV}O(\alpha,2\text{-tdt})_2]$ is considerably deviated from 90° (av. 18.2°) in all complexes studied here.

Table III. Absorption Parameters of Oxomolybdenum(IV) Thiolate Complexes.

Complex	*d-d* (ε)	LMCT (ε)
$(NEt_4)_2[Mo^{IV}O(S\text{-}p\text{-}C_6H_4Cl)_4]$	588 (480)	313 (29800)
$(NEt_4)_2[Mo^{IV}O(bdt)_2]$	457 (370)	324 (8100)
$(NEt_4)_2[Mo^{IV}O(\alpha,2\text{-}tdt)_2]$	588 (200)	385 (4200)
$(NEt_4)_2[Mo^{IV}O(edt)_2]$ (**1a**)	480 (250)	338 (1900)
$(NEt_4)_2[Mo^{IV}O(1,2\text{-}pdt)_2]$ (**2**)	480 (95)	360 (4200)
$(NEt_4)_2[Mo^{IV}O(2,3\text{-}budt)_2]$ (**3**)	478 (110)	360 (3800)
$(NEt_4)_2[Mo^{IV}O(1,3\text{-}pdt)_2]$ (**4b**)	528 (110)	363 (1740)

The complex $(NEt_4)_2[Mo^{IV}O(S\text{-}p\text{-}C_6H_4Cl)_4]$ also shows the lower energy *d-d* transition (588 nm).[6] This complex has relatively little deviated O-Mo-S-C torsion angles (deviation from 90° is av. 7.0°) and relatively large Mo-S-C bond angles (av. 116.3°). Although these parameters are similar to those of **4c**, this complex shows a lower energy *d-d* transition. This smaller *d-d* splitting is caused by the weaker ligand field of non-chelating arenethiolate ligands. Actually, the Mo-S bond distances of $(PPh_4)_2[Mo^{IV}O(S\text{-}p\text{-}C_6H_4Cl)_4]$ (av. 2.415 Å) are longer than those of **4c** (av. 2.398 (A) and 2.400 Å (B)).

Electrochemical Properties. The redox properties of the complexes **1-4** were studied using cyclic voltammetry (CV) in MeCN solution. The voltammogram of **4b** is shown in Figure 4. The electrochemical data of oxomolybdenum(IV) thiolate complexes thus studied are summarized in Table IV. All complexes displayed a quasi-reversible Mo(V)/Mo(IV) redox couple and irreversible oxidation to the Mo(VI) state. The complexes having alkanedithiolate ligands show a relatively more negative Mo(V)/Mo(IV) redox couple compared with those of the complexes having arenethiolate ligand, because of strong $p\pi$ donor character of the alkanethiolate ligands.

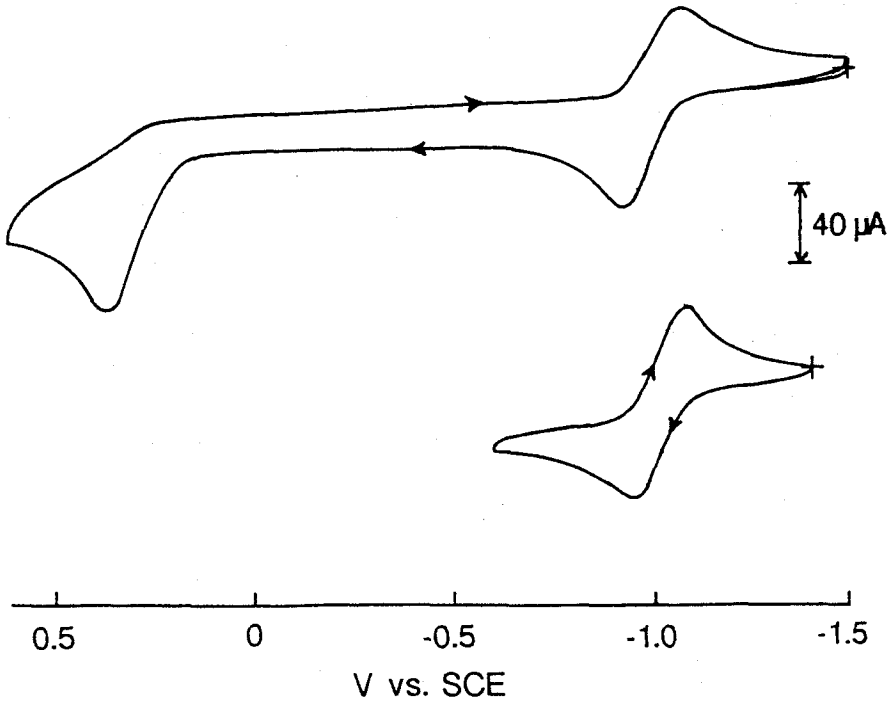

Figure 4. CV of $(PPh_4)_2[Mo^{IV}O(1,3\text{-pdt})_2]$ (**4b**) in MeCN (2 mM) solution.

The redox potentials of **2**-**4** show more negative Mo(V)/Mo(IV) redox couples compared with **1**. The negative couples for **2** and **3** are mainly due to the electronic effect of methyl substituents on the chelate ligands. **4b** has a more negative redox couple compared with **2** or **3**. This negative redox couple of **4b** is due not only to the electronic effect, but also to the steric effect of the 1,3-pdt chelate ligand.

The present Mo(V)/Mo(IV) electrochemical reaction is interpreted by removal of one electron from the HOMO orbital, and addition to the resulting single occupied SOMO orbital. Thus, the redox potential depends on the HOMO energy level. The EHMO calculation shows that the HOMO increases to the higher energy level as the O-Mo-S-C torsion angle deviates from 90°, or the Mo-S-C bond angle changes from 105° to 115° (*vide infra*). Because the deviation from 90° of the torsion angle of **1b** and **4c** is similar,

Table IV. Redox couples of Oxomolybdenum(IV) Thiolate Complexes in MeCN solution (2 mM) at 25 °C.

Complex	Mo(V)/Mo(IV)a)		Mo(VI)/Mo(V)a)
		ipa/ipc	
$(NEt_4)_2[Mo^{IV}O(S\text{-}p\text{-}C_6H_4Cl)_4]$	-0.65	1.00	0.54
$(NEt_4)_2[Mo^{IV}O(bdt)_2]$	-0.37	1.00	0.65
$(NEt_4)_2[Mo^{IV}O(\alpha,2\text{-tdt})_2]$	-0.74	0.98	0.65
$(NEt_4)_2[Mo^{IV}O(edt)_2]$ (**1a**)	-0.84	1.00	0.48
$(NEt_4)_2[Mo^{IV}O(1,2\text{-pdt})_2]$ (**2**)	-0.86	1.00	0.52
$(NEt_4)_2[Mo^{IV}O(2,3\text{-budt})_2]$ (**3**)	-0.92	1.00	0.48
$(NEt_4)_2[Mo^{IV}O(1,3\text{-pdt})_2]$ (**4b**)	-1.01	1.00	0.52

a) vs. SCE

it is concluded that the negative redox couple of **4** compared with **1**-**3** is mainly due to the larger Mo-S-C bond angles (av. 116.1° (A) and 114.7° (B) in **4c** and av. 105.1° in **1b**).

Enemark *et al.* reported that the 1,3-pdt or 1,4-propanedithiolato ligands give the negative Mo(IV)/Mo(V) redox couple compared with edt ligand in their oxomolybdenum(V) complexes $[\{BH(pyMe)_3\}Mo^{V}O(S_2R)]$ (S_2R = alkanedithiolato).[7] They suggested that this negative redox couple of the complex is due to the larger deviation of O-Mo-S-C torsion angle from 90°, or to the larger S-Mo-S bite angle. However, our conclusion is that the steric effect of the 1,3-pdt ligand is larger Mo-S-C bond angle, which affects the HOMO energy level, caused by the six-membered ring size.

Since the complex $(NEt_4)_2[Mo^{IV}O(\alpha,2\text{-tdt})_2]$ has one arenethiolate and one alkanethiolate ligands, the complex is expected to have an averaged redox potentials

between $(NEt_4)_2[Mo^{IV}O(bdt)_2]$ (- 0.37 V) and $(NEt_4)_2[Mo^{IV}O(edt)_2]$ (- 0.84 V). However, the complex $(NEt_4)_2[Mo^{IV}O(\alpha,2\text{-tdt})_2]$ shows a more negative Mo(V)/Mo(IV) redox couple (-0.74 V) than the average value (-0.61 V). The deviation of O-Mo-S-C torsion angles from 90° of this complex is relatively large (av. 18.2°), and the Mo-S-C bond angles are also relatively large (av. 111.1°). Thus, the negative Mo(V)/Mo(IV) redox couple observed in this complex is due to a combination of the both effects of the O-Mo-S-C torsion angle and Mo-S-C bond angle.

Raman Spectra. Raman spectra of **1-4** were measured with excitation at 514.5 nm. All complexes showed a sharp Mo^{IV}=O band in the range from 905 cm^{-1} to 935 cm^{-1}, and the data are summarized in Table V. Higher frequency shift of Mo^{V}=O band by an electronic effect was reported by Ellis *et al.* in their systematic study of oxomolybdenum(V) thiolate complexes.[22] They showed that the Mo^{V}=O band of $[Mo^{V}O(SAr)_4]^-$ is shifted to higher wave numbers by electron withdrawing substituents on the arenethiolate ligands. In the present study, **2-3** were found to have the lower Mo^{IV}=O bands compared with **1**, because of the electron donating effect of the methyl substituent. **4** has the slightly lower Mo^{IV}=O band (907 cm^{-1}) compared with that of **1** (910 cm^{-1}). This result shows that the Mo^{IV}=O band is not strongly affected by the steric effect of the 1,3-pdt ligand.

Our EHMO calculation suggests that the Mo^{IV}=O bond strength increases as the O-Mo-S-C torsion angle deviates from 90°. Higher Mo^{IV}=O stretching band (922 cm^{-1}) of $(NEt_4)_2[Mo^{IV}O(\alpha,2\text{-tdt})_2]$ among the related oxomolybdenum(IV) dithiolato complexes is thus ascribed to the deviated torsion angle.

NMR Spectra. Since all the known oxomolybdenum(IV) dithiolate complexes are diamagnetic, NMR spectral measurements are useful for the study of their solution structure. The ^1H and ^{13}C NMR spectra of **1-4** are shown in Figure 5 and 6. The solvents for **1** and **4a** were MeCN-d_3 and D_2O. The other complexes were measured in MeCN-d_3/MeOH-d_4 (9/1). All the measurements were carried out at 30 °C in the presence of about 0.1 equiv. of NEt_4BH_4 (or $NaBH_4$ for **4a**) to reduce the contaminated paramagnetic Mo(V) species formed by one-electron oxidation of the

Table V. Raman Spectral Data of Oxomolybdenum(IV) Thiolate Complexes.

Complex	ν(Mo=O) / cm-1	
	Mo(IV) complex	Mo(V) complex
$(NEt_4)_2[Mo^{IV}O(S\text{-}p\text{-}C_6H_4Cl)_4]$	932	942
$(NEt_4)_2[Mo^{IV}O(bdt)_2]$	905	944
$(NEt_4)_2[Mo^{IV}O(\alpha,2\text{-}tdt)_2]$	922	940
$(NEt_4)_2[Mo^{IV}O(edt)_2]$ (**1a**)	910	925
$(NEt_4)_2[Mo^{IV}O(1,2\text{-}pdt)_2]$ (**2**)	903	
$(NEt_4)_2[Mo^{IV}O(2,3\text{-}budt)_2]$ (**3**)	905	
$(PPh_4)_2[Mo^{IV}O(1,3\text{-}pdt)_2]$ (**4c**)	907	930

Mo(IV) complexes with trace amounts of air. A considerable broadening of signals of the complexes was observed by the effect of Mo(V) species in the absence of suitable reductants. The sharp signals of **1a** were obtained after about 1 week from the preparation of the solution in the presence of 0.1 equiv. of NEt_4B_4. On the other hand, for the other complexes having more negative Mo(V)/Mo(IV) couple, except for **4a**, the addition of MeOH-d_4 were necessary to obtain the sharp signals, since the reducing power of BH_4^- is enhanced in the protic solution like MeOH or H_2O. The similar NMR characteristics have been reported for the complex $(NEt_4)_2[Mo^{IV}O(\alpha,2\text{-}tdt)_2]$.[5]

1a shows the twenty-two sharp NMR signals arising from four types of methylene protons centered at 2.26 ppm with AA'BB' quartets. A singlet of methylene carbon is observed at 36.10 ppm in the no ^1H decoupled ^{13}C NMR spectrum of this complex.

^1H-^1H NOESY and ^1H-^1H, ^1H-^{13}C COSY 2D NMR spectra were effective for the assignments of NMR signals in **2** and **4**.

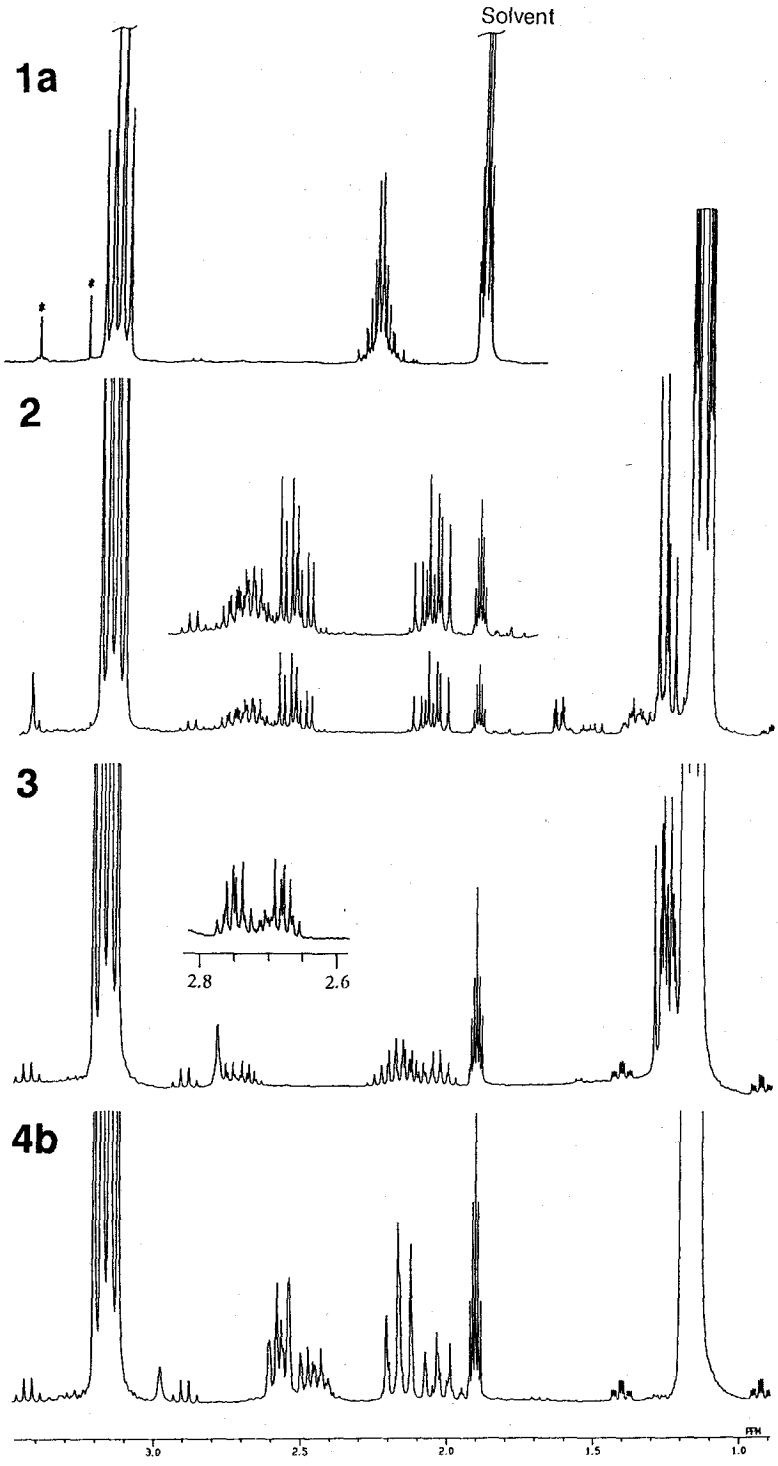

Figure 5. ^{1}H NMR spectra of oxomolybdenum(IV) complexes **1**-**4** in MeCN-*d*3 at 30°C.

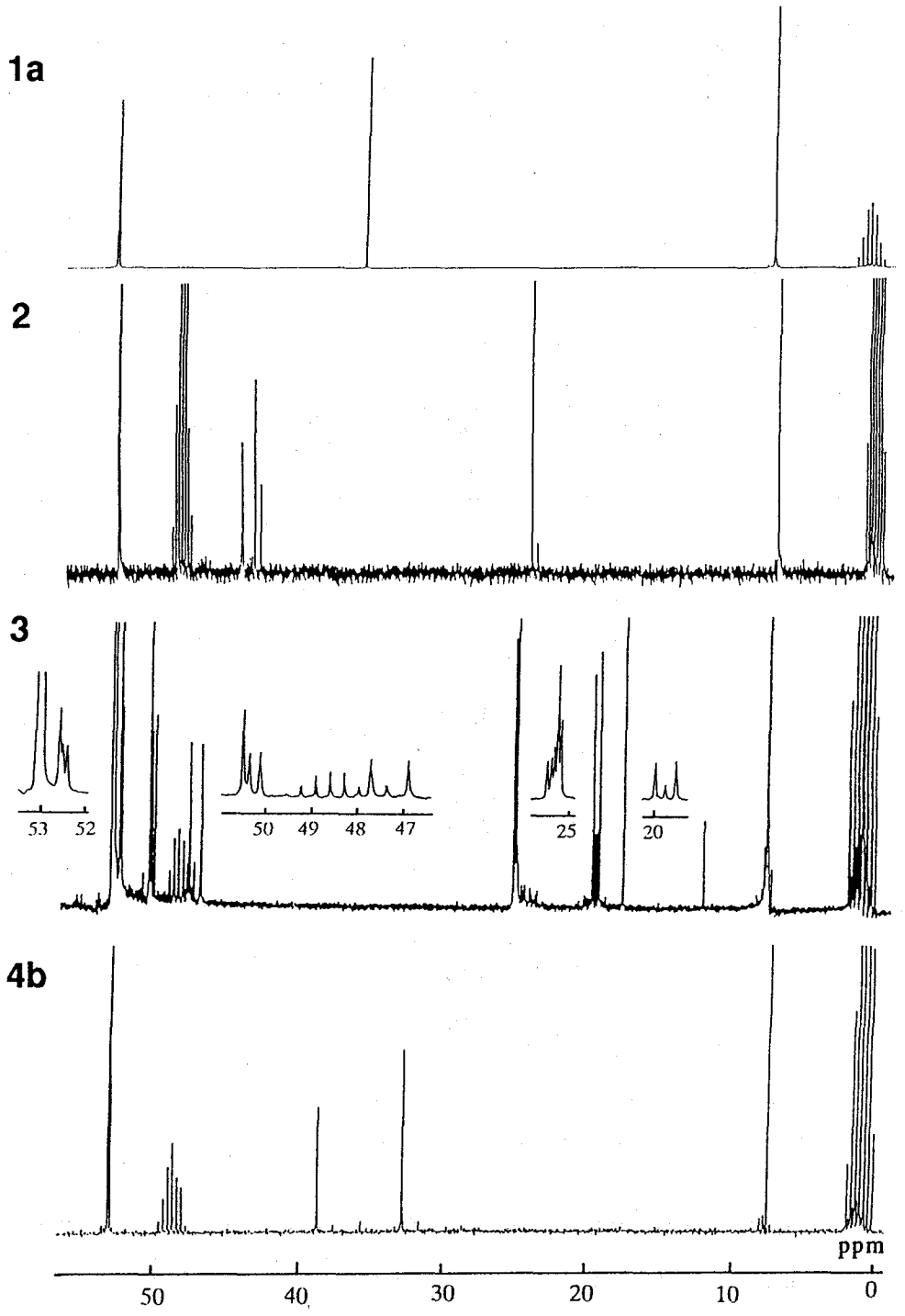

Figure 6. ^{13}C NMR spectra of oxomolybdenum(IV) complexes **1-4** in MeCN-*d*3 at 30°C.

The existence of the isomers is expected for **2** and **3** because both complexes have one or two chiral carbon atoms in their ligand skeletons. For example, the four conformational isomers, A - D, are possible for the 1,2-pdt ligand for **2** as shown in Scheme 3.

Scheme 3

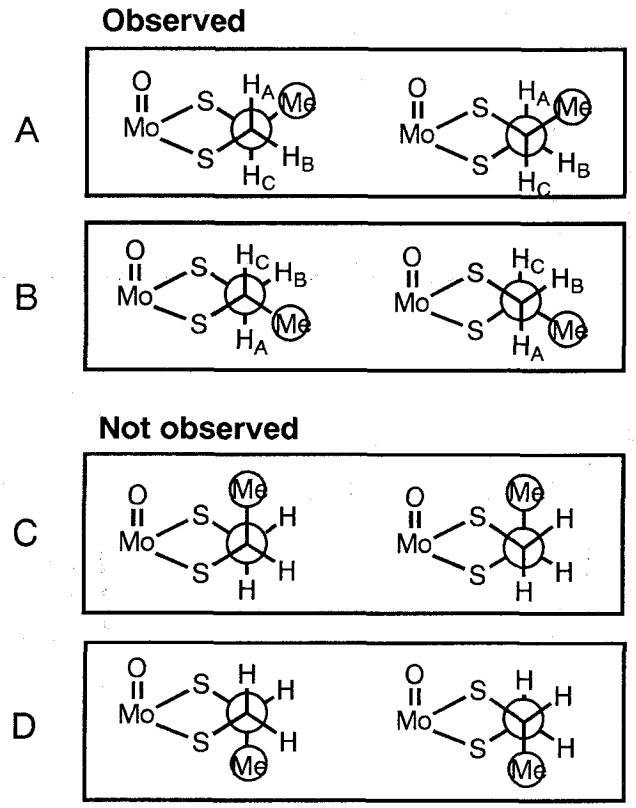

Two sets of ^{1}H NMR signals assignable to 1,2-pdt ligand of **2** were observed with similar coupling patterns and at similar regions, and were distinguished by the prime. The ^{1}H-^{1}H COSY and NOESY 2D NMR spectra of **2** are shown in Figure 7 with atom labeling scheme. Among all proton signals of the 1,2-pdt ligand, NOE were observed in the phase sensitive ^{1}H-^{1}H NOESY 2D NMR spectrum. The parameters of

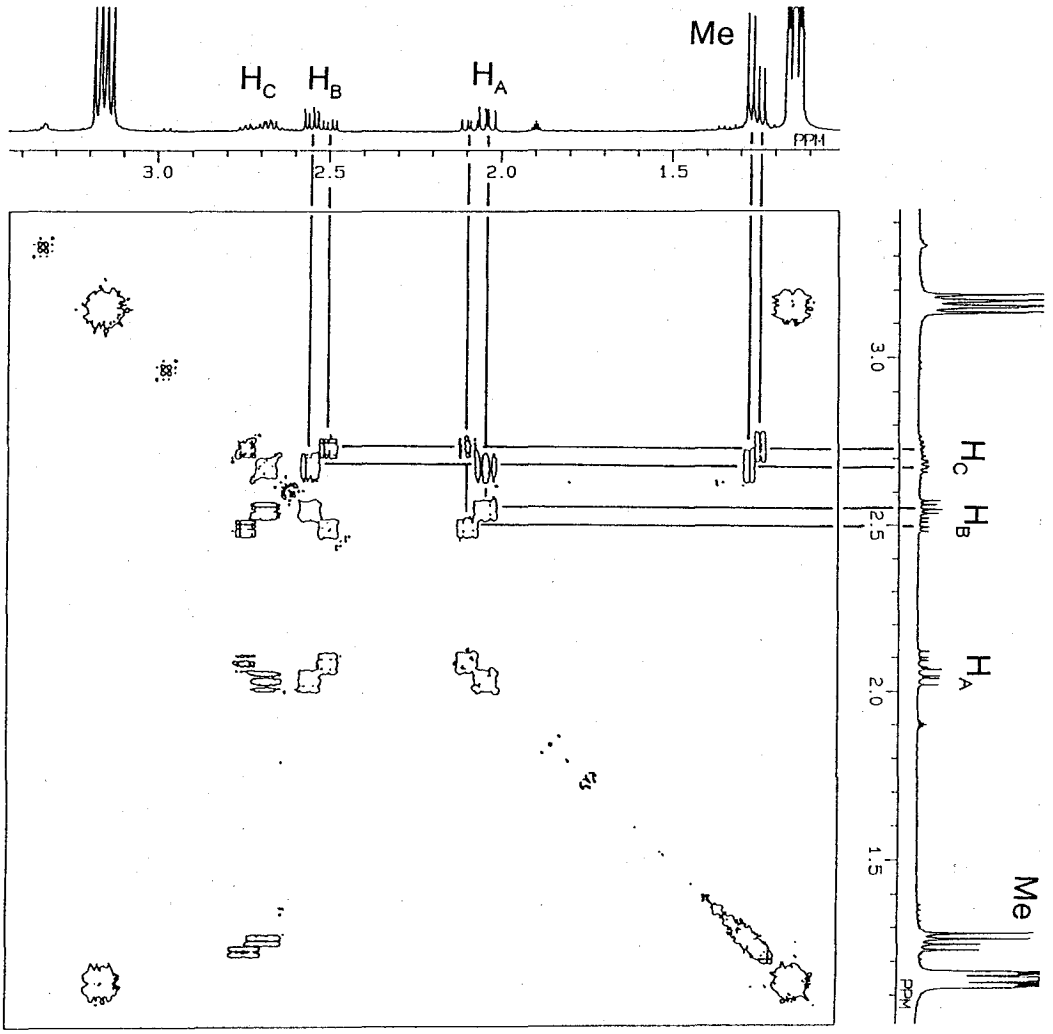

Figure 7a. The ^{1}H-^{1}H COSY 2D NMR spectrum of **2** in MeCN-d_3/MeOH-$d4$ (9/1) at 30°C

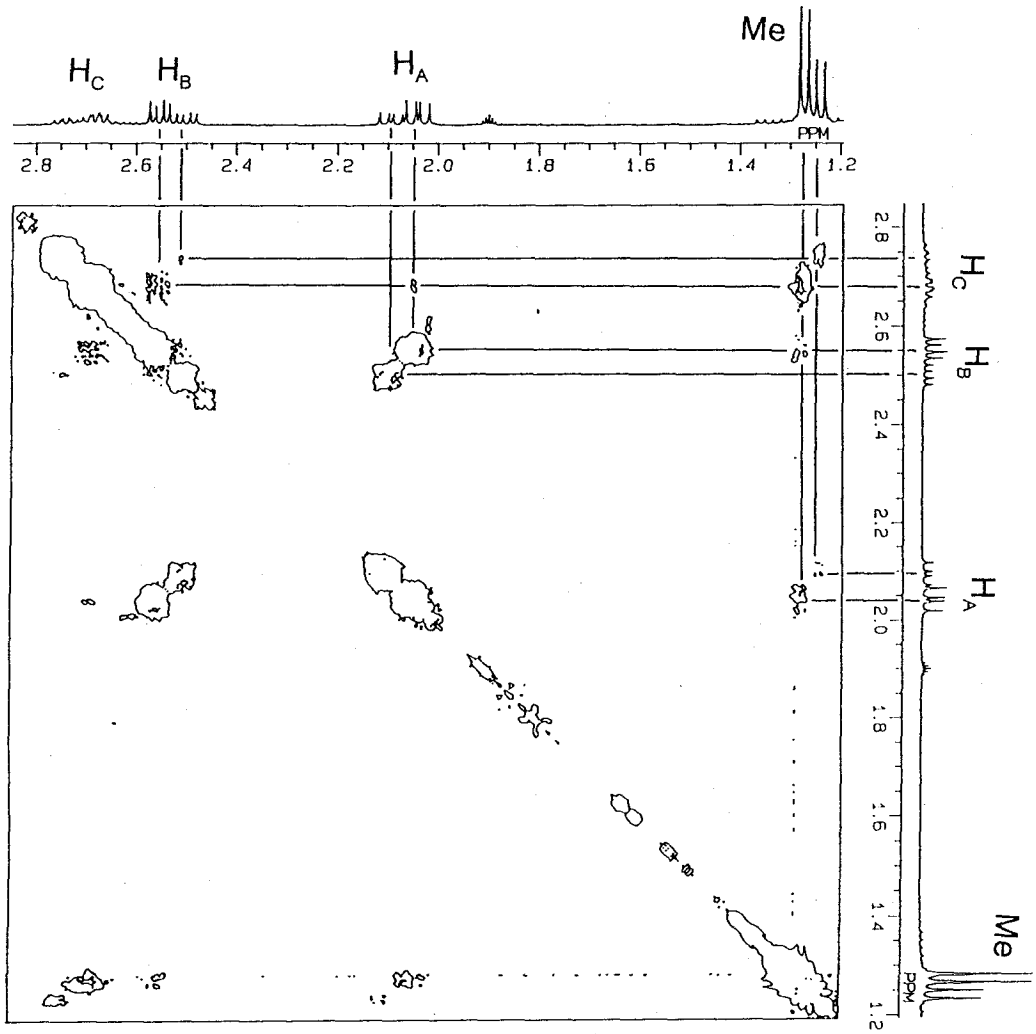

Figure 7b. The ^{1}H-^{1}H NOESY 2D NMR spectrum of **2** in MeCN-d_3/MeOH-$d4$ (9/1) at 30°C

assignable 1,2-pdt ligand protons of each conformer are i) H_A;2.04, H_B;2.55, H_C;2.69, and H_D (Me, 3H);1.27 ppm, JH_A-H_B;10.7, JH_A-H_C;7.6, JH_B-H_C;4.9, JH_C-H_D;6.6 Hz, and ii) H_A';2.10, H_B';2.50, H_C';2.74, and H_D' (Me, 3H);1.24 ppm, JH_A'-H_B';10.8, JH_A'-H_C';7.1, JH_B'-H_C';4.9, JH_C'-H_D';6.6 Hz.

H_C protons showed the cross peaks with methyl H_D protons in ^1H-^1H COSY spectrum. Relatively intense NOE between the methyl H_D protons and the two HA, H_B protons, and the weakest NOE between H_A and H_C protons indicate the methyl substituents occupy the equatorial position in the ligand skeleton. Thus, the existence of two conformational isomers A and B shown in Scheme 3 was proposed. Stronger NOE between H_B and H_C protons compared with that between H_A and H_C protons is consistent with these proposed conformers. Preferences of methyl groups to the equatorial positions are caused by the repulsion between the methyl group and the filled $p\pi$ orbital of the sulfur ligand. The configuration isomer between two intra-molecular ligands as seen in $(NEt_4)_2[Mo^{IV}O(\alpha,2\text{-tdt})_2]$[5] is not detected in these NMR measurements of **2**.

The assignment of ^{13}C signals of 1,2-pdt ligand of **2** was carried out by using ^1H-^{13}C COSY 2D NMR spectrum. The assignable ^{13}C signals of 1,2-pdt ligand of **2** were observed at 44.58 ppm for C_B, 44.53 ppm for C_B', 43.71 ppm for C_A, 43.30 ppm for C_A', and 24.67 ppm for both Me carbon atoms, where numbering scheme of C_A and C_B is shown in Scheme 4.

Scheme 4

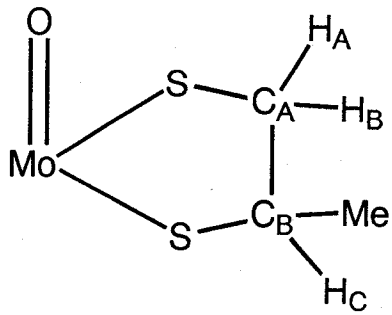

The methylene proton signals of **4b** were observed at 2.77 (2 ^{1}H) for H_B, 2.64 (1 ^{1}H) for H_D, 2.41 (2 ^{1}H) for H_A, and 2.13 ppm (1 ^{1}H) for H_C in the 1H NMR spectrum measurement. The ^{13}C signals of the 1,3-pdt ligand of **4b** were observed at 32.92 and 38.74 ppm, which were assigned to C_A and C_B carbons, respectively. The labels of carbon and hydrogen atoms for the assignments of the NMR spectra were shown in Scheme 5.

Scheme 5

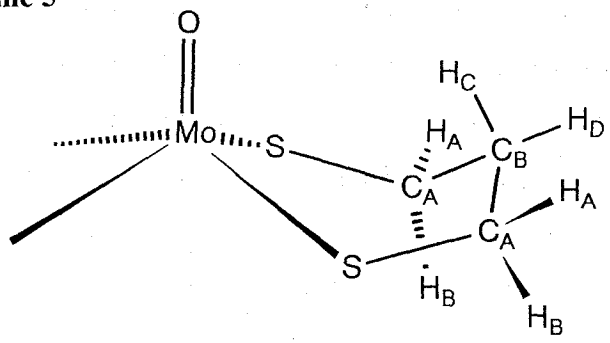

The 1,3-pdt ligand of **4a** shows the similar ^{1}H and ^{13}C NMR signals in D_2O in the presence of about 0.1 equiv. of $NaBH_4$. 2D NMR measurements for the assignment of those signals were carried out using the saturated solution of **4a**.

^{1}H-^{13}C COSY 2D NMR spectrum of **4a** shows that the C_A atom bonds to the H_A and H_B atoms, and C_B atom bonds to H_C and H_D atoms. Intense NOE between signals of H_A and H_D protons, and weak NOE between H_A and H_C protons were observed by phase sensitive ^{1}H-^{1}H NOESY 2D NMR spectrum. The X-ray crystallographic result shows that the distances of eight H_A - H_C are about 0.1 to 0.2 Å longer than those of H_A - H_D.

All the conformational isomers possible in a 2,3-budt ligand were observed in the spectrum of **3**. Four kinds of octet (doublet-quartet) protons of 2,3-budt ligand are observed in ^{1}H NMR spectrum of **3**. The full assignments of these signals were not achieved in spite of the measurements of 2D NMR spectra because diagonal noises concealed the cross peaks between proton signals at 1.9 ~ 2.2 ppm, and the overlap of

signals expected for the three methyl protons with $(NEt_4)^+$ protons at 1.12 ~ 1.17 ppm. However, distinctive eight ^{13}C signals of methyl groups were observed in the ^{13}C NMR spectrum (Figure 6), indicating that the existence of all possible four conformational isomers of 2,3-budt ligand of **3** in solution. Structural isomers of **2** and **3** shown by ^1H, ^{13}C NMR spectra were not detected by the other spectra (absorption and Raman) and CV measurements.

The present experiments show that NMR measurements are highly useful for the study of solution structure of oxomolybdenum(IV) alkanedithiolate complexes. The sharp ^1H NMR signals and the 2D NMR results of **1-4** suggest that these complexes have rigid chelating skeletons in solution at 30°C. Similar rigidity of the dithiolate ligands coordinated to the oxomolybdenum(IV) complex was already shown in the case of $(NEt_4)_2[Mo^{IV}O(\alpha,2\text{-tdt})_2]$. A quite different chemical shift of the methylene protons, CH_AH_B, was observed for this complex with an AB doublet at 2.59 and 3.92 ppm. The X-ray structure of the complex $(NEt_4)_2[Mo^{IV}O(\alpha,2\text{-tdt})_2]$ showed that this difference of the chemical shift is due to the higher shielding effect of the benzene ring of the α,2-tdt ligand to one of the methylene protons.[5]

Reaction with Oxo-Donor Reagents. All the above Mo(IV) complexes readily react with dioxygen in MeCN solution to give intense blue or purple solutions. The products have been identified as the corresponding monomeric monooxomolybdenum(V) complexes, $[Mo^{V}O(alkanedithiolato)_2]^-$, by the measurements of absorption spectra or ESR spectra.

1-4 do not react with DMSO, pyridine-*N*-oxide (PyO), and trimethylamine-*N*-oxide (Me_3NO) in MeCN or DMF at room temperature. Similar low reactivity to the oxo-donor reagents has also been reported for $(NEt_4)_2[Mo^{IV}O(\alpha,2\text{-tdt})_2]$.[5]

In general, oxomolybdenum(IV) complexes react with oxo-donor reagents such as O_2, DMSO, PyO, and Me_3NO, to produce the corresponding dioxomolybdenum(VI) complexes.[23] Recently, this oxo-transfer reaction with Me3NO was found to be a superior synthetic method for the dioxomolybdenum(VI) thiolate complexes. Thus, Yoshinaga *et al.* reported the synthesis of $[Mo^{VI}O_2(bdt)_2]^{2-}$ by the reaction between

$[Mo^{IV}O(bdt)_2]^{2-}$ and Me_3NO.[24] Attempts at the synthesis of dioxomolybdenum(VI) complexes having thiolate ligands by the direct reaction of $(Mo^{VI}O_4)^{2-}$ ion with free thiols have been unsuccessful, because the Mo(VI) ion is easily reduced to Mo(V) or Mo(IV) state by the thiols.[25]

For oxidation of the oxomolybdenum(IV) complexes with the oxo-donor reagents, two mechanisms have been proposed based on kinetic studies. Holm *et al.* suggested that the production of the intermediate, $[Mo^{IV}O(LNS_2)(X)]$ (X = R_2SO or NO_3^-) at the first step in the reaction between R_2SO or NO_3^- and $[Mo^{IV}O(LNS_2)(dmf)]$[13,26] which has a vacant coordination site. On the other hand, Roberts *et al.* proposed the dissociation of the S_2PONR_2 ligand to be the first step in the reaction between $[(HBpyMe_2)Mo^{IV}O(S_2PONR_2)]$ and Me_2SO.[27]

Recently, we reported that the asymmetric dithiolate complex, $(NEt_4)_2[Mo^{IV}O(\alpha,2\text{-tdt})_2]$, exhibits an unexpectedly low reactivity to the oxo-donor reagents such as dimethylsulfoxide (DMSO), PyO, and Me_3NO.[5] From the X-ray analysis of this complex, two possibilities were proposed for the low reactivity, *i.e.* i) the small S-Mo-S (trans) bite angle of two alkanethiolate ligands prevents the coordination of oxo-donor reagents to the position trans to Mo=O, or ii) strong Mo-S (alkanethiolate) bond prevents the rearrangement from trans-dioxo octahedral structure to the cis-dioxo octahedral structure. (Scheme 6)

Scheme 6

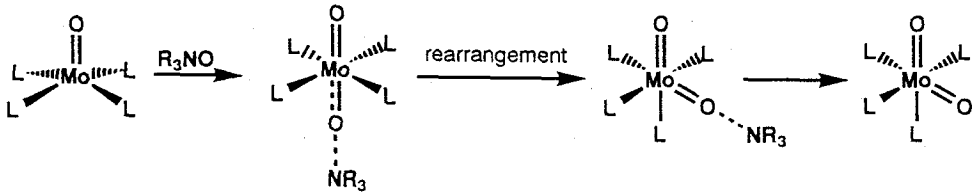

Except for $(NEt_4)_2[Mo^{IV}O(S\text{-}p\text{-}C_6H_4Cl)_4]$ and $(NEt_4)_2[Mo^{IV}O(bdt)_2]$, all the other complexes examined by us do not react with Me_3NO in MeCN or in DMF at room temperature. The S-Mo-S bite angles of **1b** and **4c** are larger (ca. 141° and ca. 144°) than

that of $(NEt_4)_2[Mo^{IV}O(\alpha,2\text{-tdt})_2]$ (ca. 135°)[5], and similar to that of $(NEt_4)_2[Mo^{IV}O(bdt)_2]$ (av. 143.7(1)°).[6] The results suggest that the inertness of **1**-**4** to Me_3NO is not due to the S-Mo-S bite angles.

Actually, the complex $[Mo^{IV}O(S\text{-}p\text{-}C_6H_4Cl)_4]^{2-}$ having weak Mo-S bonds (av. 2.415 Å) readily reacts with excess PyO, Me_3NO, and O_2 in MeCN to give intense blue solutions in 1 min, which turn its color to yellow 1 h. This complex also reacts with excess DMSO slowly in DMSO or MeCN solution to produce a yellow solution in a few hours. All these yellow solutions have an absorption maximum at about 310 nm. Similar ^1H NMR spectra were observed in these yellow reaction products, which showed two doublets at 7.2 and 7.4 ppm assignable to *p*-chlorobenzenethiolate ligand. These oxidation reaction products showed similar CV patterns in MeCN, which is an irreversible reduction at -1.52 V and an irreversible oxidation at +0.55 V (vs. SCE). Although the yellow products obtained by those oxidation reactions are too labile to be isolated and purified, their physical properties suggest that the yellow products are monomeric *cis*-dioxomolybdenum(VI) complexes, perhaps $[Mo^{VI}O_2(S\text{-}p\text{-}C_6H_4Cl)_4]^{2-}$.

The S-Mo-S (trans) bond angles (av. 144.6°) of $(PPh_4)_2[Mo^{IV}O(S\text{-}p\text{-}C_6H_4Cl)_4]$ are close to those found in **1b** (av. 144.9°) and **4c** (av. 144.0°). Thus, the differences of the reactivities between $[Mo^{IV}O(S\text{-}p\text{-}C_6H_4Cl)_4]^{2-}$ and **1**-**4** are not due to the S-Mo-S bond angle, but likely due to the Mo-S bond strengths.

These results show that the reactivities of oxomolybdenum(IV) thiolate complexes with oxo-donor reagents, such as amine-*N*-oxides, are controlled by the Mo-S bond strengths. Most probable reason for the low reactivity of **1**-**4** to the oxo-donor reagents is that a combined effect of the strong Mo-S bonds and the resulting rigid structures inhibits the structural rearrangement (trans → cis) from the species containing *trans*-O=Mo-($ONMe_3$) or *trans*-O=Mo=O coordination to the corresponding *cis* structures.

EHMO Calculation. In order to understand the differences in steric effects of thiolate ligands on physical properties of the oxomolybdenum(IV) complexes **1**, **4**, and $(NEt_4)_2[Mo^{IV}O(\alpha,2\text{-tdt})_2]$, preliminary EHMO calculation of $[Mo^{IV}O(SH)_4]^{2-}$ was carried out. Based on the differences of their molecular structures between **1b** and **4c**,

effect of the three steric parameters, O-Mo-S-C torsion angle, S-Mo-S bite angle, and Mo-S-C bond angle, were examined.

The importance of O-Mo-S-C torsion angle on the physical properties has been pointed out for some of oxomolybdenum(V) thiolate complexes.[7,8,19] For example, Enemark et al. reported the relationship of the torsion angle on absorption spectra and redox properties for a series of mono-oxomolybdenum(V) complexes, e.g. $[\{BH(pyMe)_3\}Mo^{V}O(S_2R)]$.[7] Ueyama et al. have also reported the synthesis and properties of oxomolybdenum(V) peptide complexes having unusual torsion angles (ca. 0°).[8] We performed an EHMO calculation for the qualitative studies to understand steric effect of the thiolate ligands on the physical properties in oxomolybdenum(IV) complexes based on the molecular structures of **1b** and **4c**.

Figure 8 shows the variation of HOMO and LUMO energy levels according to the change of the O-Mo-S-C torsion angle, Mo-S-C bond angles, and S-Mo-S bite angles with schematic models used for these calculations.

i) Effect of O-Mo-S-C torsion angle. The HOMO is anti-bonding between *d*xy of Mo and *p*π of the sulfur ligand in the oxomolybdenum(IV) complexes. The LUMO is anti-bonding between d_{xz}, d_{yz} of Mo and *p*π of the terminal oxo ligand. Since the contribution of HOMO which has the smallest anti-bonding character at θ = 90°, the total energy of $[Mo^{IV}O(SH)_4]^{2-}$ has a minimum at θ = 90° and has two maxima at θ = 0° and 180°. These results show that the energy difference between HOMO and LUMO has minima at θ = 0° and 180°, and a maximum at θ = 90°.

The overlap populations of Mo-O and Mo-S bonds also change according to the variation of θ. (Figure 9) The overlap population of Mo-O has a minimum at θ = 90° and maxima at θ = 0° and 180°. On the contrary Mo-S has a maximum at θ = 90° and minima at θ = 0° and 180°. The opposing relation of Mo-O and Mo-S overlap populations shown in Figure 9 is due to the repulsion between filled *p*π on terminal O atom and filled bonding orbitals formed between of d_{xz}, d_{yz} of Mo and *p*π on the sulfur.

ii) Effect of Mo-S-C bond angle. The increase of the Mo-S-C bond angles is expected in the six-membered chelate ring compared with the five-membered

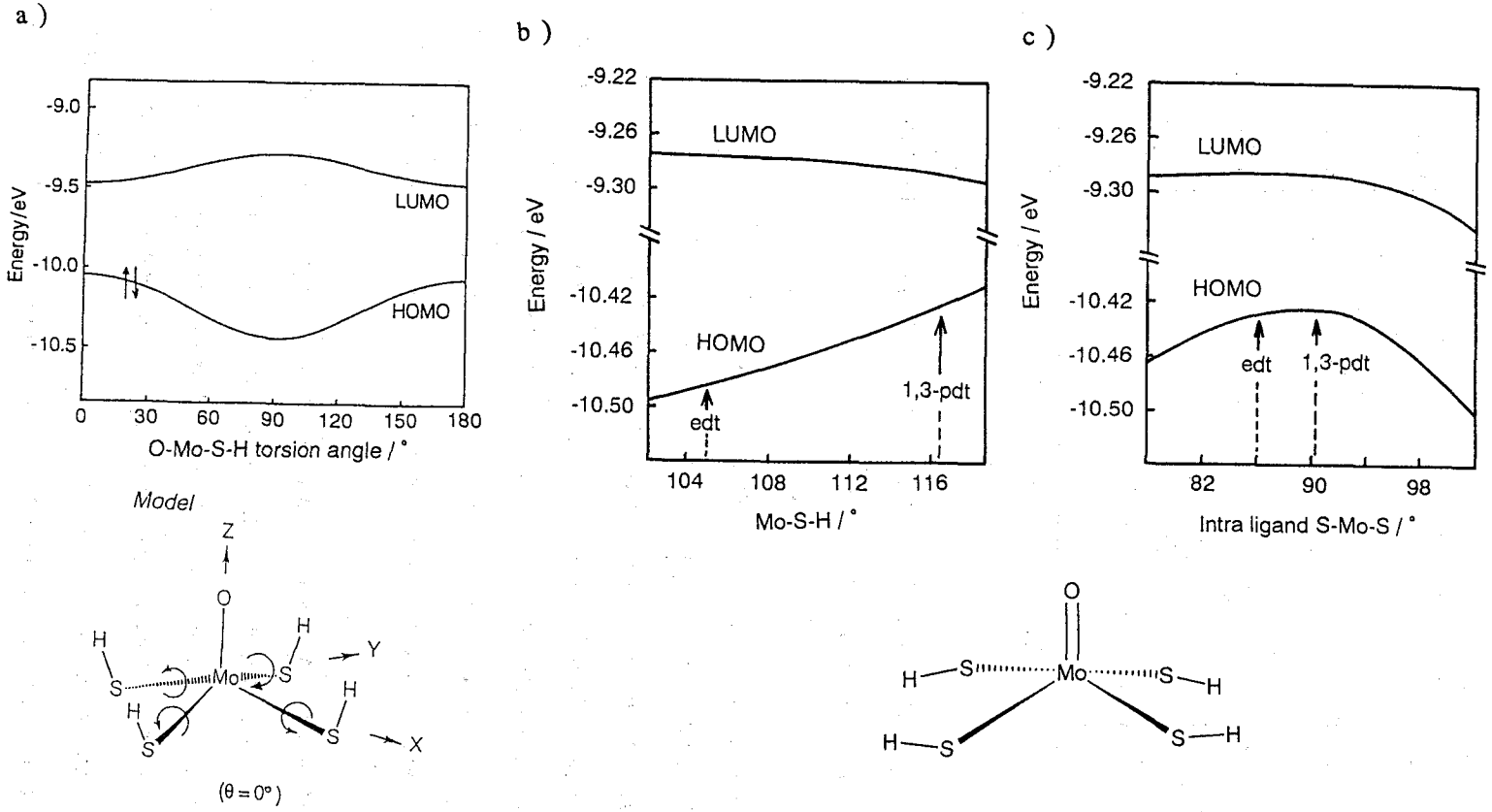

Figure 8. a) The variation of energy levels of HOMO and LUMO of $[Mo^{IV}O(SH)_4]^{2-}$ with the change of O-Mo-S-C torsion angle/θ. b) The variation of energy levels of HOMO and LUMO of $[Mo^{IV}O(SH)_4]^{2-}$ with the change of Mo-S-C bond angle/ψ. c) The variation of energy levels of HOMO and LUMO of $[Mo^{IV}O(SH)_4]^{2-}$ with the change of S-Mo-S bite angle/ϕ.

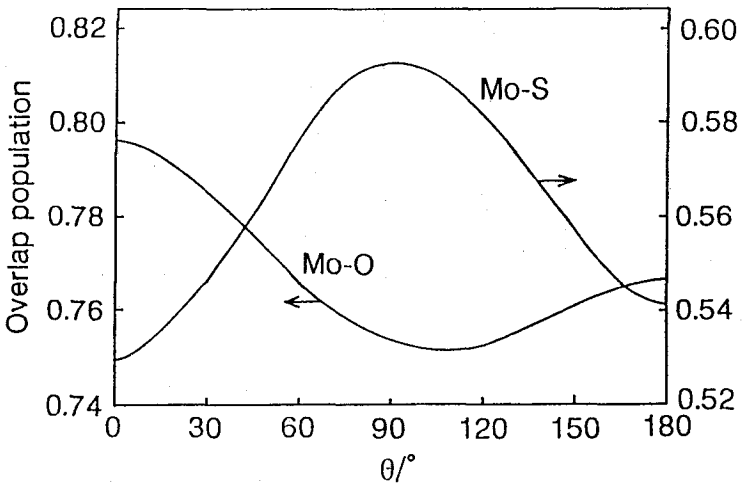

Figure 9. The overlap populations of Mo-O and Mo-S bonds of $[Mo^{IV}O(SH)_4]^{2-}$ with the changes of the O-Mo-S-C torsion angle.

chelate ring. For example, the mean Mo-S-C bond angles of **4c** (115.4°) and $(NEt_4)_2[Mo^{IV}O(\alpha,2\text{-tdt})_2]$ (111.1°) are larger than that of **1b** (105.1°). Our present calculation suggests that the energy gap between HOMO and LUMO varies according to the change of the Mo-S-C bond angle as shown in Figure 8b. The results show that the energy gap between HOMO and LUMO decreases as the Mo-S-C bond angle changes from 105° to 115°. This is mainly due to the increase of $p\pi$ component of the sulfur at 115° of Mo-S-C bond angle compared with at 103°, which results in the higher energy HOMO level.

iii) Effect of S-Mo-S bond angle. It is generally true that the five-membered chelate has smaller chelating bite angle than the six-membered chelate. Figure 8c shows the variation of HOMO and LUMO energy level according to the change of the S-Mo-S bite angle. The variation of the energy gap between HOMO and LUMO of the S-Mo-S bond angle change is relatively smaller than that of the Mo-S-C bond angle change (Figure 8b). The results suggest the shift of the *d-d* transition between **1** and **4** is due to the change of the Mo-S-C bond angles.

Conclusion.

The oxomolybdenum(IV) complexes having alkanedithiolate chelating ligands **2**-**4** were synthesized and characterized by absorption, Raman, and NMR spectra and CV measurements. The structures of the complexes **1b** and **4c** were determined by the X-ray crystallography. The complex **4** shows the negative shift of Mo(V)/Mo(IV) redox couple than that is expected in electronic effect observed in **2** and **3**. This chelating size effect of the six-membered ring compared with the five-membered chelate mainly arise from the larger Mo-S-C bond angle. Our EHMO calculation showed that the energy level of HOMO and LUMO is largely affected by the O-Mo-S-C torsion angle and Mo-S-C bite angle. The typical deviated torsion angle or bite angle are achieved in the oxomolybdenum(IV) complex having α,2-tdt ligand.

Acknowledgment. We are grateful to Prof. Kazuyuki Tatsumi of Nagoya University for his help in discussions of the EHMO calculations.

References

(1) *Molybdenum Enzymes*; Spiro, T. G., Ed.; John-Wiley: New York, 1985.

(2) Barber, M.; Neame, P. J. *J. Biol. Chem.* **1990**, 20912.

(3) Rajagopalan, K. V. In *Advances in Enzymology and Related Areas of Molecular Biology*; A. Meister, Ed.; Wiley: New York, 1991; Vol. 64; pp 215-290.

(4) Kondo, M.; Ueyama, N.; Fukuyama, K.; Nakamura, A. *Bull. Chem. Soc. Jpn.* **1993**, *66*, 1391.

(5) Ueyama, N.; Kondo, M.; Nakamura, A. *Bull. Chem. Soc. Jpn.* **1994**, *67*, 1840-1847.

(6) Boyde, S.; Ellis, S. R.; Garner, C. D.; Clegg, W. *J. Chem. Soc., Chem. Commun.* **1986**, 1541.

(7) Chang, C. S. J.; Collison, D.; Mabbs, F. E.; Enemark, J. H. *Inorg. Chem.* **1990**, *29*, 2261.

(8) Ueyama, N.; Yoshinaga, N.; Kajiwara, A.; Nakamura, A. *Chem. Lett.* **1990**, 1781.

(9) Kamata, M.; Hirotsu, K.; Higuchi, T.; Tatsumi, K.; Hoffmann, R.; Yoshida, T.; Otsuka, S. *J. Am. Chem. Soc.* **1981**, *103*, 5772.

(10) Mitchell, P. C. H.; Pygall, C. F. *Inorg. Chim. Acta* **1979**, *33*, L109.

(11) Chatt, J.; Dilworth, J. R.; Schumutz, J. A.; Zubieta, J. A. *J. Chem. Soc., Dalton Trans* **1979**, 1595.

(12) Berg, J. M.; Holm, R. H. *J. Am. Chem. Soc* **1985**, *107*, 917.

(13) Harlan, E. W.; Berg, J. M.; Holm, R. H. *J. Am. Chem. Soc.* **1986**, *108*, 6992.

(14) Schultz, B. E.; Gheller, S. F.; Muetterties, M. C.; Scott, M. J.; Holm, R. H. *J. Am. Chem. Soc.* **1993**, *115*, 2714-2722.

(15) Gheller, S. F.; Schultz, B. E.; Scott, M. J.; Holm, R. H. *J. Am. Chem. Soc.* **1992**, *114*, 6934-6935.

(16) Ellis, S. R.; Collison, D.; Garner, C. D.; Clegg, W. *J. Chem. Soc., Chem. Commun.* **1986**, 1483-1485.

(17) Bishop, P. T.; Dilworth, J. R.; Hutchinson, J.; Zubieta, J. A. *J. Chem. Soc., Chem. Commun.* **1982**, 1052.

(18) Ueyama, N.; Yoshinaga, N.; Kajiwara, A.; Nakamura, A.; Kusunoki, M. *Bull. Chem. Soc. Jpn.* **1991**, *64*, 2458.

(19) Cleland, W. E. J.; Barnhart, K. M.; Yamanouchi, K.; Collison, D.; Mabbs, F. E.; Ortega, R. B.; Enemark, J. H. *Inorg. Chem.* **1987**, *26*, 1017.

(20) Ueyama, N.; Okamura, T.; Nakamura, A. *J. Am. Chem. Soc.* **1992**, *114*, 8129-8137.

(21) Ueyama, N.; Sugawara, T.; Sasaki, K.; Nakamura, A.; Yamashita, S.; Wakatsuki, Y.; Yamazaki, H.; Yasuoka, N. *Inorg. Chem.* **1988**, 741.

(22) Ellis, S. R.; Collison, D.; Garner, C. D. *J. Chem. Soc., Dalton Trans.* **1989**, 413.

(23) Holm, R. H. *Chem. Rev.* **1987**, *87*, 1401.

(24) Yoshinaga, N.; Ueyama, N.; Okamura, T.; Nakamura, A. *Chem. Lett.* **1990**, 1655.

(25) Berg, J. M.; Hodgson, K. O.; Cramer, S. P.; Corbin, J. L.; Elseberry, A.; Pariyadath, N.; Stiefel, E. I. *J. Am. Chem. Soc.* **1979**, *101*, 2774.

(26) Caradonna, J. P.; Reddy, P. R.; Holm, R. H. *J. Am. Chem. Soc.* **1988**, *110*, 2139.

(27) Roberts, S. A.; Young, C. G.; Cleland, W. E. J.; Ortega, R. B.; Enemark, J. H. *Inorg. Chem.* **1988**, *27*, 3044.

Chapter V

Conproportionation Reactions between Oxomolybdenum(IV) and Dioxomolybdenum(VI) Complexes having Thiolate Ligands

Introduction

Oxomolybdenum ion exists at the active site of molybdooxidoreductases such as sulfite oxidase, xanthine oxidase, or aldehyde oxidase.[1] EXAFS studies have shown that the molybdenum ion has two or three S ligands.[1,2] Rajagopalan et al. showed that the dithiolene ligand containing a pterin derivative coordinates to the Mo ion by analyzing of the degradation products.[3] Recently, a cysteine coordination to the Mo ion is suggested from the presence of the invariant cysteine residue in amino acid sequences of nitrate reductases.[4] EXAFS studies have also shown that the $Mo^{VI}(=O)_2$ or $Mo^{VI}(=O)(=S)$ cores are present in the oxidized state, and $Mo^{IV}(=O)$ core is in the reduced state. Isotope labeling method has shown that the terminal oxo ligand of $Mo^{VI}(=O)(=S)$ core of xanthine oxidase is transferred to the xanthine.[5]

As model compounds of these active sites, a number of dioxomolybdenum(VI) complexes have been synthesized, and their structures, properties, and reactivities have been studied.[6] In these complexes, $[Mo^{VI}O_2(dtc)_2]$ (dtc = diethyldithiocarbamate) shows the highest oxo-transfer reactivity to the phosphines (PPh_3, PPh_2Et, PEt_3, etc.) or benzoin. However, when catalytic oxidation reaction is carried out by using this complex as a catalyst, a rapid deactivation is observed.[6,7] This is due to the formation of the unreactive μ-oxo dimer, $[(dtc)_2Mo^{V}(O)\text{-}O\text{-}Mo^{V}O(dtc)_2]$, by the reaction between $[Mo^{VI}O_2(dtc)_2]$ and $[Mo^{IV}O(dtc)_2]$which is the product after oxidation of phosphines or benzoin. Among these complexes, the equilibrium reaction exists in the solution[8,9] (eq. 1).

$$[Mo^{VI}O_2(dtc)_2] + [Mo^{IV}O(dtc)_2] \rightleftharpoons [(dtc)_2Mo^{V}(O)\text{-}O\text{-}Mo^{V}O(dtc)_2] \quad (1)$$

It has been shown that the binucleation (*i.e.* comproportionation reaction) is prevented by the steric hindrance of the ligands.[6,10] Holm et al. showed that the bulky ligand inhibits the formation of the μ-oxo dimer in the catalytic reaction. They synthesized dioxomolybdenum(VI) complexes having a bulky ligand, $[Mo^{VI}O_2(L\text{-}N_2S)]$ (L-NS_2 = 2,6-bis(2,2-diphenyl-2-mercaptoethyl)pyridine(2-)), and showed that this complex does not give the μ-oxo dimer complex.[11-13] Then, this complex catalytically oxidizes phosphines or other oxo-acceptor substrates without deactivation.

The reactivity between oxomolybdenum(IV) complex and dioxomolybdenum(VI) complex having thiolate ligands has not been studied to date, because of the limited suitable complexes. Attempts of the synthesis of dioxomolybdenum(VI) complex by direct reaction between $Mo^{VI}(=O)_2^{2+}$ ion and free thiol give the reduced Mo(V) complex. The synthesis of oxomolybdenum(IV) complex has also been difficult because of the limited synthetic method.

In general, it has been to be very likely that an oxomolybdenum(IV) complex readily reacts with a dioxomolybdenum(VI) complex to produce a μ-oxo dimer complex. We synthesized the dioxomolybdenum(VI) complex having bdt^{2-} (1,2-benzenedithiolato) ligand by oxidation of $(NEt_4)_2[Mo^{IV}O(bdt)_2]$ with Me_3NO.[14] Our kinetic studies of this oxidation reaction has shown absence of the comproportionation reaction between the Mo(IV) complex and Mo(VI) complex.[15] Actually, $(NEt_4)_2[Mo^{IV}O(bdt)_2]$ catalyzes the oxidation of phosphines with pyO or O_2 without deactivation.[16]

Recently, we synthesized some oxomolybdenum(IV) complexes having chelating alkanedithiolate ligands as appropriate model compounds for the reduced active sites of molybdoenzymes.[17,18] These complexes, *e.g.* $[Mo^{IV}O(\alpha,2\text{-tdt})_2]^{2-}$ (α,2-tdt = α,2-toluenedithiolato) or $[Mo^{IV}O(edt)_2]^{2-}$ (edt = 1,2-ethanedithiolato), show unexpected inertness to the oxo-transfer reagents such as trimethyl amine-*N*-oxide and dimethyl sulfoxide. It was proposed that the unexpected reactivity is due to the strong Mo-S

(alkanethiolate) bond which prevents the intramolecular rearrangement of the complexes in the process of catalysis.

The reaction mechanism of an oxo-transfer reaction between trimethyl amine-*N*-oxide and oxomolybdenum(IV) complexes is regarded to be similar to that of comproportionation reaction between dioxomolybdenum(IV) complexes and oxomolybdenum(IV) complexes because the first step of the both reactions is the coordination of the O atoms to the Mo(IV) ion in the trans position of Mo=O.

We studied the reactivity of the comproportionation between oxomolybdenum(IV) and dioxomolybdenum(VI) complex having S containing ligands. In this paper, the results and the reaction mechanism of the comproportionation reaction are described.

Experimental Section

All syntheses and physical measurements were carried out under argon atmosphere using standard Schlenk technique. Acetonitrile (MeCN), and *N,N*-dimethylformamide (DMF) were dried over calcium hydride, distilled under argon atmosphere before using. 1,2-Dimethoxyethane (DME) was distilled from sodium benzophenone ketyl prior to use.

Materials. The four oxomolybdenum(IV) complexes, $[Mo^{IV}O(dtc)_2]$[19], $(NEt_4)_2[Mo^{IV}O(p\text{-}ClC_6H_4S)_4]$ (p-ClC_6H_4S = p-chlorobenzenethiolato),[20] $(NEt_4)_2[Mo^{IV}O(bdt)_2]$[15,21], $(NEt_4)_2[Mo^{IV}O(\alpha,2\text{-}tdt)_2]$[17], and three dioxomolybdenum(VI) complex, $[Mo^{VI}O_2(dtc)_2]$[22], $(NEt_4)_2[Mo^{VI}O_2(bdt)_2]$,[14] and $[Mo^{VI}O_2(cys\text{-}OMe)_2]$[23] were synthesized by the literature methods. $(NEt_4)_2[Mo^{IV}O(edt)_2]$ was prepared by the ligand exchange reaction between $(NEt_4)_2[Mo^{IV}O(p\text{-}ClC_6H_4S)_4]$ and 1,2-ethanedithiol in DME.[18]

Synthesis of $(NEt_4)_2[Mo^{IV}O(SC_6F_5)_4]$. Ellis et al. synthesized $(HNEt_3)_2[Mo^{IV}O(SC_6F_5)_4]$ by the reaction of $[Mo^{IV}OCl_2(PPh_2Me)_3]$ with pentafluorobenzenethiol.[24] The oxomolybdenum(IV) complex having two NEt_4^+ cations

$(NEt_4)_2[Mo^{IV}O(SC_6F_5)_4]$ was conveniently prepared by the reduction of $(NEt_4)[Mo^{V}O(SC_6F_5)_4]$ with NEt_4BH_4 in DME. This oxomolybdenum(V) complex was prepared according to the reported procedure by Ellis et al.[24]

$(NEt_4)[Mo^{V}O(SC_6F_5)_4]$ (0.15 g, 0.15 mmol) and NEt_4BH_4 (0.025 g, 0.17 mmol) were stirred in 2 mL of DME at room temperature for 10 hours. DME (9 mL) was added to the deep red solution to dissolve the purple precipitation. The solution was filtered, and reduced in volume to about 1 mL under reduced pressure. Red-brown powder was obtained by careful addition of 3 mL of diethyl ether to the solution. The product was collected by filtration, and dried *in vacuo*. The purification was carried out by reprecipitation from DME/diethyl ether. Yield, 0.10 g (77%). Anal. Calcd for $C_{40}H_{40}N_2OMoS_4F_{20}$: C, 41.1; H, 3.45; N, 2.40. Found: C, 40.77; H, 3.75; 2.40.

Conproportionation Reactions Between Oxomolybdenum(IV) complex and the Dioxomolybdenum(VI) complex. The reactions between oxomolybdenum(IV) complex and dioxomolybdenum(VI) complex were carried out by mixing of a MeCN solution of the Mo(IV) complex (2.0 mM, 1.0 mL) with a MeCN solution of the Mo(VI) complex (2.0 mM, 1.0 mL) at room temperature (ca. 24 °C). The absorption spectra of the reaction mixture were measured within 3 min after the mixing.

Physical Measurements. Absorption spectra were measured on a Jasco Ubest-30 spectrometer with 1 mm matched silica cells. ESR spectrum was recorded on a JEOL JES-FE1X spectrometer in MeCN/DMF (4:1) solution at 77 K. Cyclic voltammograms were taken on a Yanaco P-1100 polarographic analyzer in MeCN solution with a glassy carbon electrode and $(n\text{-Bu})_4NClO_4$ (100 mM) as supporting electrolyte.

Results

The Reaction Between $[Mo^{IV}O(dtc)_2]$ and $[Mo^{VI}O_2(dtc)_2]$. This is the typical example of the μ-oxo dimer formation. This reaction has been studied repeatedly to date.[6,8,25,26] An intense red-purple solution is immediately obtained when the Mo(IV) complex (pink solution) and the Mo(VI) complex (yellow solution) are mixed. The absorption spectrum change of the reaction solutions (2mM/2mM) is shown in Figure 1. The band at 510 nm is assignable to the μ-oxo dimer $[(dtc)_2Mo^{V}(O)\text{-}O\text{-}Mo^{V}O(dtc)_2]$. This band does not obey the Lambert-Beer's rule, because of the equilibrium reaction between $[Mo^{IV}O(dtc)_2]$ and $[Mo^{VI}O_2(dtc)_2]$ complexes and the μ-oxo dimer.

The Reaction Between $[Mo^{IV}O(dtc)_2]$ and $(NEt_4)_2[Mo^{VI}O_2(bdt)_2]$. The absorption spectrum of this reaction mixture shows the occurrence of some reactions (Figure 2). This reaction mixture shows absorption maxima at 510 nm and 726 nm, and a shoulder at 380 nm. The curve obtained is similar to that of the reaction mixture of $(NEt_4)_2[Mo^{IV}O(bdt)_2]$ and $[Mo^{VI}O_2(dtc)_2]$ (*vide infra*). Because the band at 510 nm does not obey the Lambert-Beer's rule, and shows the rapid decrease by dilution, this band is assigned to the $[(dtc)_2Mo^{V}(O)\text{-}O\text{-}Mo^{V}O(dtc)_2]$. The band at 726 nm obeys the Lambert-Beer's rule, indicating this band is due to the $[Mo^{V}O(bdt)_2]^-$ [27]. The yields of the each products are quite low (< 10 %) estimated from the absorption intensities. Unidentified byproducts in this reaction are perhaps polymeric compounds bridged by μ-oxo ligand.

The redox potentials of $[Mo^{IV}O(dtc)_2]$ (0.52 V) and $(NEt_4)_2[Mo^{VI}O_2(bdt)_2]$ (-1.0 V) show that the electronic reduction of the Mo(VI) complex is implausible. Proposal reaction mechanism of this reaction is via the μ-oxo dimer formation (eq. 2-3).

$$[Mo^{IV}O(dtc)_2] + (NEt_4)_2[Mo^{VI}O_2(bdt)_2] \rightleftharpoons [(dtc)_2Mo^{V}(O)\text{-}O\text{-}Mo^{V}O(bdt)_2] \rightleftharpoons [Mo^{IV}O(bdt)_2] + (NEt_4)_2[Mo^{VI}O_2(dtc)_2] \quad (2)$$

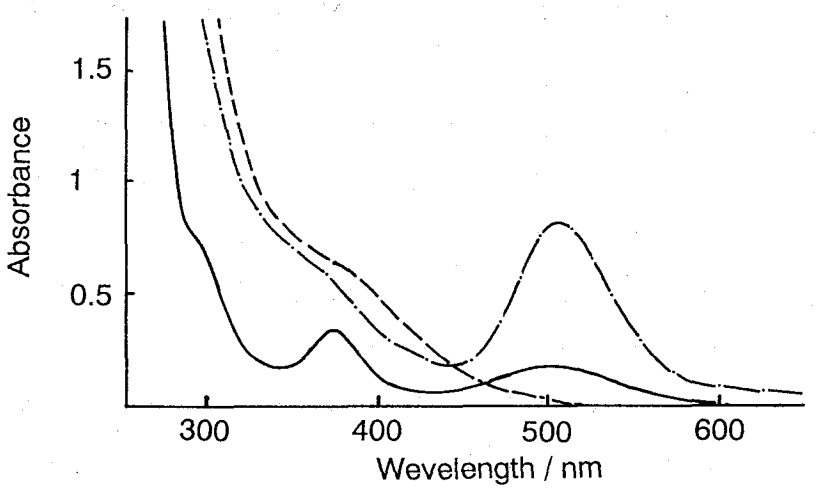

Figure 1. Absorption spectra of $[Mo^{IV}O(dtc)_2]$ (2.0 mM) (—), $[Mo^{VI}O_2(dtc)_2]$ (2.0 mM) (----), and the reaction mixture (— · —) in MeCN.

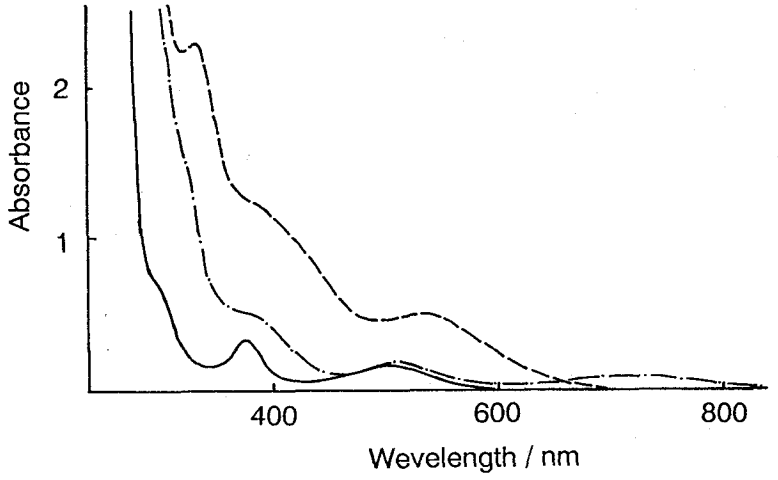

Figure 2. Absorption spectra of $[Mo^{IV}O(dtc)_2]$ (2.0 mM) (—), $[Mo^{VI}O_2(bdt)_2]$ (2.0 mM) (----), and the reaction mixture (— · —) in MeCN.

$$[Mo^{VI}O_2(bdt)_2] + [Mo^{IV}O(dtc)_2] \rightarrow [Mo^{V}O(bdt)_2]^- + [(dtc)_2Mo^{V}(O)\text{-}O\text{-}Mo^{V}O(dtc)_2] \quad (3)$$

The comproportionation reaction between $[Mo^{IV}O(dtc)_2]$ and $[Mo^{VI}O_2(bdt)_2]^{2-}$ gives the hetero μ-oxo dimer, $[(dtc)_2Mo^{V}(O)\text{-}O\text{-}Mo^{V}O(bdt)_2]^{2-}$. The dimer complex gives the $[Mo^{VI}O_2(dtc)_2]$ and $[Mo^{IV}O(bdt)_2]^{2-}$ by the equilibrium reaction. As shown in below, these two complexes react to produce the $[(dtc)_2Mo^{V}(O)\text{-}O\text{-}Mo^{V}O(dtc)_2]$ and $[MoO^{V}(bdt)_2]^-$, which were observed in the reaction.

The Reaction Between $[Mo^{IV}O(dtc)_2]$ and $[Mo^{VI}O_2(cys\text{-}OMe)_2]$. Figure 3a shows the absorption spectrum of this reaction mixture with each starting solution. The spectra show the additive properties among the three solutions, showing that no oxo or electron transfer reactions occur between these complexes.

The Reaction Between $(NEt_4)_2[Mo^{IV}O(SC_6F_5)_4]$ and $[Mo^{VI}O_2(dtc)_2]$. The reaction solution immediately gives the purple solution having 510 nm absorption band (Figure 3b). This band is characteristic of the μ-oxo dimer. Actually, this band does not obey Lambert-Beer's rule. The CV of this purple solution shows the irreversible reduction of $Mo^{VI}O_2^{2+}$ / $Mo^{V}O^{+}$ at -0.83 and oxidation at 0.40 V (vs. SCE) of $Mo^{VI}O^{2+}$ - $Mo^{V}O^{3+}$. These redox behavior is similar to that of $[(dtc)_2Mo^{V}(O)\text{-}O\text{-}Mo^{V}O(dtc)_2]$. Each redox is due to the $[Mo^{VI}O_2(dtc)_2]$ and $[Mo^{IV}O(dtc)_2]$ species, (Table II), which are equilibrium components. These absorption and redox results show no formation of hetero μ-oxo dimer $[(SC_6F_5)_4Mo^{V}(O)\text{-}O\text{-}Mo^{V}O(dtc)_2]$.

No observation of the characteristic band of $[Mo^{V}O(SC_6F_5)_4]^-$ species show that $(NEt_4)_2[Mo^{IV}O(SC_6F_5)_4]$ does not act as one-electron reduction reagent shown in the reaction between $(NEt_4)_2[Mo^{IV}O(p\text{-}ClC_6H_4S)_4]$ and $[Mo^{VI}O_2(dtc)_2]$. Neither slow diffusion mixing method of the two complexes nor the reaction of excess Mo(IV) complex with Mo(VI) complexes gives the $[Mo^{V}O(SC_6F_5)_4]^-$ complex. This reactivity contrast to that of the reaction between $(NEt_4)_2[Mo^{IV}O(p\text{-}ClC_6H_4S)_4]$ and $(NEt_4)_2[Mo^{VI}O_2(dtc)_2]$ (*vide infra*).

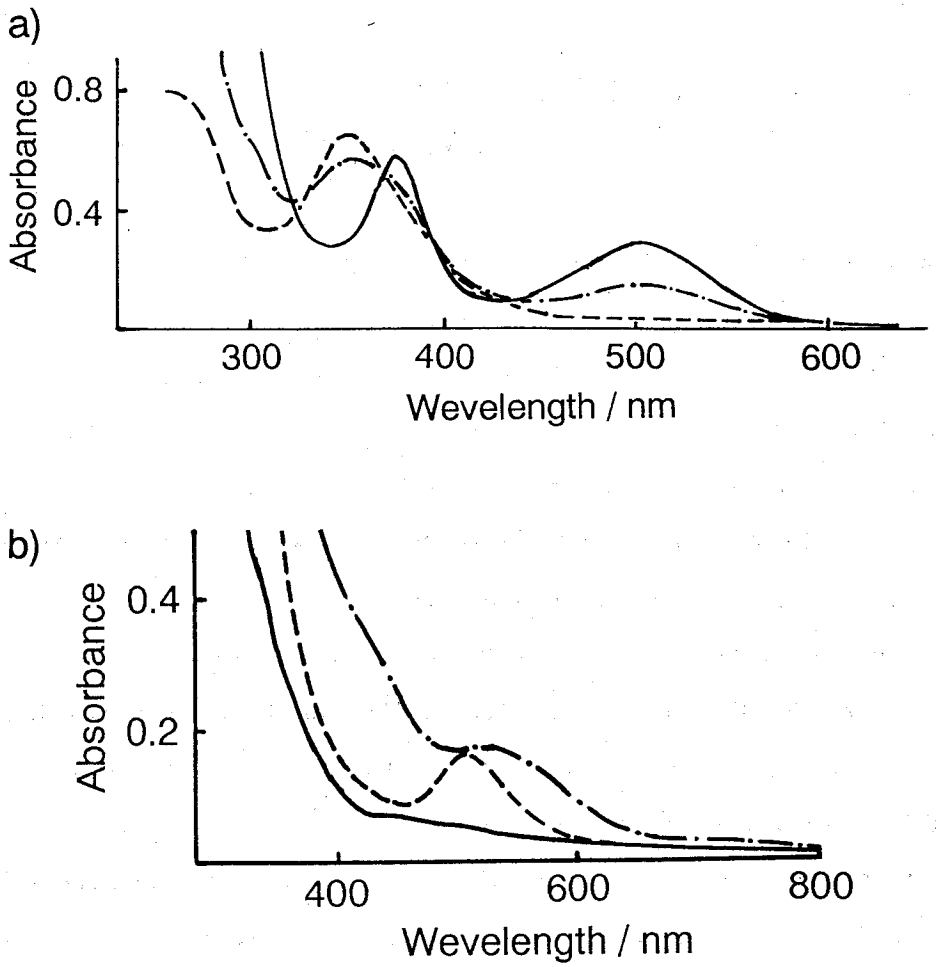

Figure 3. a) Absorption spectra of $[Mo^{IV}O(dtc)_2]$ (2.0 mM) (—), $[Mo^{VI}O_2(cys\text{-}OMe)_2]$ (2.0 mM) (----), and the reaction mixture (— ·—) in MeCN. b) Absorption spectra of $(NEt_4)_2[Mo^{IV}O(SC_6F_5)_4]$ (2.0 mM) (—), $[Mo^{VI}O_2(dtc)_2]$ (2.0 mM) (----), and the reaction mixture (— ·—) in MeCN.

Proposed reaction mechanism of this reaction is as follows.

$$[Mo^{IV}O(SC_6F_5)_4] + [Mo^{VI}O_2(dtc)_2] \rightleftharpoons [(dtc)_2Mo^{V}(O)\text{-}O\text{-}Mo^{V}O(dtc)_2] \rightleftharpoons [Mo^{IV}O(dtc)_2] + [Mo^{VI}O_2(SC_6F_5)_4] \quad (4)$$

$$[Mo^{VI}O_2(dtc)_2] + [Mo^{IV}O(dtc)_2] \rightleftharpoons [(dtc)_2Mo^{V}(O)\text{-}O\text{-}Mo^{V}O(dtc)_2] \quad (1)'$$

The product $[Mo^{VI}O_2(SC_6F_5)_4]$ likely changes to the dimeric or polymeric complex because of the thermal instability of the Mo(VI) complex having monodentate thiolate ligand.[18] Monomeric oxomolybdenum(V) complex having thiolate ligand shows characteristic CT band (S → Mo) at visible region.[28] On the contrary, μ-oxo dimer complex does not show the characteristic band at the visible region.[29]

The Reaction Between $(NEt_4)_2[Mo^{IV}O(SC_6F_5)_4]$ and $[Mo^{VI}O_2$(bdt or cys-OMe)$_2]$. Both absorption spectra show additive spectra between the reaction mixture and the starting complexes, indicating no reaction between these complexes.

The Reaction Between $(NEt_4)_2[Mo^{IV}O(bdt)_2]$ and $[Mo^{VI}O_2(dtc)_2]$. The mixing of $(NEt_4)_2[Mo^{IV}O(bdt)_2]$ (orange solution) with $[Mo^{VI}O_2(dtc)_2]$ (yellow solution) MeCN solution gives a deep purple coloration immediately. The absorption spectrum change is shown in Figure 4a. The reaction mixture exhibits new bands at 510 nm and 727 nm. The band at 510 nm does not depend on the concentration and rapidly decreases by dilution, whereas the band at 710 nm obeys the Lambert-Beer's rule. These observations show that the absorption band at 510 nm is due to the formation of a μ-oxo dimer, $[(dtc)_2Mo^{V}(O)\text{-}O\text{-}Mo^{V}O(dtc)_2]$. The reaction mixture also shows the intense ESR signal in MeCN/DMF (4:1) solution at 77 K (Figure 4b). The ESR parameters obtained, g_{11}= 2.022, g = 1.984, 1.976, is consistent with that of $(NEt_4)[Mo^{V}O(bdt)_2]$, demonstrating the band at 710 nm is due to the formation of $[Mo^{V}O(bdt)_2]^-$. The formation of $[Mo^{V}O(bdt)_2]^-$ is also detected by the CV measurement ($E_{1/2}$ = -0.37 V vs

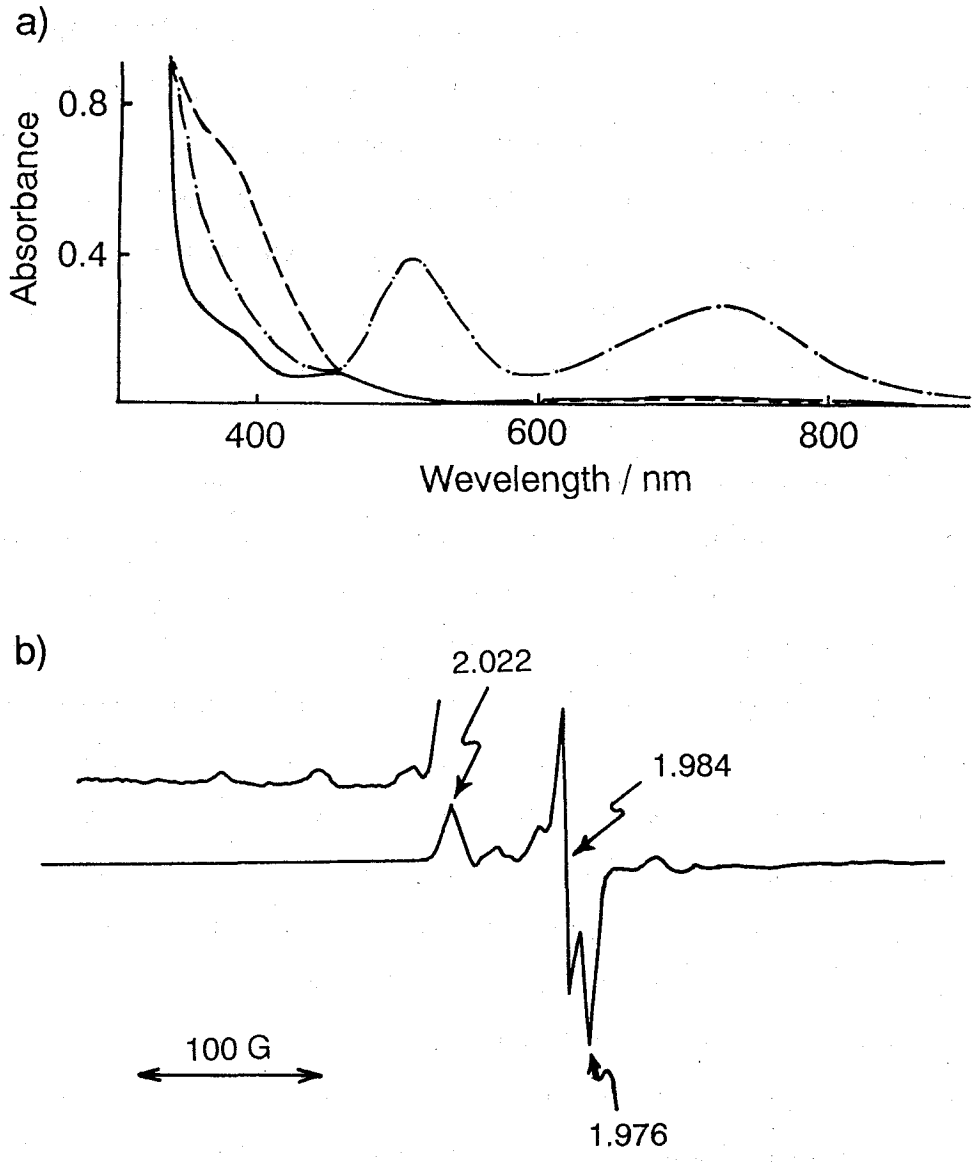

Figure 4. a) Absorption spectra of $(NEt_4)_2[Mo^{IV}O(bdt)_2]$ (2.0 mM) (—), $(NEt_4)_2[Mo^{VI}O_2(dtc)_2]$ (2.0 mM) (----), and the reaction mixture (— ·—) in MeCN. b) ESR spectrum of the reaction mixture in MeCN/DMF (4:1) at 77 K.

SCE). The yield of this complex is estimated to be ca. 30 % from the absorption intensity at λ_{max} of 727 nm (ε = 7700).

These results show that the reaction between $(NEt_4)_2[Mo^{IV}O(bdt)_2]$ and $[Mo^{VI}O_2(dtc)_2]$ does not give the hetero μ-oxo dimer complex, $[(bdt)_2Mo^{V}(O)\text{-}O\text{-}Mo^{V}O(dtc)_2]^{2-}$, but $[(dtc)_2Mo^{V}(O)\text{-}O\text{-}Mo^{V}O(dtc)_2]$ and $[Mo^{V}O(bdt)_2]^-$ as the results of the electron transfer reaction. This reaction mechanism is discussed in the Discussion.

The Reaction Between $(NEt_4)_2[Mo^{IV}O(bdt)_2]$ and $(NEt_4)_2[Mo^{VI}O_2(bdt)_2]$. The absorption spectral change of the reaction between $(NEt_4)_2[Mo^{IV}O(bdt)_2]$ and $(NEt_4)_2[Mo^{VI}O_2(bdt)_2]$ is shown in Figure 5a. Additivity among three spectra shows absence of reactions between the two complexes.

The Reaction Between $(NEt_4)_2[Mo^{IV}O(bdt)_2]$ and $[Mo^{VI}O_2(cys\text{-}OMe)_2]$. The absorption spectrum of this reaction mixture solution also shows the additivity. That is, no oxo or electron transfer reactions occurs in these complexes.

The Reaction Between $(NEt_4)_2[Mo^{IV}O(p\text{-}ClC_6H_4S)_4]$ and $(NEt_4)_2[Mo^{VI}O_2(dtc)_2]$. This reaction mixture gave purple coloration immediately, finally blue solution within 3 s. The spectrum of the final blue solution shows a characteristic band of $[Mo^{V}O(p\text{-}ClC_6H_4S)_4]^-$ at 600 nm in *ca.* 40 % yield, and shows no band for assignable to $[(dtc)_2Mo^{V}(O)\text{-}O\text{-}Mo^{V}O(dtc)_2]$ around 510 nm (Figure 5b). Since i) the absorption measurement of the slow diffusion solution of $[Mo^{VI}O_2(dtc)_2]$ into $(NEt_4)_2[Mo^{IV}O(p\text{-}ClC_6H_4S)_4]$ showed the clear shoulder band at 510 nm, and ii) reaction between $(NEt_4)_2[Mo^{IV}O(p\text{-}ClC_6H_4S)_4]$ and 4 equiv.. of $[Mo^{VI}O_2(dtc)_2]$ gives the purple solution having band at 510 nm of μ-oxo dimer $[(dtc)_2Mo^{V}(O)\text{-}O\text{-}Mo^{V}O(dtc)_2]$ with no band around 600 nm, the observation of purple solution in the initial stage is due to the formation of the μ-oxo dimer $[(dtc)_2Mo^{V}(O)\text{-}O\text{-}Mo^{V}O(dtc)_2]$. The results show that the reaction product between $(NEt_4)_2[Mo^{IV}O(p\text{-}ClC_6H_4S)_4]$ and $(NEt_4)_2[Mo^{VI}O_2(dtc)_2]$ contains the $[Mo^{V}O(p\text{-}ClC_6H_4S)_4]^-$ and $[Mo^{IV}O(dtc)_2]$.

Yield of the formation of $[Mo^{V}O(p\text{-}ClC_6H_4S)_4]^-$ (*ca.* 40 %) suggests that 0.4 equiv. of $(NEt_4)_2[Mo^{IV}O(p\text{-}ClC_6H_4S)_4]$ acts as one-electron reducing source in this reaction. Since $[Mo^{VI}O_2(dtc)_2]$ is completely reduced to the Mo(IV) state, the occurrence

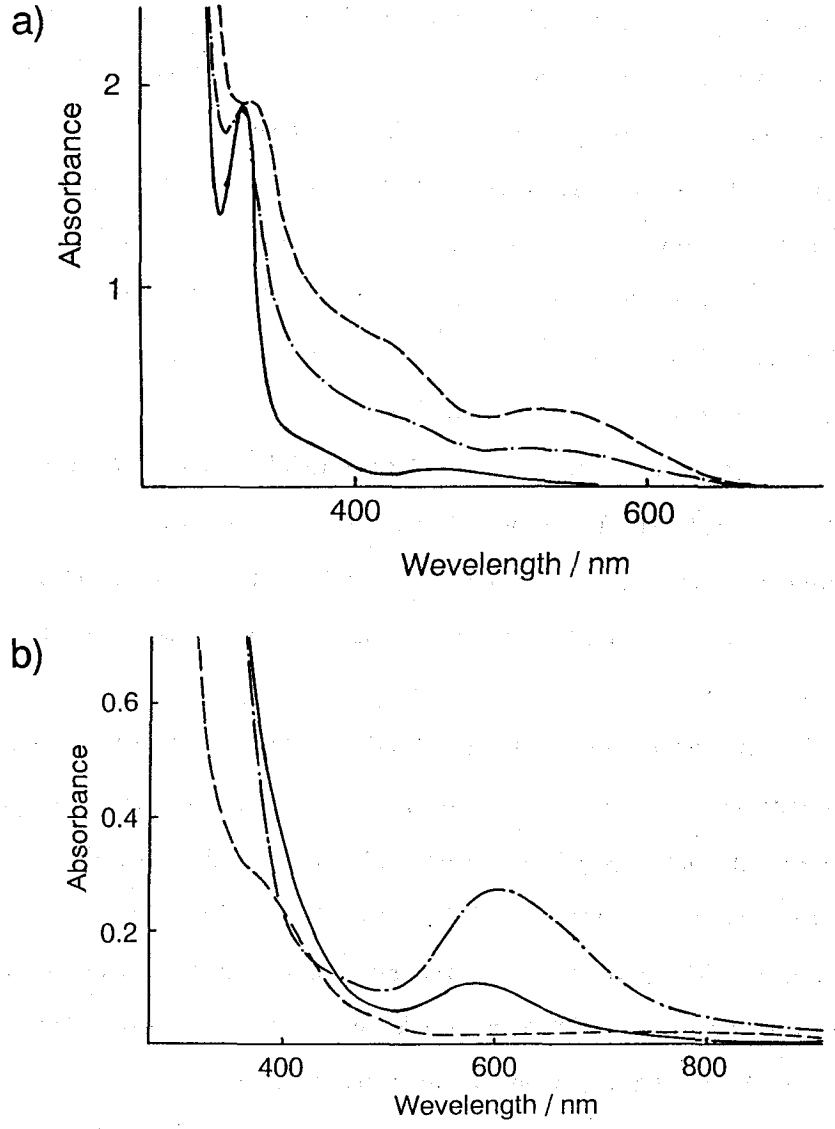

Figure 5. a) Absorption spectra of $(NEt_4)_2[Mo^{IV}O(bdt)_2]$ (2.0 mM) (—), $(NEt_4)_2[Mo^{VI}O_2(bdt)_2]$ (2.0 mM) (----), and the reaction mixture (— ·—) in MeCN. b) Absorption spectra of $(NEt_4)_2[Mo^{IV}O(p\text{-}ClC_6H_4S)_4]$ (2.0 mM) (—), $[Mo^{VI}O_2(dtc)_2]$ (2.0 mM) (----), and the reaction mixture (— ·—) in MeCN.

of 1.6 equiv. of other reducing source is proposed. This source may be free thiolate ligand p-$ClC_6H_4S^-$, which is eliminated from the Mo(IV or V) - (p-ClC_6H_4S) complex. Actually reaction between $(NEt_4)[Mo^VO(p\text{-}ClC_6H_4S)_4]$ and equimolar $[Mo^{VI}O_2(dtc)_2]$ readily proceed to give the red purple solution having intense band around 510 nm from the μ-oxo dimer $[(dtc)_2Mo^V(O)\text{-}O\text{-}Mo^VO(dtc)_2]$. $(NEt_4)[Mo^VO(p\text{-}ClC_6H_4S)_4]$ may change to the multinuclear complex having no characteristic band.

The Reaction Between $(NEt_4)_2[Mo^{IV}O(p\text{-}ClC_6H_4S)_4]$ and $(NEt_4)_2[Mo^{VI}O_2(bdt)_2]$. Although the absorption spectrum of the yellow-orange reaction mixture shows the formation of $[Mo^VO(p\text{-}ClC_6H_4S)_4]^-$ in ca. 12 %, broad absorption around 500 nm suggests the existence of non-reacted $(NEt_4)_2[Mo^{VI}O_2(bdt)_2]$. Thus, this reaction does not proceed substantially.

The Reaction Between $(NEt_4)_2[Mo^{IV}O(p\text{-}ClC_6H_4S)_4]$ and $[Mo^{VI}O_2(cys\text{-}OMe)_2]$. The absorption spectrum shows a band at 600 nm. Although the absorption maxima suggest the production of *ca.* 2 % of $[Mo^VO(p\text{-}ClC_6H_4S)_4]^-$, the spectra roughly shows the additive property among these complexes. Thus, no reaction occurs in this system.

The Reaction Between $(NEt_4)_2[Mo^{IV}O(\alpha,2\text{-tdt or edt})_2]$ and $[Mo^{VI}O_2(dtc)_2]$. These reactions give the similar results to that of the reaction between $(NEt_4)_2[Mo^{IV}O(bdt)_2]$ and $[Mo^{VI}O_2(dtc)_2]$. All these reactions give the monooxomolybdenum(V) complexes, $[Mo^VO(L)_2]^-$ (L = α,2-tdt, edt), and the μ-oxo dimer, $[(dtc)_2Mo^V(O)\text{-}O\text{-}Mo^VO(dtc)_2]$. The results show that the oxomolybdenum(IV) complexes having chelating dithiolate ligands do not afford the μ-oxo dimer by the reaction with $[Mo^{VI}O_2(dtc)_2]$, but the electron transfer reaction.

The Reaction Between $(NEt_4)_2[Mo^{IV}O(edt)_2]$ and $(NEt_4)_2[Mo^{VI}O_2(bdt)_2]$. The absorption spectrum of the brownish reaction solution obtained shows the intense CT band of $[Mo^VO(edt)_2]^-$, which consists of characteristic bands at 448 (750), 519 (690), and 625 nm (890 $M^{-1}cm^{-1}$), and the broad band around 400 - 550 nm (Figure 6). The yield of $[Mo^VO(edt)_2]^-$ is *ca.* 70 %. No change of the

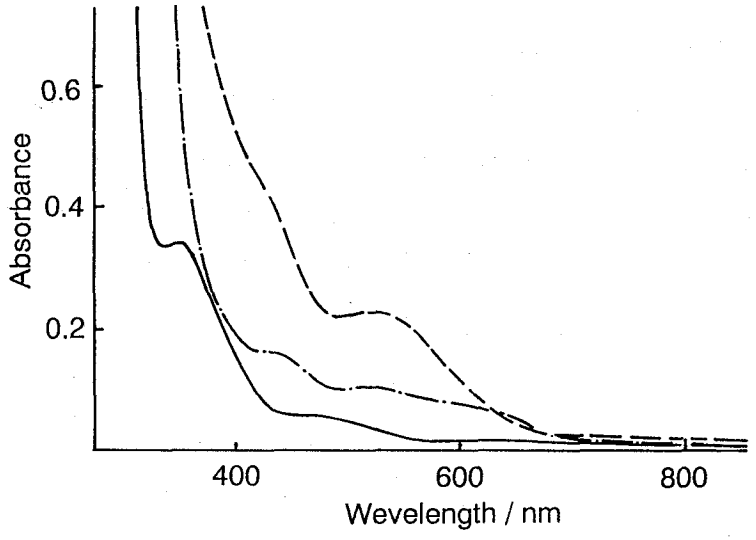

Figure 6. Absorption spectra of $(NEt_4)_2[Mo^{IV}O(edt)_4]$ (2.0 mM) (—), $(NEt_4)_2[Mo^{VI}O_2(bdt)_2]$ (2.0 mM) (----), and the reaction mixture (— ·—) in MeCN.

absorption spectrum by O_2 bubbling to the obtained solution indicates the absence of $[Mo^{IV}O(bdt)_2]^{2-}$, but the decomposed product.

The Reaction Between $(NEt_4)_2[Mo^{IV}O(edt)_2]$ and $[Mo^{VI}O_2(cys\text{-}OMe)_2]$. The absorption spectrum of the reaction solution is almost consistent with that of $[Mo^{V}O(edt)_2]^-$ complex, indicating the production of $[Mo^{V}O(edt)_2]^-$ complex in quantitative yield. The reaction system does not produce the μ-oxo dimer $[(cys\text{-}OMe)_2Mo^{V}(O)\text{-}O\text{-}Mo^{V}O(cys\text{-}OMe)_2]$. The expected reaction product $[Mo^{VI}O_2(cys\text{-}OMe)_2]$ is not detected.

Discussion

The conproportionation reactions.

The results are summarized in Table I. Although all these complexes studied in here do not have any bulky ligands, only the one well-known reaction between $[Mo^{IV}O(dtc)_2]$ and $[Mo^{VI}O_2(dtc)_2]$ forms the thermally and kinetically stable μ-oxo dimer. The μ-oxo dimer formation as an intermediate is proposed in the two reactions i) between $(NEt_4)_2[Mo^{IV}O(SC_6F_5)_4]$ and $[Mo^{VI}O_2(dtc)_2]$, and ii) between $[Mo^{IV}O(dtc)_2]$ and $(NEt_4)_2[Mo^{VI}O_2(bdt)_2]$. All other reactions showed no evidence for the μ-oxo dimer formation. Table I shows that the comproportionation reactivity is apparently affected by the reactivity of both oxomolybdenum(IV) and dioxomolybdenum(VI) complexes.

Since the molybdenum ions of the μ-oxo dimer have the oxidation number of five, the formation of the μ-oxo dimer involves the electron transfer reaction between the Mo(IV) ion and Mo(VI) ion. Even if the redox potential of ($Mo^{IV}O^{2+}$ / $Mo^{V}O^{+}$) of oxomolybdenum(IV) complex is more positive than that of ($Mo^{VI}O_2^{2+}$ / $Mo^{V}O_2^{+}$) of dioxomolybdenum(VI) complex, the μ-oxo dimer forms in the present studies. For example, the dtc complexes, which readily form the μ-oxo dimer, the oxidation potential of $[Mo^{IV}O(dtc)_2]$ (0.52 V) is more positive than the reduction potential of $[Mo^{VI}O_2(dtc)_2]$ (-0.87 V). The results show that this reaction is not the simple electron transfer reaction between two molecules. Thus, it is proposed that the electron transfer reaction occurs after the coordination of oxo ligand of the dioxomolybdenum(VI) complex to the Mo(IV) complex.

The X-ray structure of the μ-oxo dimer molybdenum(V) complexes have been reported in some complexes, *e.g.* $[(L)_2Mo^{V}(O)\text{-}O\text{-}Mo^{V}O(L)_2]$ (L = S_2CS-*i*-Pr,[30] S_2COEt,[31] $S_2CN(n\text{-}Pr)_2$,[32] $S_2P(OEt)_2$,[33], 2-salicylideneamino(benzenethiolato)[34], and $[(NCS)_4Mo^{V}(O)\text{-}O\text{-}Mo^{V}O(NCS)_4]^{4-}$,[35] indicating that the bridging and terminal oxo ligands are in mutually cis configuration. Thus, the rearrangement of the cis to trans configuration is proposed for the final step.

Table I. Conproportionation reaction results between oxomolybdenum(IV) and dioxomolybdenum(VI) complexes.

$[Mo^{IV}O(L)_2]^{n-}$ Complexes \	$[Mo^{VI}O_2(L)_2]^{n-}$ Complexes		
L	L = dtc (n = 0)	bdt (n = 2)	cys-OMe (n = 0)
dtc (n = 0)	μ-oxo dimer formation	μ-oxo dimer formation	no reaction
C_6F_5S (n = 2)[a]	electron transfer reaction	no reaction	no reaction
bdt (n = 2)	electron transfer reaction	no reaction	no reaction
p-ClC_6H_4S (n = 2) [b]	electron transfer reaction	no reaction	no reaction
α,2-tdt (n = 2)	electron transfer reaction	any reaction occurs	electron transfer reaction
edt (n = 2)	electron transfer reaction	any reaction occurs	electron transfer reaction

a) $[Mo^{IV}O(SC_6F_5)_2]^{2-}$

b) $[Mo^{IV}O(p\text{-}ClC_6H_4S)_2]^{2-}$

Thus, the following reaction mechanism is proposed for the μ-oxo dimer formation, which consists of three steps. (Scheme 1) The first step (**I**) is the coordination of the terminal oxo ligand of dioxomolybdenum(VI) complex to the vacant site of oxomolybdenum(IV) complex. The second step (**II**) is the electron transfer reaction from the Mo(IV) ion to the Mo(VI) complex to form the μ-oxo dimer having a straight linear $O{=}Mo^{V}{-}O{-}Mo^{V}$ geometry. The third step (**III**) is the intramolecular rearrangement of *trans*-O=Mo-O to *cis*-O=Mo-O configuration.

Table II. Redox properties of oxomolybdenum(IV) and dioxomolybdenum(VI) complexes.

Mo(IV)/Mo(V) redox potentials (vs SCE) of oxomolybdenum(IV) complexes.

Complex	Redox potential	References
$[Mo^{IV}O(dtc)_2]$	0.52	44
$(NEt_4)_2[Mo^{IV}O(SC_6F_5)_4]$	-0.03	this work
$(NEt_4)_2[Mo^{IV}O(p\text{-}ClC_6H_4S)_2]$	-0.66	20
$(NEt_4)_2[Mo^{IV}O(bdt)_2]$	-0.37	45
$(NEt_4)_2[Mo^{IV}O(\alpha,2\text{-}tdt)_2]$	-0.74	17
$(NEt_4)_2[Mo^{IV}O(edt)_2]$	-0.84	18

Mo(VI)/Mo(V) redox potentials (vs SCE) of dioxomolybdenum(VI) complexes.

Complex	Redox potential	References
$[Mo^{VI}O_2(dtc)_2]$	-0.87	46
$(NEt_4)_2[Mo^{VI}O_2(bdt)_2]$	-1.0	14
$[Mo^{VI}O_2(cys\text{-}OMe)_2]$	-1.25	46

The second reaction process (**II**) accompanies an electron transfer from $Mo^{IV}O^{2+}$ to $Mo^{VI}O_2^{2+}$ and the Mo^{VI}=O bond cleavage. The strong electron transfer ability of the Mo(IV) complex and the accepting ability or the activated Mo^{VI}=O bond of Mo(VI) complex are expected to facilitate this electron transfer reaction step. The electron donating ability of the Mo(IV) complex is evaluated by the oxidation potential of $Mo^{IV}O^{2+}$ to $Mo^{V}O^{+}$, which is detected by CV measurement. The electrochemical data of the related oxomolybdenum(IV) and dioxomolybdenum(VI) complexes are summarized in Table II. The data show that the reducing ability is relatively high in the thiolate complexes (0 ~ -0.84 V), and low in $[Mo^{IV}O(dtc)_2]$ (0.52 V). However, these

oxomolybdenum(IV) complexes except for $(NEt_4)_2[Mo^{IV}O(SC_6F_5)_4]$ did not produce the μ-oxo dimer, but afford the oxomolybdenum(V) complexes in the reaction with $[Mo^{VI}O_2(dtc)_2]$. Although the oxidation potentials of all these oxomolybdenum(IV) complexes (0.52 ~ -0.84 V) are more positive than reduction potential of $[Mo^{VI}O_2(dtc)_2]$ (-0.87 V), the oxidation reaction occurs. These oxomolybdenum(V) complexes are produced by the irreversible dissociation reaction of the intermediate having linear O=Mo-O-Mo geometry to the oxomolybdenum(V) complex and dioxomolybdenum(V) complex (Scheme. 2).

In general, these oxomolybdenum(V) complexes having thiolate ligand are so stable that these are readily produced by one-electron oxidation of the corresponding oxomolybdenum(IV) complexes. Actually, the redox couple of $Mo^{IV}O^{2+}$ / $Mo^{V}O^{+}$ of these thiolate complexes is quasi reversible. On the contrary, $[Mo^{IV}O(dtc)_2]$ shows the irreversible wave. These results show that the strong electron donating ability of the oxomolybdenum(IV) thiolate complex is not necessarily facilitate the μ-oxo dimer formation, because formation of the oxomolybdenum(V) complex is preferred.

The activity of dioxomolybdenum(VI) complex is reflected in the oxo transfer reactivity to the substrates such as triphenylphosphine. For instance, $[Mo^{VI}O_2(dtc)_2]$ shows the highest oxo-transfer reactivity to PPh_3 in dioxomolybdenum(VI) complexes studied to date.[6]

The reactivity of the oxo transfer reaction of dioxomolybdenum(VI) complexes is enhanced by the i) coordinating ligand type, ii) redox property, and iii) trans influence. The reduction reactivity of $Mo^{VI}O^{2+}$ ion by phosphines is enhanced by the type of the donor sets as in the following order.[36]

$S_4 > NS_2 > N_2S_2 > ONS >> NO_2$

Actually, the oxo transfer reactivity of $[Mo^{VI}O_2(cys\text{-}OMe)_2]$ (N_2S_2 set) is extremely lower than that of $[Mo^{VI}O_2(dtc)_2]$ (S_4 set).

The oxo-transfer reactivity to the phosphines is enhanced as the Mo(VI)/Mo(V) redox couple shifts to the positive side.[36] The Mo^{VI}=O bond of dioxomolybdenum(VI) complex is also expected to be activated by the trans influence from the donating atoms in

Scheme 1

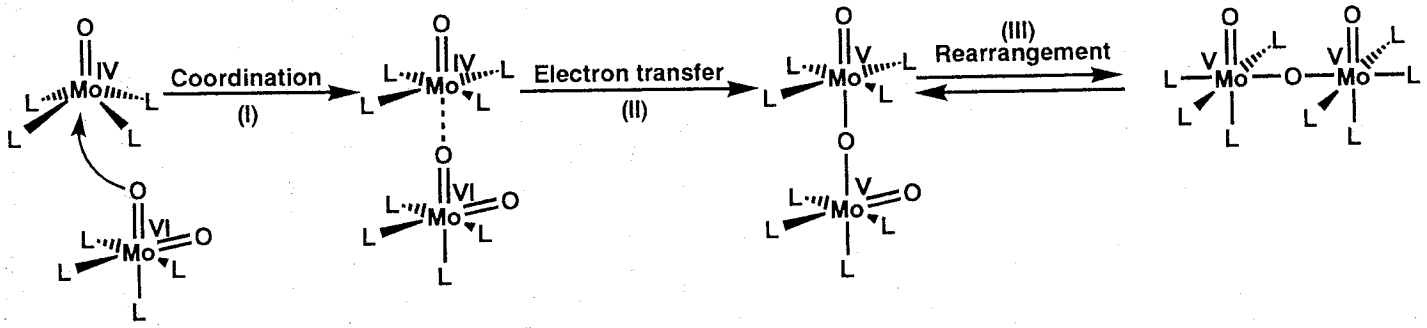

Scheme 2

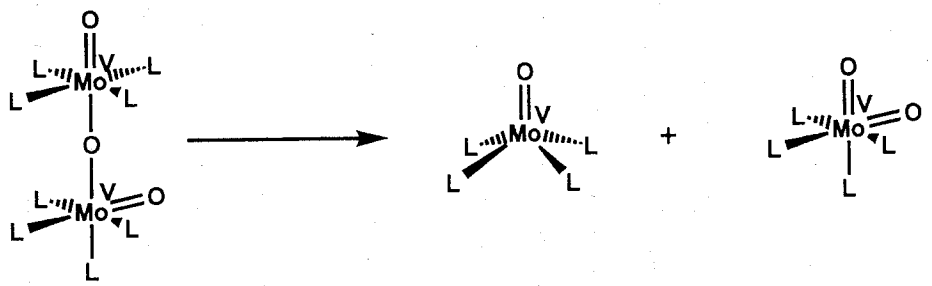

the trans position to Mo^{VI}=O. $(NEt_4)_2[Mo^{VI}O_2(bdt)_2]$ is an only example having thiolate ligand trans to the Mo^{VI}=O in dioxomolybdenum(VI) complexes synthesized to date. Actually, this complex shows the lower $\nu(Mo^{VI}=O)$ band (860, 832 cm^{-1}) in Raman spectrum compared with that of $[Mo^{VI}O_2(dtc)_2]$ (907, 878 cm^{-1} (IR spectrum))[37]. However, the comproportionation reactivity is higher in $[Mo^{VI}O_2(dtc)_2]$ than that of $(NEt_4)_2[Mo^{VI}O_2(bdt)_2]$ in the reaction with $(NEt_4)_2[Mo^{IV}O(SC_6F_5)_4]$. This is likely that the more negative reduction potential of $Mo^{VI}O_2^{2+}$ / $Mo^{V}O_2^{+}$ of $(NEt_4)_2[Mo^{VI}O_2(bdt)_2]$ inhibits the reaction.

For the achievement of the rearrangement of the third step (**III**) of the comproportionation reaction, the temporary dissociation of the coordinating ligand or the spread space of the coordination sphere is necessary. (Scheme 3) The chelating ligands *i.e.* bdt, edt, α,2-tdt, hardly dissociate because of the chelating effect. Especially, alkanedithiolate ligand (edt and α,2-tdt) makes the strong chelating skeleton because of the strong σ character of the alkanethiolate. Actually, these oxomolybdenum(IV) complexes having these chelating ligands do not achieve the μ-oxo dimer formation. The monodentate ligands *i.e.* $SC_6F_5^-$ and *p*-$ClC_6H_4S^-$, may allow the temporary dissociation. Although $(NEt_4)_2[Mo^{IV}O(SC_6F_5)_4]$ forms the μ-oxo dimer in the reaction with $[Mo^{VI}O_2(dtc)_2]$, $(NEt_4)_2[Mo^{IV}O(p\text{-}ClC_6H_4S)_4]$ does not form the μ-oxo dimer because of the production of the unreactive oxomolybdenum(V) complex $(NEt_4)[Mo^{V}O(p\text{-}ClC_6H_4S)_4]$.

The dtc ligand has the sterically enough coordination sphere as seen in some of the seven coordinated dtc-molybdenum complexes. For example, $[Mo^{VI}N(dtc)_3]$[38,39], $[Mo^{VI}(NS)(S_2CNMe_2)_2]$[40], and $[Mo^{VI}O(S_2)(dtc)_2]$[41] are known to date. This is due to the relatively narrow S-Mo-S bite angle (*ca.* 69°) of the dtc ligand.[42] Although, $(NEt_4)_2[Mo^{VI}O_2(bdt)_2]$ reacts with $[Mo^{IV}O(dtc)_2]$, this complex does not react with $(NEt_4)_2[Mo^{IV}O(SC_6F_5)_4]$ or $(NEt_4)_2[Mo^{IV}O(p\text{-}ClC_6H_4S)_4]$ in spite of their more negative ($Mo^{IV}O^{2+}$ / $Mo^{V}O^{+}$) redox potential (-0.03 and -0.66 V). This is likely that the steric hindrance between the arene ligand of the Mo(IV) complexes and the bdt ligand of

Scheme 3

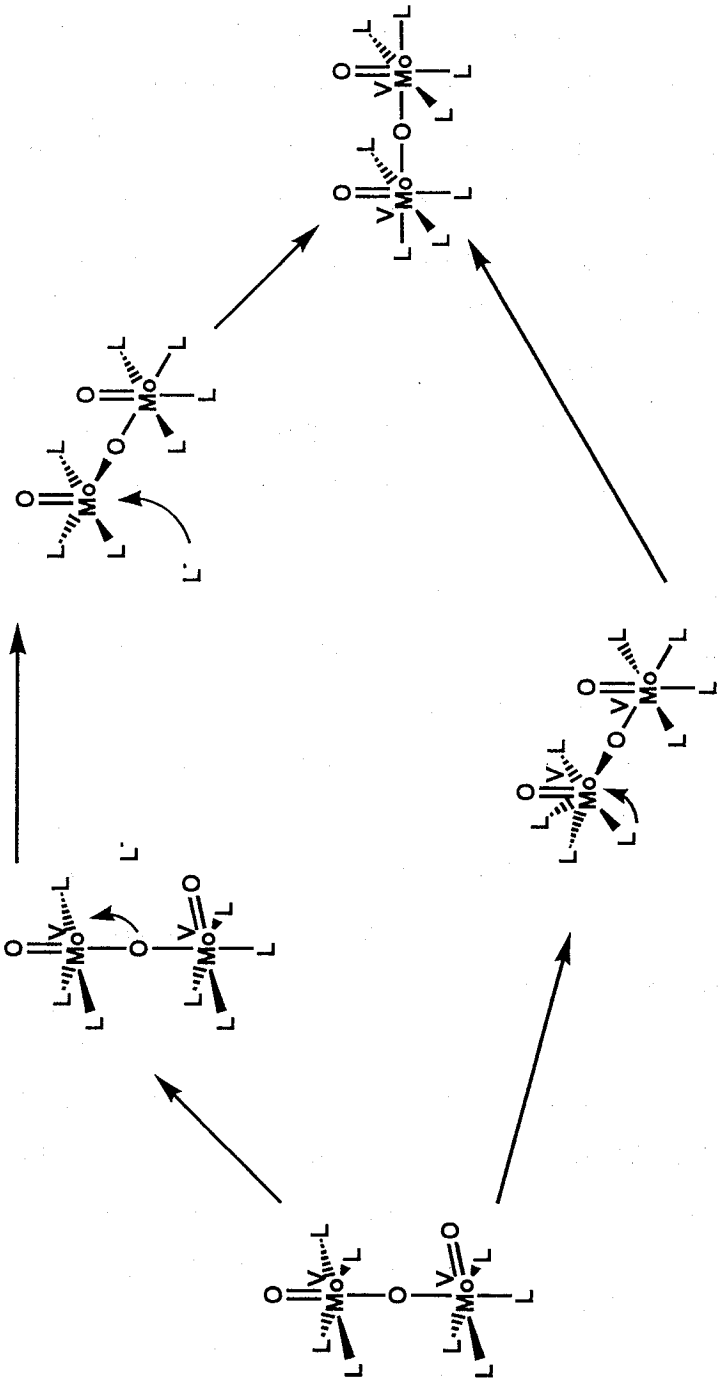

the Mo(VI) complex, and the lower acidity of the Mo(IV) ion of the two complexes weakening the coordinating of the oxo ligand of Mo(VI) to Mo(IV) complex (step **I**).

Although, $(NEt_4)_2[Mo^{VI}O_2(bdt)_2]$ affords the μ-oxo dimer as an intermediate only in the reaction with $[Mo^{IV}O(dtc)_2]$, this complex does not react with $(NEt_4)_2[Mo^{IV}O(SC_6F_5)_4]$, $(NEt_4)_2[Mo^{IV}O(bdt)_2]$, or $(NEt_4)_2[Mo^{IV}O(p\text{-}ClC_6H_4S)_4]$. $[Mo^{IV}O(dtc)_2]$ has lower $Mo^{IV}O^{2+}$ / $Mo^{V}O^{+}$ redox potential than that of other three Mo(IV) complexes, indicating the enough coordinating space highly facilitate the formation of the μ-oxo dimer. Thus, the rearrangement (step **III**) is an important step for the achievement of the μ-oxo dimer formation. Although the bdt ligand has no steric hindrance, no reaction occur between $(NEt_4)_2[Mo^{IV}O(bdt)_2]$ and $(NEt_4)_2[Mo^{VI}O_2(bdt)_2]$. This is also due to the inhibition of the rearrangement of the trans to the cis configuration. In the reaction with $(NEt_4)_2[Mo^{IV}O(\alpha,2\text{-tdt or edt})_2]$, the production of the oxomolybdenum(V) complexes is due to the extreme negative redox potential (-0.74, -0.84 V of $Mo^{IV}O^{2+}$ / $Mo^{V}O^{+}$).

$[Mo^{VI}O_2(cys\text{-}OMe)_2]$ is quite inert to the μ-oxo dimer formation reaction in the reaction studied in here. This is due to the negative redox of $Mo^{VI}O_2^{2+}$ / $Mo^{V}O^{2+}$ (-1.25 V) of this complex and the low reactivity of the oxo ligand because of the weak trans effect of the N ligand to Mo=O.[6,36,43] When the catalytic oxidation of triphenylphosphine or benzoin by $[Mo^{VI}O_2(cys\text{-}OMe)_2]$ is carried out, the μ-oxo dimer $[(cys\text{-}OMe)_2Mo^{V}(O)\text{-}O\text{-}Mo^{V}O(cys\text{-}OMe)_2]$ is formed.[7] Thus, $[Mo^{VI}O_2(cys\text{-}OMe)_2]$ reacts with $[Mo^{IV}O(cys\text{-}OMe)_2]$ to give the μ-oxo dimer. This formation is due to the high reactivity of the $[Mo^{IV}O(cys\text{-}OMe)_2]$. Actually, this oxomolybdenum(IV) complex has not been isolated to date.

Relevance to the reaction between oxomolybdenum(IV) complexes with amine-*N*-oxide.

In general, oxomolybdenum(IV) complex has been expected to react with oxo-donating reagents such as pyO, Me_3NO, or DMSO to produce the dioxomolybdenum(VI) complex.[6] For example, $[Mo^{IV}O(dtc)_2]$[19] readily reacts with these reagents to give the dioxomolybdenum(VI) complexes.

Although $(NEt_4)_2[Mo^{IV}O(bdt)_2]$ reacts with Me_3NO to give the $(NEt_4)_2[Mo^{VI}O_2(bdt)_2]$, this Mo(IV) complex does not react with pyO or DMSO, indicating that the oxo-accepting reactivity of this Mo(IV) complex is weaker than that of $[Mo^{IV}O(dtc)_2]$.[14,15] Recently, we showed that $[Mo^{IV}O(\alpha,2\text{-tdt})_2]^{2-}$ did not react with DMSO, pyO, and Me_3NO, and suggested that this is due to the strong Mo-S bond preventing the rearrangement from the trans-Mo(O)(OR) form to the cis form in the oxo-transfer process.[17] This proposed reaction mechanism is quite similar to that of the formation of the μ-oxo dimer by the comproportionation reaction between oxomolybdenum(IV) and dioxomolybdenum(VI) complexes.

Thus, the first step is the coordination of the oxo-donating reagent to the Mo(IV) complex. Since these oxo-donating reagents do not accept one-electron, the production of oxomolybdenum(V) complex does not occur. The following reaction is the rearrangement of *cis* to the *trans* configuration of the *trans*-O=Mo-ONR_3 complex, or *trans*-O=Mo=O complex which is the two electron transfer reaction product. No oxo-accepting reaction is due to the inhibition of the rearrangement by the alkanedithiolate chelating ligand. Thus, the strong Mo-S bond of the alkanedithiolate chelating ligand inhibits the rearrangement of the *cis*-O=Mo-ONR3 to *trans*-O=Mo-ONR_3 complex.

References

(1) *Molybdenum Enzymes*; Spiro, T. G., Ed.; John-Wiley: New York, 1985.

(2) Cramer, S. P.; Wahl, R.; Rajagopalan, K. V. *J. Am. Chem. Soc.* **1981**, *103*, 7721.

(3) Rajagopalan, K. V. In *Advances in Enzymology and Related Areas of Molecular Biology*; A. Meister, Ed.; Wiley: New York, 1991; Vol. 64; pp 215-290.

(4) Barber, M.; Neame, P. J. *J. Biol. Chem.* **1990**, 20912.

(5) Hille, R.; Sprecher, H. *J. Biol. Chem.* **1987**, *262*, 10914.

(6) Holm, R. H. *Chem. Rev.* **1987**, *87*, 1401.

(7) Ueyama, N.; Kamabuchi, K.; Nakamura, A. *J. Chem. Soc., Dalton Trans.* **1985**, 635.

(8) Newton, W. E.; Corbin, J. L.; Bravard, D. C.; Searles, J. E.; McDonald, J. *Inorg. Chem.* **1974**, *13*, 1100.

(9) Matsuda, T.; Tanaka, K.; Tanaka, T. *Inorg. Chem.* **1979**, *18*, 454.

(10) Roberts, S. A.; Young, C. G.; Cleland, W. E. J.; Ortega, R. B.; Enemark, J. H. *Inorg. Chem.* **1988**, *27*, 3044.

(11) Caradonna, J. P.; Reddy, P. R.; Holm, R. H. *J. Am. Chem. Soc.* **1988**, *110*, 2139.

(12) Harlan, E. W.; Berg, J. M.; Holm, R. H. *J. Am. Chem. Soc.* **1986**, *108*, 6992.

(13) Craig, J. A.; Holm, R. H. *J. Am. Chem. soc.* **1989**, *111*, 2111.

(14) Yoshinaga, N.; Ueyama, N.; Okamura, T.; Nakamura, A. *Chem. Lett.* **1990**, 1655.

(15) Oku, H.; Ueyama, N.; Kondo, M.; Nakamura, A. *Inorg. Chem.* **1994**, *33*, 209-216.

(16) Ueyama, N.; Yoshinaga, N.; Okamura, T.; Zaima, H.; Nakamura, A. *J. Mol. Catal.* **1991**, *64*, 247.

(17) Ueyama, N.; Kondo, M.; Nakamura, A. *Bull. Chem. Soc. Jpn.* **1994**, *67*, 1840-1847.

(18) Kondo, M.; Ueyama, N.; Nakamura, A.; Waters, J. M.; Ainscough, E. W.; Brodie, A. M. *to be submitted*

(19) Mitchell, P. C. H.; Scarle, R. D. *J. Chem. Soc., Dalton Trans.* **1975**, 2552.

(20) Kondo, M.; Ueyama, N.; Fukuyama, K.; Nakamura, A. *Bull. Chem. Soc. Jpn.* **1993**, *66*, 1391.

(21) Ueyama, N.; Yoshinaga, N.; Okamura, T.; Zaima, H.; Nakamura, A. *J. Mol. Catal.* **1989**, *55*, 284.

(22) Jowitt, R. N.; Mitchell, P. C. H. *J. Chem. Soc. A.* **1970**, 1702.

(23) Kay, A.; Mitchell, P. C. H. *J. Chem. Soc. A.* **1968**, 2421.

(24) Ellis, S. R.; Collison, D.; Garner, C. D. *J. Chem. Soc., Dalton Trans.* **1989**, 413.

(25) Barral, R.; Bocard, C.; Sérée de Roch, I.; Saus, L. *Tetrahedron Lett.* **1972**, 1693.

(26) Reynolds, M. S.; Berg, J. M.; Holm, R. H. *Inorg. Chem.* **1984**, *23*, 3057.

(27) Ellis, S. R.; Collison, D.; Garner, C. D.; Clegg, W. *J. Chem. Soc., Chem. Commun.* **1986**, 1483-1485.

(28) Hanson, G. R.; Brunette, A. A.; McDonell, A. C.; Murray, K. S.; Wedd, A. G. *J. Am. Chem. Soc.* **1981**, *103*, 1953.

(29) Dance, I. E.; Wedd, A. G.; Boyd, I. W. *Aust. J. Chem.* **1978**, *31*, 519.

(30) Zubieta, J. A.; Maniloff, G. B. *Inorg. Nucl. Chem. Lett.* **1976**, *12*, 121.

(31) Blake, A. B.; Cotton, F. A.; Wood, J. S. *J. Am. Chem. Soc.* **1964**, *86*,

(32) Ricard; Estienne, J.; Karagiannidis, P.; Toledano, P.; Fischer, J.; Nitschler, A.; Weiss, R. *J. Coor. Chem.* **1974**, *3*, 277.

(33) Knox, J. R.; Prout, C. K. *Acta Crystallogr., Sect. B: Struct. Crystallot. Cryst. Chem.* **1969**, *B25*, 2281.

(34) Craig, J. A.; Harlan, E. W.; Snyder, B. S.; Whitener, M. A.; Holm, R. H. *Inorg. Chem.* **1989**, *28*, 2082.

(35) Bino, A.; Cohen, S.; Tsimering, L. *Inorg. Chim. Acta.* **1983**, *77*, L19.

(36) Topich, J.; Lyon, J. T., III *Inorg. Chem.* **1984**, *23*, 3202.

(37) Newton, W. E.; McDonald, J. W. *Less-Commmon Met.* **1977**, *54*, 51.

(38) Chatt, J.; Dilworth, J. R. *J. Chem. Soc., Dalton Trans.* **1974**, 517-518.

(39) Hursthouse, M. B.; Motevalli, M. *J. Chem. Soc., dalton Trns.* **1979**, 1362.

(40) Bishop, M. W.; Chatt, J.; Dilworth, J. R. *J. Chem. Soc., Dalton Trans.* **1979**, 1.

(41) Harmer, M. A.; Halbert, T. R.; Coyle, W.-H. P. C. L.; Cohen, S. A.; Stiefel, E. I. *Polyhedron* **1986**, *5*, 341.

(42) Berg, J. M.; Hodgson, K. O. *Inorg. Chem.* **1980**, *19*, 2180.

(43) Buchanan, I.; Minelli, M.; Ashby, M. T.; King, T. J.; Enemark, J. H.; Garner, C. D. *Inorg. Chem.* **1984**, *23*, 495.

(44) De Hayes, L. J.; Faulkner, H. C.; Koub, W. H. J.; Sawyer, D. T. *Inorg. Chem.* **1975**, *14*, 2110.

(45) Boyde, S.; Ellis, S. R.; Garner, C. D.; Clegg, W. *J. Chem. Soc., Chem. Commun.* **1986**, 1541.

(46) Ueyama, N.; Yoshinaga, N.; Nakamura, A. *J. Chem. Soc., Dalton Trans.* **1990**, 387.

Chapter VI

Ligand Exchange Reaction of $[Mo^{IV}O(p\text{-}ClC_6H_4S)_4]^{2-}$ with a Tetradentate Peptide Ligand.

Introduction

Molybdenum ion at the active site of the molybdenum enzymes such as oxomolybdoenzymes or nitrogenase shows the specific catalytic reactivity to the several substrates. Recently, it has been reported that the chelating peptide Z-cys-Pro-Leu-cys-OMe gives the highly reactive oxomolybdenum(V and IV) complexes.[1] These complexes exist in the two conformational isomers *i.*e. parallel- and anti-parallel type complexes. (see Figure 5 in Chapter I) In the two isomers, only parallel-type one shows a more positive Mo(V)/Mo(IV) redox potential. The oxomolybdenum(IV) complex having parallel-type peptide chelation was prepared by the one-electron reduction from the Mo(V) complex, and showed the specific reactivity to the several substrates such as benzonitrile, phenylacetylene, or trimethylsilylazide.[1] Although the selective synthesis of parallel-type oxomolybdenum(V) complex was attempted by using the tetradentate peptide chelate *cis*-1,2-cyclohexylene(CO-cys-Pro-Leu-cys-OMe)$_2$, the complex obtained was thermally unstable at room temperature.

We have shown that the oxomolybdenum(IV) complexes are synthesized by the ligand exchange reaction between $[Mo^{IV}O(p\text{-}ClC_6H_4S)_4]^{2-}$ and dithiols in DME. As shown in the study of the oxomolybdenum(V) complex having peptide thiolate ligands such as Z-cys-Pro-Leu-cys-OMe, the active state of the oxomolybdenum complex is expected to be at the Mo(IV) state. Then, an attempt to the synthesis of the oxomolybdenum(IV) complex having tetradentate chelation was carried out by the ligand exchange reaction between $[Mo^{IV}O(p\text{-}ClC_6H_4S)_4]^{2-}$ and a novel tetradentate peptide chelate, *cis*-1,2-cyclohexylene(CO-Ala-cys-Pro-Leu-cys-Gly-Ala-OMe)$_2$. This tetradentate chelate contains the sequence of the cys-Pro-Leu-cys, which was shown to

be effective for the synthesis of the highly reactive oxomolybdenum(IV) complex. An Ala residue is inserted between the cyclohexyl ring and cys residues to confer the thermal stability to the tetradentate chelate of *cis*-1,2-cyclohexylene(CO-cys-Pro-Leu-cys-OMe)$_2$. Chelation of a Cys-Pro-Leu-Cys fragment to iron has been found in the active site of rubredoxin.[2]

Experimental Section

All manipulations were carried out under Ar atmosphere using standard Schlenk techniques. 1,2-Dimethoxyethane (DME) and diethyl ether (Et_2O) were distilled from sodium/benzophenone ketyl, and acetonitrile (MeCN) was distilled over calcium hydride just before use under Ar.

The tetradentate peptide chelate ligand cis-1,2-cyclohexylene(CO-cys-Pro-Leu-Cys-Gly-Ala-OMe)$_2$ was prepared stepwise by the mixed anhydride (MA) method.[3] The starting complexes $(NEt_4)[Mo^{V}O(SPh)_4]$[4] and $(NEt_4)_2[Mo^{IV}O(p\text{-}ClC_6H_4S)_4]$[5] were prepared by the literature method.

Synthesis of $(NEt_4)[Mo^{V}O\{$*cis*-1,2-cyclohexylene(CO-Ala-cys-Pro-Leu-cys-Gly-Ala-OMe)$_2\}]$. $(NEt_4)_2[Mo^{IV}O(p\text{-}ClC_6H_4S)_4]$ (1.9 mg, 2.0 x 10^{-6} mol) and the cis-1,2-cyclohexylene(CO-Ala-Cys-Pro-Leu-Cys-Gly-Ala-OMe)$_2$ (13 mg, 9.2 x 10^{-6} mol) were stirred in DME (8 mL) at room temperature for overnight. The pink solution obtained was filtered, and reduced in volume to about 2 mL. Diethyl ether (10 mL) was carefully added to the solution to give the pink precipitation.

Physical measurement. Absorption and CD spectra were recorded on JASCO Ubest-30 and JASCO J-40 spectrometers, respectively, in DME solution with 1 mm matched silica cells. ESR spectrum was recorded on a JEOL JES-FE1X spectrometer in DME (4:1) solution at room temperature and 77 K. Cyclic voltammograms were taken on a Yanaco P-1100 polarographic analyzer in DME solution with a glassy carbon electrode and $(n\text{-}Bu)_4NClO_4$ (100 mM) as supporting electrolyte.

Results and Discussion

Synthesis. The ligand exchange reaction between $(NEt_4)_2[Mo^{IV}O(p\text{-}ClC_6H_4S)_4]$ and the tetradentate peptide ligand cis-1,2-cyclohexylene(CO-Ala-Cys-Pro-Leu-Cys-Gly-Ala-OMe)$_2$ produces only oxomolybdenum(V) complex as evidenced by the visible and ESR spectrum. The unsuccessful synthesis of the oxomolybdenum(IV) complex is due to the extreme negative Mo(V)/Mo(IV) redox potential (> -1 V vs. SCE). Attempts to reduce this Mo(V) complex to the Mo(IV) state by the BH_4^- reagent in DME or DME/MeOH solution were unsuccessful. However, this novel tetradentate peptide affords the thermally stable oxomolybdenum(V) complex, probably by the effect of an addition of the Ala residue between CO connecting to the cyclohexylene and Cys in the peptide sequence.

In general, oxomolybdenum(V and IV) complexes show the quasi-reversible Mo(V)/Mo(IV) redox couple in the CV measurement in the range between 0 and -1 V (vs. SCE).[5-9] However, the oxomolybdenum(V)-peptide complex obtained in this study does not show the redox couple in the range between 0 V and -1.5 V (vs. SCE). The Mo(V)/Mo(IV) redox reaction is the adding of one electron to the SOMO orbital, and the removing from the resulting HOMO orbital. The results indicate this peptide Mo(V)complex has high SOMO orbital.

In general, oxomolybdenum(V and IV) complexes having alkanethiolate ligand show the more negative Mo(V)/Mo(IV) redox potential than that of the arenethiolate complexes because of the strong electron donating ability.[5,8-10] We studied the several oxomolybdenum(IV) complexes having alkanedithiolate chelate, and showed that the deviated O-Mo-S-C torsion angle from 90° also affords the high energy HOMO orbital. For example, the Mo(V)/Mo(IV) redox potential of $[Mo^{IV}O(\alpha,2\text{-tdt})_2]^{2-}$ (α,2-tdt^{2-} = α,2-toluenedithiolato) (-0.74 V) is more negative than that of the mean value of $[Mo^{IV}O(bdt)_2]^{2-}$ (bdt^{2-} = 1,2-benzenedithiolato) (-0.37 V) and $[Mo^{IV}O(edt)_2]^{2-}$ (edt^{2-} = 1,2-ethanedithiolato) (-0.84 V). This is due to the deviated O-Mo-S-C torsion angle from

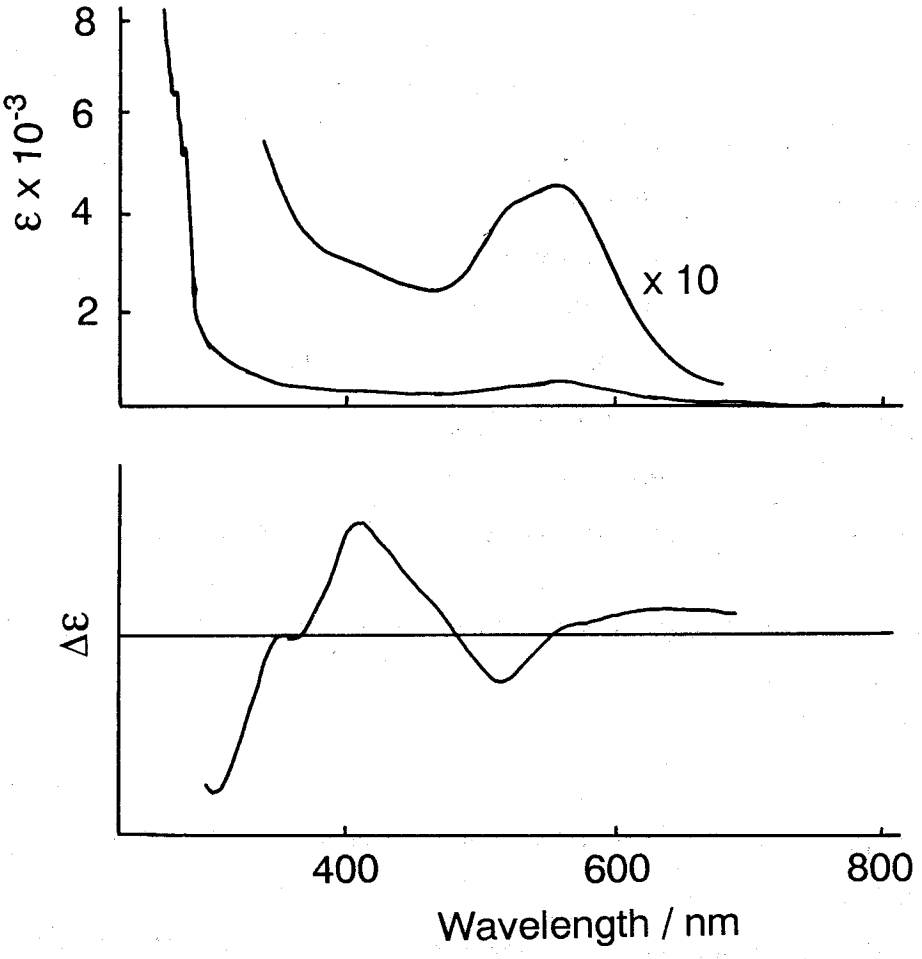

Figure 1. The absorption (top) and the CD (bottom) spectra of (NEt4)[$Mo^{V}O$\{*cis*-1,2-cyclohexylene(CO-Ala-cys-Pro-Leu-cys-Gly-Ala-OMe)$_2$\}] in DME solution.

Table I. Absorption Parameters of Oxomolybdenum(V) Thiolate Complexes.

Complex	LMCT (ε)	References
$(NEt_4)[Mo^VO(cy(acplcga)_2)]$[a]	558 (470)	this work
$(NEt_4)[Mo^VO(cplc)_2]$[b]	540 (parallel)	1
	509 (anti-parallel)	
$(NEt_4)[Mo^VO(SPh)_4]$	598 (6600)	4
$(NEt_4)[Mo^VO(bdt)_2]$	452 (470)	11
$(NEt_4)[Mo^VO(\alpha,2\text{-tdt})_2]$	454 (2300), 520 (4100),	
	600 (5200), 720 (2300)	12
$(NEt_4)[Mo^VO(edt)_2]$	448 (750), 519 (690), 625 (886)	remeasured

a) cy(acplcga)$_2$ = *cis*-1,2-cyclohexylene(CO-Ala-cys-Pro-Leu-cys-Gly-Ala-OMe)$_2$

b) cplc = Z-cys-Pro-Leu-cys-OMe

90° of the $[Mo^{IV}O(\alpha,2\text{-tdt})_2]^{2-}$ (*ca.* 18°) compared with those of $[Mo^{IV}O(bdt)_2]^{2-}$ (*ca.* 0°) and $[Mo^{IV}O(edt)_2]^{2-}$ (*ca.* 9°).[9,10]

Physical Properties. The peptide complex $(NEt_4)[Mo^VO\{$*cis*-1,2-cyclohexylene(CO-Ala-cys-Pro-Leu-cys-Gly-Ala-OMe)$_2\}]$ obtained has CT transition maximum at 558 nm (ε; 470) and the shoulder band at 530 nm (ε; 430) in DME solution (Figure 1). The electronic spectral data of oxomolybdenum(V) complexes having thiolate ligands are summarized in Table I. In general, the oxomolybdenum(V) thiolate complexes show the LMCT transition in the visible region.[11] The band energy and the strength (ε) of this tetradentate peptide complex are similar to that of some related oxomolybdenum(V) complexes having alkanedithiolate chelating *e.g.* $[Mo^VO(edt)_2]^-$ or $[Mo^VO(Z\text{-cys-Pro-Leu-cys-OMe})_2]^-$.[1]

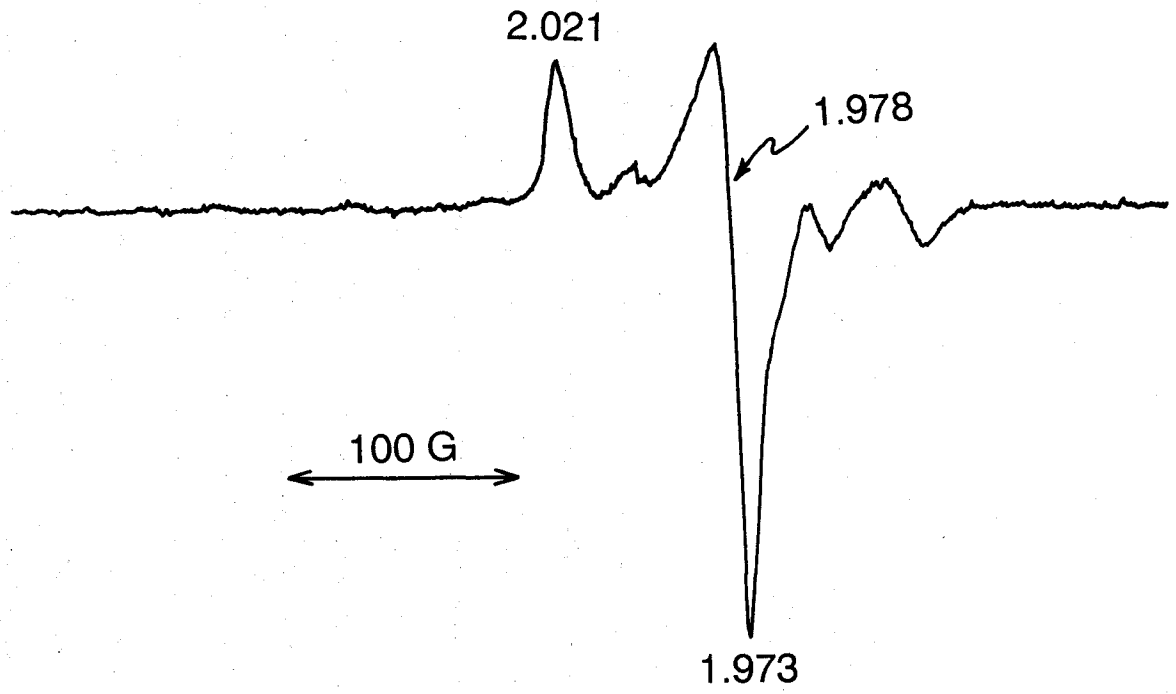

Figure 2. ESR spectrum of $(NEt_4)[Mo^{V}O\{cis\text{-}1,2\text{-}cyclohexylene(CO\text{-}Ala\text{-}cys\text{-}Pro\text{-}Leu\text{-}cys\text{-}Gly\text{-}Ala\text{-}OMe)}_2\}]$ in DME solution at 77K.

Table II. ESR parameters of Oxomolybdenum(V) Thiolate Complexes.

Complex	g_z	g_x	g_y	g_{av}	references
$(NEt_4)[Mo^VO(cy(acplcga)_2)]$[a]	2.021	1.978		1.988	this work
$(NEt_4)[Mo^VO(cplc)_2]$[b] (parallel type)	2.028	1.981	1.961	1.990	1
(anti-parallel type)	2.016	1.966		1.980	
$(NEt_4)[Mo^VO(bdt)_2]$	2.022	1.984	1.976	1.994	11
$(NEt_4)[Mo^VO(\alpha,2\text{-tdt})_2]$	2.035	1.980	1.976	1.997	12
$(NEt_4)[Mo^VO(edt)_2]$	2.050	1.983			

a) $cy(acplcga)_2$ = *cis*-1,2-cyclohexylene(CO-Ala-cys-Pro-Leu-cys-Gly-Ala-OMe)$_2$

b) cplc = Z-cys-Pro-Leu-cys-OMe

The present peptide complex shows the intense ESR signal at room temperature and 77 K. Figure 2 shows the ESR spectrum of this complex at the low temperature. The $g_\perp$, $g_{//}$ and g_{av} values are 2.021, 1.978, and 1.988 respectively.

The ESR spectra for the peptide complex in fluid and frozen DME solutions indicate that the only one ESR active molybdenum species is present. The ESR pattern and the g values of this tetradentate peptide complex is close to that of the anti-parallel type of the peptide complex $[Mo^VO(Z\text{-cys-Pro-Leu-cys-OMe})_2]^-$ than that of the parallel type complex. This result indicates that the coordinating conformation regulated in the tetradentate ligand *cis*-1,2-cyclohexylene(CO-cys-Pro-Leu-cys-OMe)$_2$ is near the anti-parallel type coordination than that of parallel type in Z-cys-Pro-Leu-cys-OMe chelation.

Ueyama et al. reported that the ESR spectrum of $(NEt_4)[Mo^VO\{$*cis*-1,2-cyclohexylene(CO-cys-Pro-Leu-cys-OMe)$_2\}]$ is quite similar to that of the parallel-type complex of $[Mo^VO(Z\text{-cys-Pro-Leu-cys-OMe})_2]^-$, indicating that the coordinating environments both complexes are similar.[1] The results indicate that the effect of this

tetradentate chelating is not similar to that of the desired parallel-type complex of $[Mo^{V}O(Z\text{-cys-Pro-Leu-cys-OMe})_2]^-$.

Conclusion

The tetradentate peptide chelating *cis*-1,2-cyclohexylene(CO-Ala-cys-Pro-Leu-cys-Gly-Ala-OMe)$_2$ affords the thermally stable oxomolybdenum(V) complex at room temperature. The ESR spectrum of this complex suggests that the electronic state of this complex is close to that of the anti-parallel type of $[Mo^{V}O(Z\text{-cys-Pro-Leu-cys-OMe})_2]^-$ than that of the parallel-type complex.

Acknowledgment. We are grateful to Professor Mikiharu Kamachi and Dr. Atsushi Kajiwara for the measurements of electron spin resonance spectroscopy in the department of Macromolecular Science, Faculty of Science, Osaka University.

References

(1) Ueyama, N.; Yoshinaga, N.; Kajiwara, A.; Nakamura, A. *Chem. Lett.* **1990**, 1781.

(2) Adman, E. T.; Sieker, L. C.; Jensen, L. H.; Bruschi, M.; LeGall, J. *J. Mol. Biol.* **1987**, *112*, 113.

(3) Sun, W.-Y. Doctoral thesis Thesis, Osaka University, 1993.

(4) Boyd, I. W.; Dance, I. G.; Murray, K. S.; Wedd, A. G. *Aust. J. Chem.* **1978**, *31*, 279.

(5) Kondo, M.; Ueyama, N.; Fukuyama, K.; Nakamura, A. *Bull. Chem. Soc. Jpn.* **1993**, *66*, 1391.

(6) Bradbury, J. R.; Masters, A. F.; McDonell, A. C.; Brunette, A. A.; Bond, A. M.; Wedd, A. G. *J. Am. Chem. Soc.* **1981**, *103*, 1959.

(7) Ellis, S. R.; Collison, D.; Garner, C. D. *J. Chem. Soc., Dalton Trans.* **1989**, 413.

(8) Boyde, S.; Ellis, S. R.; Garner, C. D.; Clegg, W. *J. Chem. Soc., Chem. Commun.* **1986**, 1541.

(9) Ueyama, N.; Kondo, M.; Nakamura, A. *Bull. Chem. Soc. Jpn.* **1994**, *67*, 1840-1847.

(10) Kondo, M.; Ueyama, N.; Nakamura, A.; Waters, J. M.; Ainscough, E. W.; Brodie, A. M. *to be submitted*

(11) Hanson, G. R.; Brunette, A. A.; McDonell, A. C.; Murray, K. S.; Wedd, A. G. *J. Am. Chem. Soc.* **1981**, *103*, 1953.

(12) Oku, H.; Ueyama, N.; Kondo, M.; Nakamura, A. *Inorg. Chem.* **1994**, *33*, 209-216.

(13) Ueyama, N.; Yoshinaga, N.; Kajiwara, A.; Nakamura, A.; Kusunoki, M. *Bull. Chem. Soc. Jpn.* **1991**, *64*, 2458.

Chapter VII

Synthesis and Properties of a Nitridomolybdenum(VI) Complex Having Benzenedithiolate Ligand. Effect of the Thiolate on the Activation of the Nitride Ligand

Introduction

A number of dinitrogen molybdenum(0) complexes have been synthesized to date using phosphorus ligands as model compounds of active sites of nitrogenase.[1,2] However, when those complexes are treated with strong acids such as HCl, only less than 50 % yield of ammonia is produced. During the reduction process, production of a nitridomolybdenum complex as an intermediate has been suggested (Scheme 1).

Scheme 1

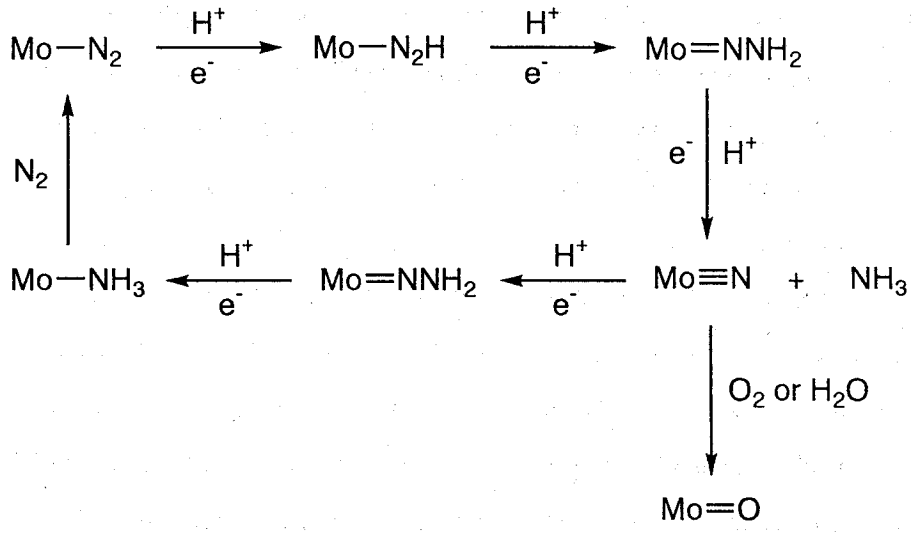

Proposed reduction mechanism of dinitrogen ligand of molybdenum complex.

Table I. Yield of ammonia production by the reductive hydrolysis of nitridomolybdenum complexes.

Reagent	Yield of ammonia (%) (based on Mo) $[(n\text{-Bu}4)4N][Mo^{VI}NCl4]$	$[(n\text{-Bu}4)4N][Mo^{VI}N(S\text{-}t\text{-Bu})4]$
$NaBH_4$	1.2	10.6
$NaBH_4$-HCl	19.2	12.1
H_2SO_4	0.0	18.3
NaOH	13.0	22.3

Conditions; 2 h, 30 °C, solvent; THF/EtOH (3 mL/1 mL).
Complex, 5 x 10^{-2} mmol; Reagents/Mo = 20 (mol/mol).

It has been proposed that the low yield of the ammonia production is due to the difficulty of the hydrolytic reduction of the metal-nitride triple bond ($Mo^{VI}\equiv N$). Actually, nitridomolybdenum complexes having P, N, or O ligands give only a small amount of ammonia in the reaction with strong acids.[3] Therefore, activation of the nitride ligand is one of the most important steps for the achievement of the catalytic reduction of dinitrogen to ammonia.

EXAFS studies have shown that the Fe-Mo cluster having many S ligands exists at the active site of nitrogenase.[4] Actually, a recent X-ray analysis of *Azobacter vinelandii* shows the Fe-Mo cluster ligated by many S ligands.[5] The synthesis of nitridomolybdenum(VI) complexes having bulky thiolate ligands, $[Mo^{VI}N(S\text{-}^{t}Bu)4]^{-}$, has been attempted in this laboratory. Although the isolation was difficult because of the thermal instability, this complex shows the increase of ammonia production compared with $[Mo^{VI}NCl4]^{-}$ in the reaction with acids or bases (Table I).

In order to understand the i) activation effect of the thiolate on the nitride ligand and ii) function of the molybdenum ion in the active site of nitrogenase, a nitridomolybdenum(VI) complex having 1,2-benzenedithiolate (bdt) ligand was synthesized. The extremely air-sensitive nitridomolybdenum(VI) complex obtained was characterized by Raman, IR, absorption, and NMR spectroscopic method.

Experimental Section

All manipulations were carried out under Ar atmosphere using standard Schlenk techniques. 1,2-Dimethoxyethane (DME) and tetrahydrofuran (THF) were distilled from sodium/benzophenone ketyl, and dimethylformamide (DMF), acetonitrile (MeCN), MeCN-d_3, dimethylsulfoxide (DMSO), and dichloromethane (CH_2Cl_2) were distilled over calcium hydride before use under Ar.

The starting complex $(NEt_4)[Mo^{VI}NCl_4]$[3,6] and 1,2-benzenedithiol (H_2-bdt)[7,8] were prepared by the literature method. Dilithium 1,2-benzenedithiolate (Li_2-bdt) was prepared by the reaction of H_2-bdt with *n*-butyl lithium (1.6 M, *n*-hexane soln.) in DME at 0 °C. This dilithium salt has a dme molecule as a crystalline solvent.

Synthesis of $(NEt_4)_2[Mo^{VI}N(bdt)_2Cl]$ (1). The complex $(NEt_4)[Mo^{VI}NCl_4]$ (0.18 g, 0.47 mmol) was added dropwise to the Li-bdt•dme (0.29 g, 1.2 mmol) in DMF/THF (5 mL/10 mL) solution with stirring on the dry ice-methanol bath (*ca.* -70 °C). The reaction mixture was stirred at the low temperature for 30 min. and room temperature for 2 h. The green precipitate obtained was collected by filtration, and dissolved in 60 mL of MeCN. After removal of insoluble solids by centrifugation, the solution was reduced in volume to about 5 mL in vacuum. The green microcrystals obtained were collected by filtration, dried *in vacuo*. Yield, 0.048 mmol, 23 %. Elemental analysis, Calcd for $C_{28}H_{48}ClN_3S_4Mo$: C,49.00; H,7.05; N,6.12. Found: C,50.46; H,7.47; N,5.43. Low carbon analysis value is inevitable for this complex, and is due to the extreme air-sensitivity.

Reaction of 1 with oxygen gas in solid state. The O_2-oxidized sample was prepared by the mixing of green microcrystals of **1** (about 20 mg) with 5 equimolar of oxygen gas for about 5 min. at room temperature. The atmosphere was evacuated and admitted of Ar gas for three times. The obtained brownish sample was then transferred into an IR cell under Ar, and measured by IR spectra using O_2-free nujol. For the Raman spectrum measurement, KBr pellet containing the solid powdered sample was prepared and fixed in the glass tube by using cellophane, and sealed under Ar. The measurement was carried out at room temperature with 514.5 nm excitation.

The IR spectrum of the O_2-oxidized sample was prepared in the similar oxidizing condition was also measured using O_2-free nujol without any reducing pressure process.

Reaction of 1 with oxygen gas at solution state.

i) Stoichiometric reaction for absorption spectrum. To a MeCN solution of **1** (8.7 mM, 0.6 mL, 5.2×10^{-6} mol), 0.1 mL of oxygen gas (5×10^{-6} mol) was bubbled at room temperature. The red purple solution changed to blue. Then, absorption spectrum of the solution was measured.

ii) Stoichiometric reaction for ^{1}H-NMR. **1** (4.2 mg, 6.1×10^{-6} mol) was dissolved in 0.6 mL of MeCN-d_3. To the solution, 0.2 mL of oxygen gas (9×10^{-6} mol) was bubbled at room temperature. The red-purple solution changed to blue solution. This solution showed no clear bdt ligand signals in ^{1}H NMR spectrum, because of the paramagnetic effect of the oxomolybdenum(V) complex produced in low yield.

iii) Reaction with excess O_2 gas. To the MeCN-d_3 solution (0.6 mL) of **1** (2.3 mg, 3.4×10^{-6} mol), 0.4 mL of oxygen gas (2×10^{-5} mol) was bubbled to give a yellow solution. And the ^{1}H NMR spectrum was measured.

Reaction of $(NEt_4)_2[Mo^{IV}O(bdt)_2]$ with excess oxygen gas. To the complex $(NEt_4)_2[Mo^{IV}O(bdt)_2]$ (1.6 mg, 2.5×10^{-6} mol) in 1 mL of MeCN-d_3, 1 mL of O_2 gas (4×10^{-5} mol) was bubbled at room temperature. The ^{1}H NMR spectrum of the yellow solution obtained was measured.

Reaction of $(NEt_4)[Mo^{VI}NCl_4]$ with oxygen gas. This reaction was followed by the absorption spectrum. To the complex $(NEt_4)[Mo^{VI}NCl_4]$ in CH_2Cl_2 (4 mM, 0.6 mL, 2×10^{-6} mol), 0.05 mL of oxygen gas (2×10^{-6} mol) was bubbled. After absorption measurement, excess oxygen gas (0.5 mL, 2×10^{-5} mol) was bubbled to the solution. The time course of the absorption was recorded at 20 min intervals.

Reaction of 1 with H_2O. To the MeCN red-purple solution of **1** (20 mM, 0.6 mL), 2 equimolar of O_2-free H_2O was added to give yellow-orange solution. The reaction was followed by absorption spectrum.

For the preparation of the oxidized sample for the IR spectrum measurement, H_2O (0.02 g, 1×10^{-3} mol) in MeCN (10 mL) was added to the MeCN solution (10 mL) of **1** (0.016 g, 2.3×10^{-5} mol) with stirring at room temperature for 30 min. The brownish solution obtained was evaporated to give yellow-orange powder. The product was dried *in vacuo*. IR spectrum of the product was measured using KBr pellet.

Physical measurement. Absorption spectra were recorded on a JASCO Ubest-30 spectrometer in MeCN solution with 1 mm matched silica cells. Raman spectra were obtained on a JASCO R-800 spectrometer in solid state with 514.5 nm excitation. ^1H NMR spectrum was measured on a JEOL EX 270 spectrometer in MeCN-d_3, and was internally referenced to the residual protio solvent impurity (MeCN-d_2, $\delta \equiv 1.90$). ^{14}N NMR spectrum was taken on a JEOL JNH-GSX spectrometer in DMSO/MeCN-d_3 (4:1) solution, and the chemical shifts were reported relative to external reference of $NaNO_3$.

Results and Discussion

Synthesis. The diamagnetic nitridomolybdenum(VI) complex having bdt ligand, **1**, was synthesized by the reaction of $(NEt_4)[Mo^{VI}NCl_4]$ with excess Li_2-bdt in DMF/THF solution. This reaction was carried out at low temperature (ca. -70 °C) in order to prevent the reduction of Mo(VI) ion to Mo(V) state. This complex was obtained as extreme air-sensitive green microcrystals. Elemental analysis shows this complex has a chloro ligand.

Although a number of nitridomolybdenum(VI) complexes have been synthesized, no complexes ligated by thiolate ligands have been reported. As an example of nitridomolybdenum complex having S ligand, $[Mo^{VI}N(S_2CNEt_2)_3]$[9,10] has been synthesized to date. However, the S ligand of this complex is thioketone like. The bdt ligand has been used for the syntheses of oxo- or dioxomolybdenum(IV, V, or VI) complexes[11,12] because of the higher stabilization effects on the monomeric molybdenum ion by the chelation and electronic delocalization through the phenyl ring compared with benzenethiolate or 1,2-ethanedithiolate ligands. This chelate ligand gave the thermally stable nitridomolybdenum(VI) complex **1**.

Raman and IR Spectra. **1** shows the intense $\nu(Mo^{VI}\equiv N)$ band at 1010 cm^{-1} in the Raman spectrum in the solid state. (Figure 1a) This band disappears in the O_2-oxidized product, which is oxomolybdenum(IV) complex (Figure 1b) (*vide infra*). The differential spectrum between **1** and the oxidized sample more clearly shows the $\nu(Mo^{VI}\equiv N)$ band at 1010 cm^{-1} (Figure1c). This band is lower in 45 cm^{-1} than that of $(NEt_4)_2[Mo^{VI}NCl_4]$ (1055 cm^{-1})[3]. The shift indicates that the $Mo^{VI}\equiv N$ bond of **1** is weaker than that of $(NEt_4)_2[Mo^{VI}NCl_4]$. The lower $\nu(Mo^{VI}\equiv N)$ band of **1** compared with $(NEt_4)[Mo^{VI}NCl_4]$ is due to the competitive $p\pi$-donation from S ligand to $d\pi$ of the Mo atom (Scheme 2) and the trans influence from the Cl ligand to the $Mo^{VI}\equiv N$ bond.

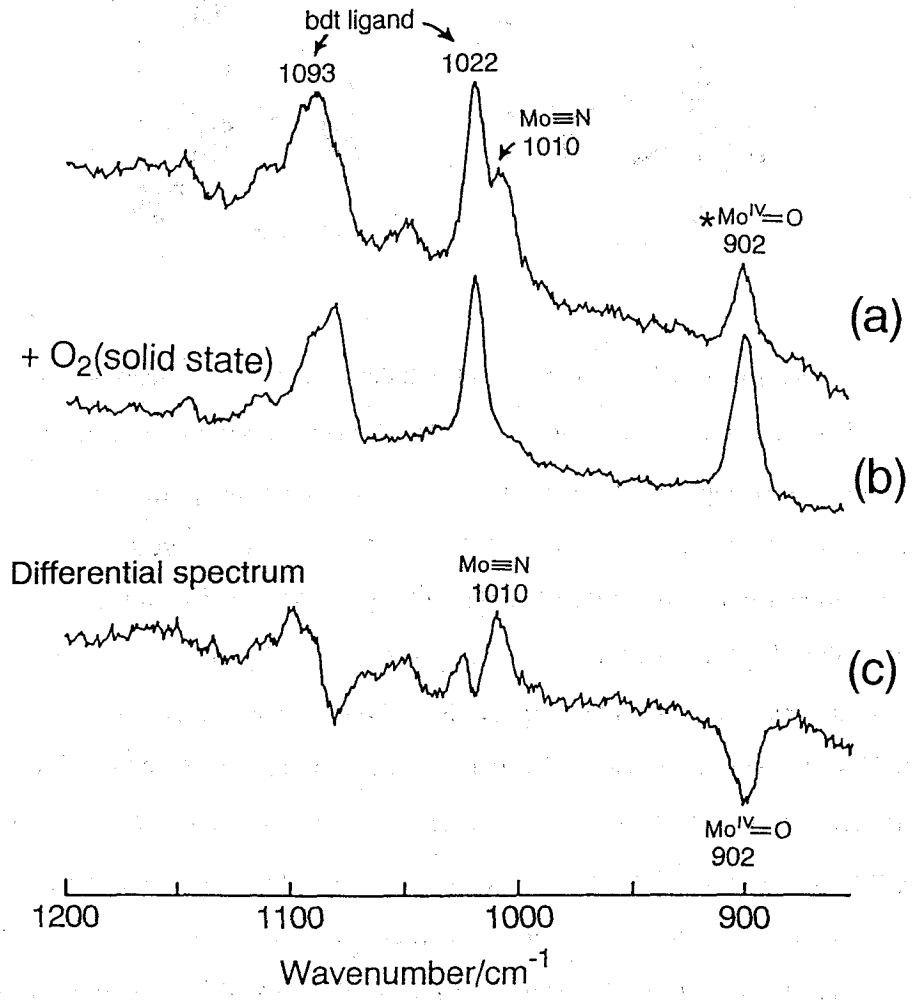

Figure 1. Raman spectra of **1** (a), the oxidized product (b), and the differential spectrum (c).

Scheme 2

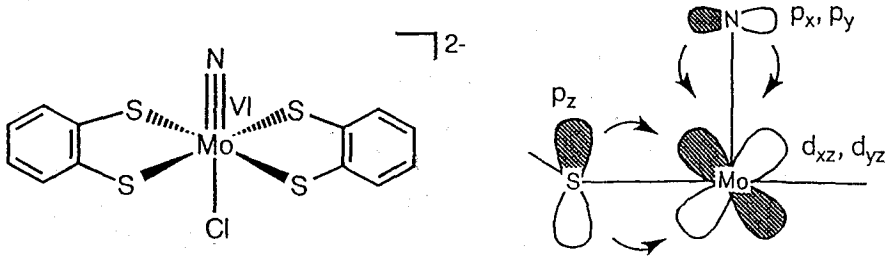

A number of ν(Mo≡N) bands of nitridomolybdenum complexes have been reported to date. Table II summarizes the ν(Mo≡N) data of several nitridomolybdenum complexes, showing that the band is affected by coordinating ligands, molecular structure, and crystal structure. The $[Mo^{VI}NCl_4]^-$ anions have different ν(Mo≡N) band for the several cations; NEt_4^+ (1055 cm^{-1})[3], NMe_4^+ (1054 cm^{-1})[6], $AsPH_4^+$ (1060 cm^{-1})[6,13], PPh_4^+ (1060 cm^{-1})[14], and $Cl_3PNPCl_3^+$ (995 cm^{-1}) [15]. The X-ray crystallographic studies of these complexes have shown that this extremely lower shift of $Cl_3PNPCl_3^+$ complex is due to the trans influence of the infinite -Mo≡N---Mo≡N-- structure. Actually, the Mo≡N bond distance (1.75 (4) Å) of $Cl_3PNPCl_3^+$ complex is longer than those of $AsPH_4^+$ (1.66 (4) Å) or PPh_4^+ (1.637 (4) Å) complexes. The Cl ligand coordination to the trans position of nitrido ligand also gives the lower sift of the triple bond vibration. Thus, the ν(Mo≡N) band of $(NEt_4)_2[Mo^{VI}NCl_5]$ (1028 cm^{-1}) is lower by 27 cm^{-1} than that of $(NEt_4)[Mo^{VI}NCl_4]$.[16] The results show that the coordination to the trans position of the Mo≡N ligand weakens the triple bond by the trans influence.

On the other hand, the complexes having soft ligands such as O, N, S give the lower $\nu(Mo^{VI}\equiv N)$ band compared with that of $(NEt_4)[Mo^{VI}NCl_4]$. For example, $[Mo^{VI}NCl_3(bpy)]$, $[Mo^{VI}N(N_3)_3(bpy)]$, $[Mo^{VI}NCl_3(OPPh_3)_2]$, $(PPh_4)[Mo^{VI}N(OPh)_4]$, $[Mo^{VI}N(t\text{-}BuO)_3]$, and $[Mo^{VI}N(S_2CNEt)_3]$ show the ν(Mo≡N) bands at 1027[3], 972[17], 1042[3], 1033[18],1020[19], and 1015 cm^{-1},[9] respectively,

Table II. Frequencies of $Mo^{VI}{\equiv}N$ bond of nitridomolybdenum complexes.

Complex	$\nu(Mo^{VI}{\equiv}N)/cm^{-1}$	Mo≡N/Mo--N/Å	References
$(NEt_4)[Mo^{VI}NCl_4]$	1056(1055)[a]		3
$(NMe_4)[Mo^{VI}NCl_4]$	1050(1058)[a]		3
	1054		6
$[(n\text{-}Bu)_4N][Mo^{VI}NCl_4]$	1065(1063)[a]		3
	1065		33
$(AsPh_4)[Mo^{VI}NCl_4]$	1060[b]	1.66 (4)	13
$(PPh_4)[Mo^{VI}NCl_4]$	1060	1.637 (4)	14
$(Cl_3PNPCl_3)[Mo^{VI}NCl_4]$[c]	995	1.75 (4) / 2.43 (4)	15
$(AsPh_4)[Mo^{VI}NF_4]$	969	1.83 (4)	20
$(PPh_4)[Mo^{VI}NBr_4]$	1060	1.63 (2)	32
$(NEt_4)_2[Mo^{VI}NCl_5]$	1028		16
$[Mo^{VI}NCl_3]$[d]	1045	1.64 (1) / 2.13	32
		1.67 (1)	
$[Mo^{VI}NCl_3(bpy)]$[e]	1027(1023)[a]		3
	1009		2
$\{HB(Me_2pz)_3\}Mo^{VI}N(N_3)_2$[f]	1023	1.646 (4)	16
$[Mo^{VI}N(N_3)_2Cl(terpy)]$[g]	1005	1.662 (7)	17
$[Mo^{VI}N(N_3)_3(bpy)]$	972	1.642 (5)	17
$[Mo^{VI}NCl_3(OPPh_3)_2]$	1042 (1038)[a]		3
	1038		2
$(PPh_4)[Mo^{VI}N(OPh)_4]$	1033		18
$[Mo^{VI}N(t\text{-}BuO)_3]$[c]	1020	1.661 (4) / 2.883 (8)	19
$[Mo^{VI}N(S_2CNEt_2)_3]$	1015	1.641 (9)	9
$(NEt_4)_2[Mo^{VI}N(bdt)_2Cl]$ (**1**)	1010		this work
$(NEt_4)_2[Mo^{V}NCl_4]$	1050		16
$\{HB(Me_2pz)_3\}Mo^{V}NCl_2$	1020		16

[a] Raman (IR) values. [b] The $\nu(Mo^{VI}{\equiv}N)$ value was sited from Dehnicke et al.[6] [c] polymeric structure; $-Mo^{VI}{\equiv}N\text{--}Mo^{VI}{\equiv}N-$. [d] tetrameric structure; $(Mo^{VI}{\equiv}N)_4$ unit. [e] bpy = bipyridine. [f] $\{HB(Me_2pz)_3\}$ = tris(3,5-dimethylpyrazol-1-yl)hydroborate. [g] terpy = terpyridine.

which are lower than that of $(NEt_4)[Mo^{VI}NCl_4]$ (1056 cm^{-1}). The low wavenumber shifts of these complexes are due to the competitive π-donation from pπ of N, S, O ligands to the Mo dπ. This effect has also been observed in the F ligand, *i.e.* $\nu(Mo^{VI}\equiv N)$ band of $(AsPh_4)[Mo^{VI}NF_4]$ is observed at 969 cm^{-1}.[20]

The $\nu(Mo^{VI}\equiv N)$ band of **1** is not clearly assigned in IR spectrum, because of the hindrance of the strong bands ascribed to phenyl rings. However, the differential spectrum between **1** and the slightly O_2-oxidized sample shows the intensity decrease of the 1004 cm^{-1} band, which is assigned to $\nu(Mo^{VI}\equiv N)$ band. This value is close to that of the Raman result (1010 cm^{-1}).

The absorption spectrum. The green microcrystals of **1** gives a deep red color by dissolution in MeCN. Figure 2 shows the absorption spectrum of **1**. The distinct absorption maxima of **1** appeared at 325 (2880), 448 (220), and 566 nm (200 $M^{-1}cm^{-1}$). Since **1** has no d electron, these two bands at 448 and 566 nm are assigned as CT transition from S pπ to Mo dπ. This transition supports the electronic interaction between S pπ and Mo dπ as suggested from the results of the Raman and IR spectra. Similar CT transition was reported in the dioxomolybdenum(VI) complex having two bdt ligands. Thus, $(NEt_4)_2[Mo^{VI}O_2(bdt)_2]$ shows two CT bands at 420 and 540 nm in MeCN solution.[21] These results show that the electronic state of **1** is similar to that of the dioxomolybdenum(VI) complex $(NEt_4)_2[Mo^{VI}O_2(bdt)_2]$.

NMR Studies. The ^1H NMR and ^{14}N NMR spectra of diamagnetic **1** were measured in MeCN-d_3 and DMSO/MeCN-d_3 (4:1), respectively. The broad proton signals of bdt ligands are observed at 7.48 and 6.74 ppm in ^1H NMR spectrum measurement, because of the rapid spin exchange between **1** and paramagnetic $[Mo^{V}O(bdt)_2]^-$ contaminated by the oxidation reaction with a trace amount of air. (Figure 3a) The sharp signals were obtained by reduction of the contaminated Mo(V) complex by addition of 0.01 equiv. (to **1**) of NEt_4BH_4 (Figure 3b). Similar broadened signals by rapid spin exchange between Mo(IV) and Mo(V) states were observed in ^1H NMR spectrum measurement of an oxomolybdenum(IV) complex, $(NEt_4)_2[Mo^{IV}O(bdt)_2]$ (Figure 3c,d).

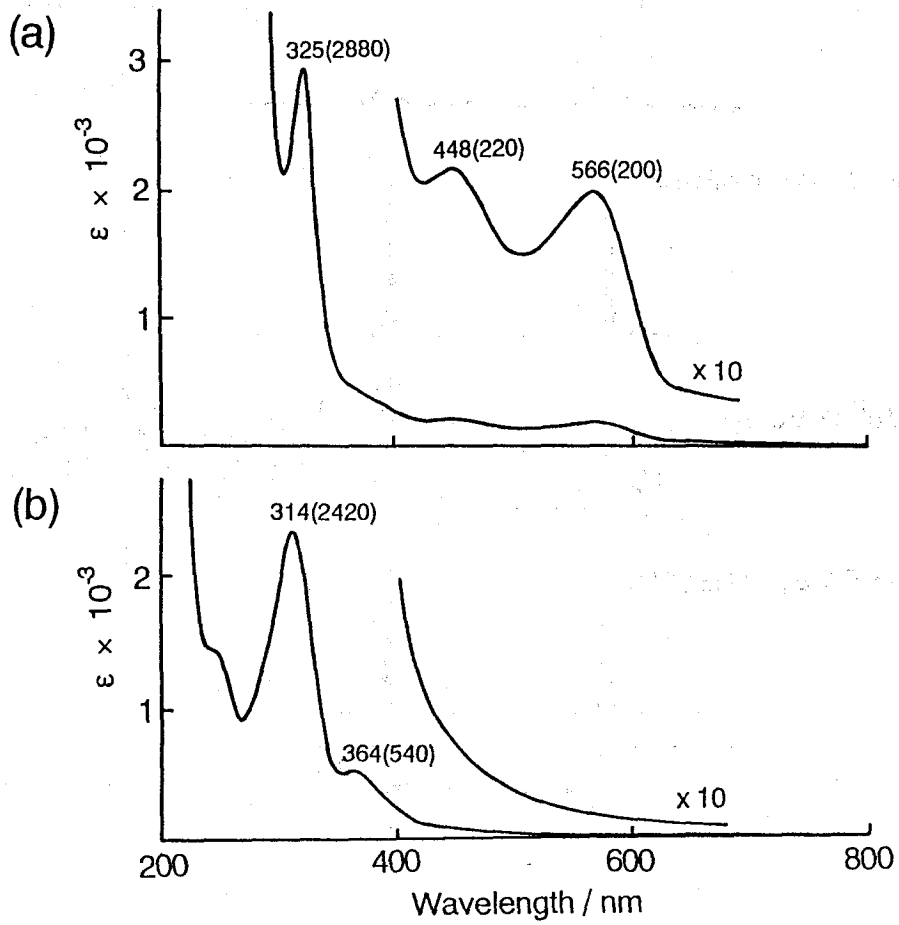

Figure 2. Absorption spectra of $(NEt_4)_2[Mo^{VI}N(bdt)_2Cl]$ (**1**) (a) and $(NEt_4)[Mo^{VI}NCl_4]$ (b) in MeCN solution.

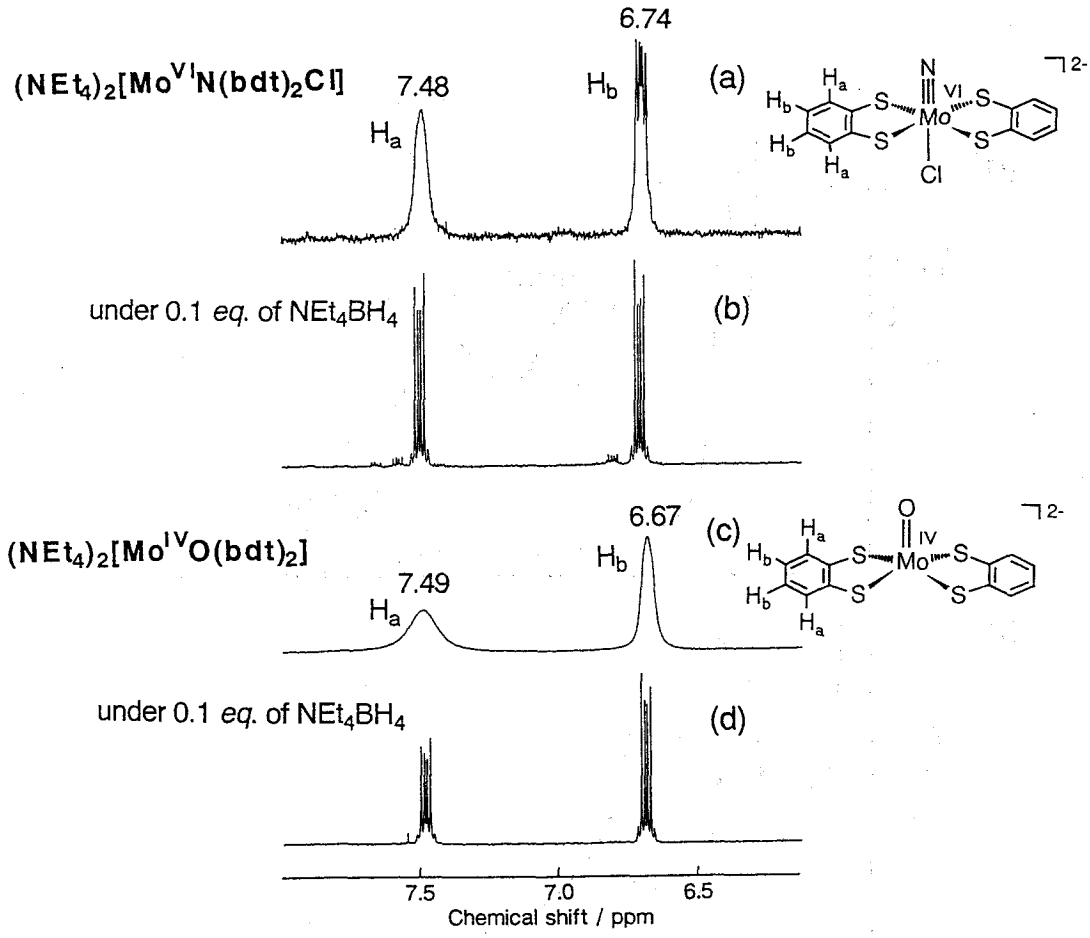

Figure 3. ^{1}H NMR spectra of $(NEt_4)_2[Mo^{VI}N(bdt)_2Cl]$ (**1**) in MeCN-d_3 (a) and MeCN-d_3 in the presence of 0.01 equimolar NEt_4BH_4 (b), and $(NEt_4)_2[Mo^{VI}O_2(bdt)_2]$ in MeCN-d_3 (c) and MeCN-d_3 in the presence of the NEt_4BH_4 (d).

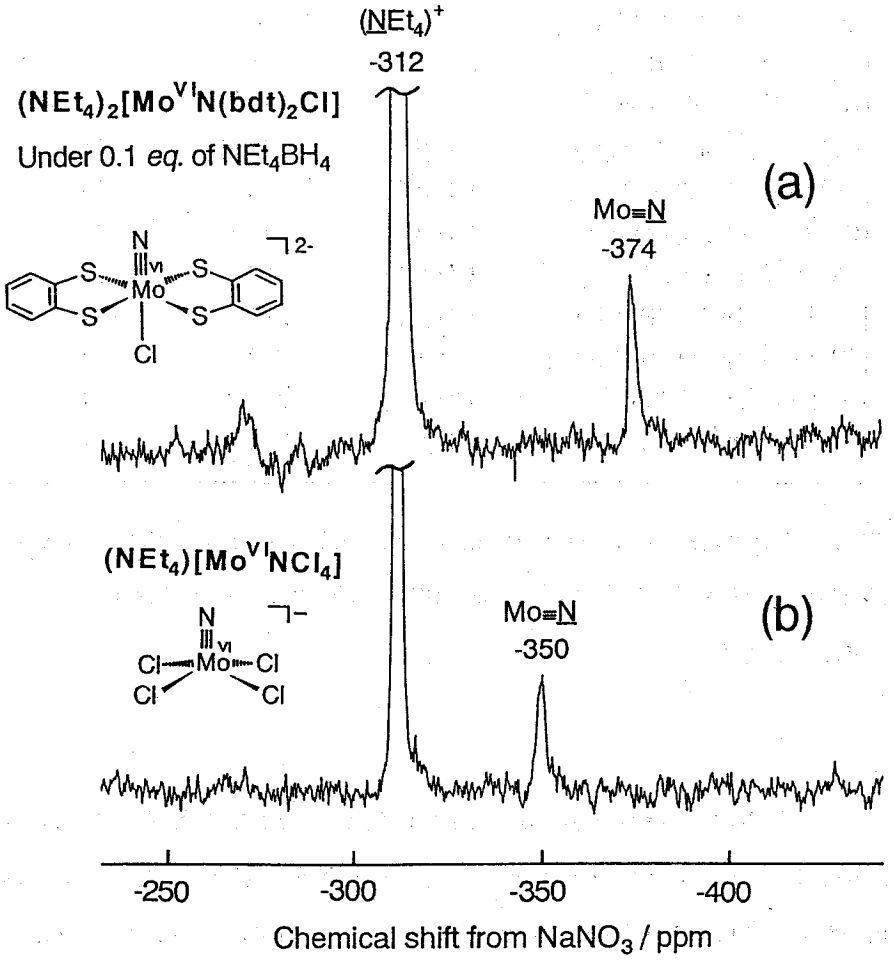

Figure 4. ^{14}N NMR spectra of $(NEt_4)_2[Mo^{VI}N(bdt)_2Cl]$ (**1**) (a) and $(NEt_4)[Mo^{VI}NCl_4]$ (b) in DMSO/MeCN-d_3 (4/1).

Table III. ^{14}N- or ^{15}N NMR data of nitrido complexes

Complex	Solvent	δ [a]	References
trans-[$Mo^{VI}Cl(^{15}N)(dppe)_2$]	THF	166.8	24
trans-[$Mo^{VI}Br(^{15}N)(dppe)_2$]	THF	190.6	24
$(NEt_4)_2[Mo^{VI}N(bdt)_2]$ [b]	c	-374 [d]	This work
$(NEt_4)_2[Mo^{VI}N(bdt)_2]$ [b]	c	-350 [d]	This work
$[Re^{V}Cl_2(^{15}N)(PnPrPh_2)_2]$	CH_2Cl_2	85.8	23
$[Re^{V}Cl_2(^{15}N)(PMe_2Ph)_3]$	CH_2Cl_2	68.2	23
$[Re^{V}Cl_2(^{15}N)(dppe)_2]Cl$ [e]	CH_2Cl_2	67.1	23
$[Mo^{VI}(^{15}N)(S_2CNEt_2)_3]$	CH_2Cl_2	40.0	23
$[W^{VI}_2(^{15}N)Cl_9 \cdot CH_3CN]$	CD_2Cl_2	211.2	34
$[\{W^{VI}(^{15}N)Cl_3 \cdot CH_3CN\}_4]$	CD_2Cl_2	222.7	34
$PPh_4[W^{VI}(^{15}N)Cl_4]$	CH_2Cl_2	258.8	34
$PPh_4[W^{VI}_2(^{15}N)Cl_{10}]$	CH_2Cl_2	251.0	34

[a]Chemical shifts relative to nitromethane. [b]bdt = 1,2-benzenedithiolate. [c]solvent = DMSO-d_6/MeCN-d_3 (4/1). [d]Chemical shifts relative to $NaNO_3$. [e]dppe = $Ph_2CH_2CH_2PPh_2$.

^{14}N NMR signal of nitride ligand of **1** and $(NEt_4)[Mo^{VI}NCl_4]$ appears at -374 ppm and -350 ppm (relative to $NaNO_3$), respectively. (Figure 4) Thus, the nitride ligand of $(NEt_4)[Mo^{VI}NCl_4]$ is more deshielded than that of **1**, indicating the lower electron density of the nitrido ligand of **1** compared with that of $(NEt_4)[Mo^{VI}NCl_4]$. This result is consistent with those of Raman, IR, and absorption spectral results.

Only a few ^{15}N NMR spectra of nitride complexes of molybdenum, tungstenum, or rhenium have been reported to date.[22] Table III summarizes the ^{14}N and ^{15}N NMR spectral data of those complexes. These investigations have shown that the chemical shifts of the nitride ligand depend on the coordination number at the metal center, the type of the ligand, and also on the electron density of the ligand. Thus, the decrease in π-donation of the nitride ligand to the metal ion leads to the upfield of the chemical shift.

The ^{15}N NMR data of nitridomolybdenum complexes, $[Mo^{VI}(^{15}N)(S_2CNEt_2)_3]$[23], *trans*-$[Mo^{IV}Cl(^{15}N)(dppe)_2]$ {dppe = bis (diphenylphospino) ethane}[24], and *trans*-$[Mo^{IV}Br(^{15}N)(dppe)_2]$[24] show the ^{15}N signal at 40.0, 166.8, and 190.6 ppm (relative to nitromethane, which is regarded to have the same chemical shift of $NaNO_3$), respectively. In these complexes, **1** has the most shielded nitrido ligand, suggesting the highest electron density. Observation of the ^{14}N signal of **1** and $(NEt_4)[Mo^{VI}NCl_4]$ at the upfield field region compared with other known complexes is likely due to the anion character of the complexes.

Shielding constant (σ) of the multinuclear NMR spectrum is approximately expressed by the equation 1, where σ_D is the diamagnetic term and σ_P is the paramagnetic term.[25]

$$\sigma = \sigma_D + \sigma_P \qquad (1)$$

The σ_D is expressed by the equation (2).[26]

$$\sigma_D = (3\,mc^2)^{-1} \bullet \{q^2 \langle r^{-1} \rangle\} \qquad (2)$$

where, m is mass of electron, c is velocity of light, q is electron charge density, r is quantum mechanical average. This σ_D term completely corresponds to the electron density of the nuclei. The σ_P is expressed by the equation 3.[27]

$$\sigma_P = (2e^2h^2/3\Delta Em^2c^2)(\langle r^{-3} \rangle_p Pu + \langle r^{-3} \rangle_d Du) \qquad (3)$$

where p and d indicate the p and d orbital, respectively, Pu and Du indicate the charge density bond order matrix, ΔE is related to the electronic excitation energy between the ground state and appropriately weighted excited states. Since the σ_D depends on the inner shell electron, this term is little affected by the bonding with other atoms. Thus, ^{14}N or ^{15}N NMR chemical shifts are considered to be dependent essentially on the paramagnetic term.[28] The change of the electron density of the nitride ligand affects on the Pu and Du in σ_P term.

Reaction of 1 with oxygen gas in the solid state. The reaction of **1** with oxygen gas in the solid state was monitored by Raman and IR spectra. The green microcrystals of **1** rapidly changes to the brownish powder when the sample is exposed to the excess oxygen gas. As mentioned above, the Raman spectrum of the brownish

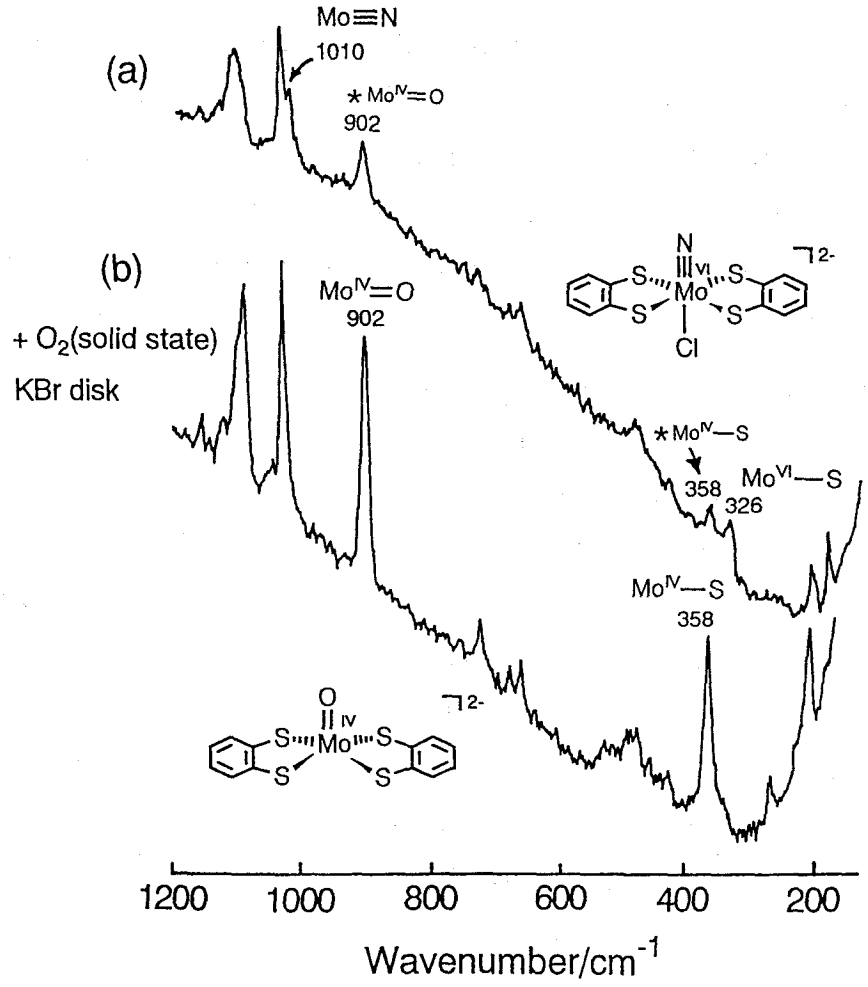

Figure 5. Raman spectra of $(NEt_4)_2[Mo^{VI}N(bdt)_2Cl]$ (**1**) (a) and the O_2-oxidized brownish powder (b).

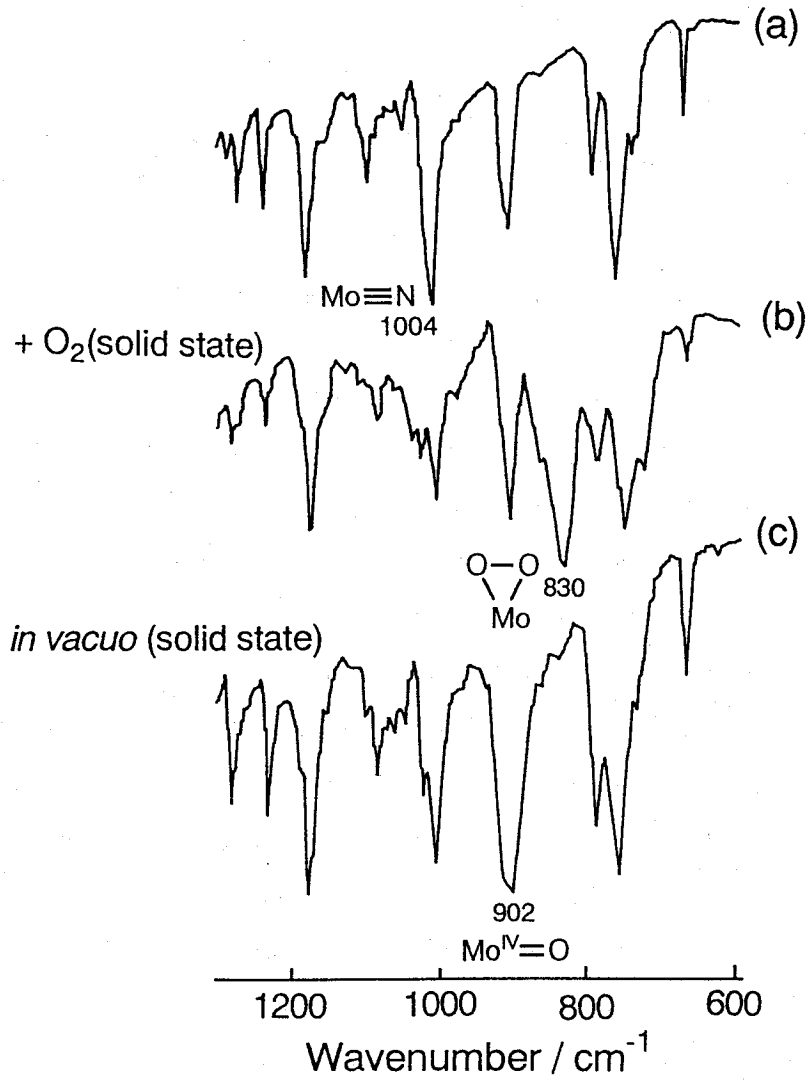

Figure 6. IR spectra of $(NEt_4)_2[Mo^{VI}N(bdt)_2Cl]$ (**1**) (a), and the O_2-oxidized product before (b) and after (c) in vacuo.

Scheme 3

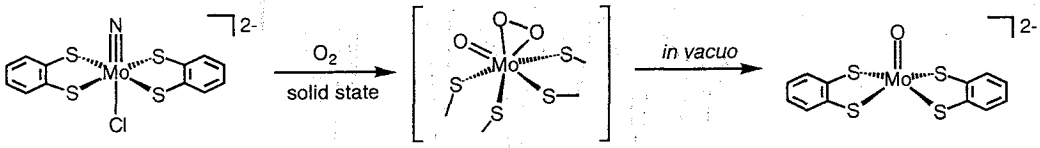

Reaction scheme of $[Mo^{VI}N(bdt)_2Cl]^{2-}$ with O_2 in the solid state

powder obtained shows the strong band at 904 cm^{-1}, which is consistent with that of the $\nu(Mo^{IV}=O)$ of $[Mo^{IV}O(bdt)_2]^{2-}$. (Figure 5)

Figure 6 shows the IR spectrum changes of the reaction of **1** with oxygen gas. Since strong band of phenyl ring around 1000 cm^{-1} hinders the $Mo^{VI}\equiv N$ band, the $\nu(Mo^{VI}\equiv N)$ band of **1** is not clear in IR spectrum. However, the differential spectrum between **1** and the slightly O_2-oxidized sample shows the decrease of 1004 cm^{-1} stretching according to the simultaneous increase of bands at 902 cm^{-1} and 830 cm^{-1}. Brownish powder obtained when **1** is exposed to excess oxygen gas shows the intense band at 830 cm^{-1}. This band disappears when the sample is exposed in reduced pressure *ca.* 5 mmHg). The spectrum of the final brownish powder is consistent with that of $(NEt_4)_2[Mo^{IV}O(bdt)_2]$ having an intense $\nu(Mo^{IV}=O)$ band at 902 cm^{-1}. The Raman and IR spectra results show that **1** reacts with O_2 to produce the oxomolybdenum(IV) complex, $[Mo^{IV}O(bdt)_2]^{2-}$.

For the explanation of the labile intense band at 830 cm^{-1}, the production of the peroxo-molybdenum(IV) complex was suggested on the basis of the lability and the frequency number. (Scheme 3) The dioxygen complex shows (O_2) band around 850 cm^{-1}. For example, $[VO(O_2)(H_2O)(bipicoline)]^-$ shows the $\nu(O_2)$ band at 839 cm^{-1}.[29] Recently, the catalytic oxidation of benzoin in the presence of dioxygen by oxomolybdenum(IV) thiolate complexes have been studied by Ueyama et al.[30,31] They

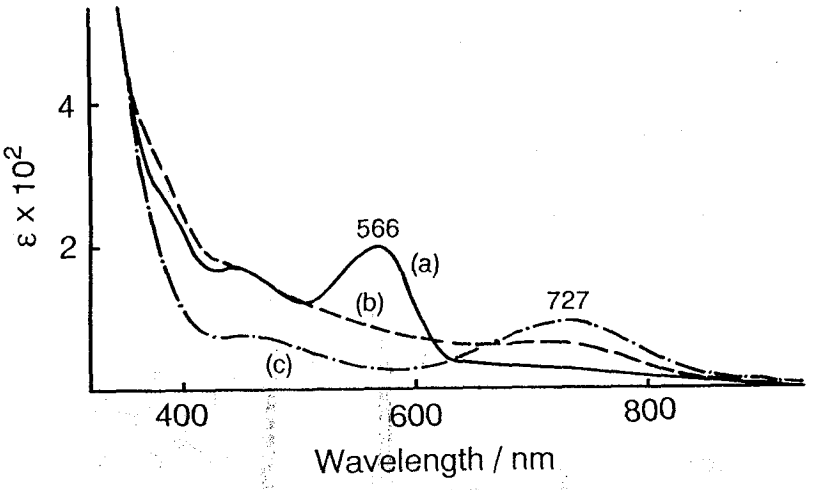

Figure 7. Absorption spectrum change for the stoichiometric reaction of $(NEt_4)_2[Mo^{VI}N(bdt)_2Cl]$ (**1**) with O_2 gas in MeCN solution.

proposed that the production of oxomolybdenum(VI) complex having dioxygen or μ-oxygen ligands as the active intermediate.

The IR spectrum and Raman spectrum results indicate that **1** reacts with O_2 to give the oxomolybdenum(IV) complex, $[Mo^{IV}O(bdt)_2]^{2-}$ as final product.

Reaction of 1 with oxygen gas in the solution state. The stoichiometric reaction of **1** with oxygen gas was carried out in MeCN or MeCN-d_3 solution. The absorption spectrum of the reaction solution exhibits the λ_{max} at 727 nm, showing the production of $[Mo^{V}O(bdt)_2]^-$ in 1 % yield. (Figure 7) This complex was produced by the 1-e$^-$ oxidation reaction of $(NEt_4)_2[Mo^{IV}O(bdt)_2]$ with O_2. The reaction of $(NEt_4)_2[Mo^{IV}O(bdt)_2]$ with air has been studied by Ueyama et al.[31] They show that the stoichiometric reaction of this complex with air gives oxomolybdenum(V) complex $[Mo^{V}O(bdt)_2]^-$ in 5 % yield. Because of the paramagnetic influence of Mo(V) complex, ^1H NMR spectrum of the reaction solution shows no clear ligand signals. Reaction of **1** with excess oxygen gas in solution gives a diamagnetic yellow product. The yellow solution does not show any characteristic absorption band at visible region. The ^1H NMR signal shows the finely separated multiplet signals at 7.1 and 6.9 ppm. (Figure 8)

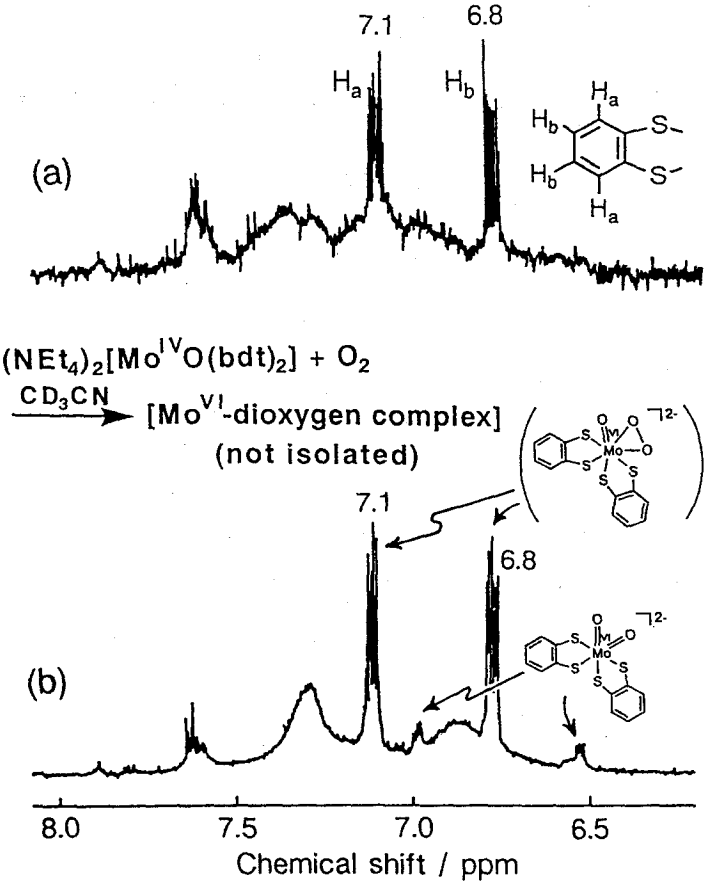

Figure 8. ^{1}H NMR spectra of the O_2-oxidized product of $(NEt_4)_2[Mo^{VI}N(bdt)_2Cl]$ (**1**) (a) and the reaction product of $(NEt_4)_2[Mo^{IV}O(bdt)_2]$ with excess O_2 in MeCN-*d*3.

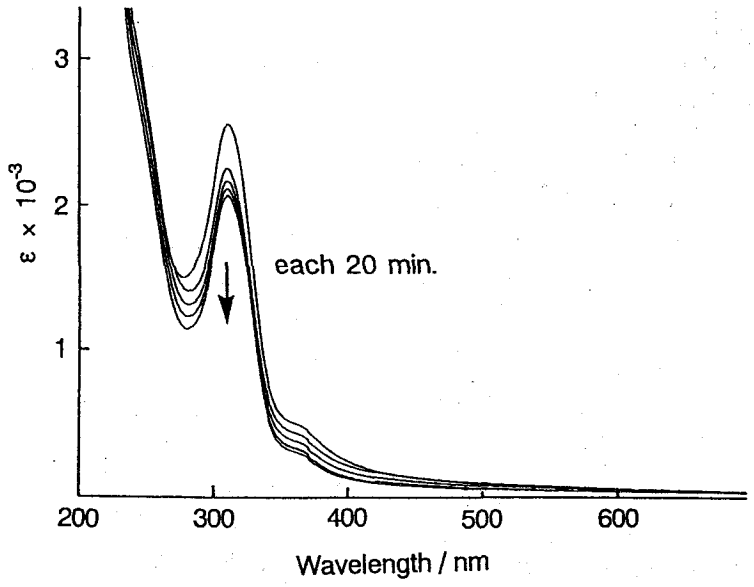

Figure 9. The absorption spectrum change of the reaction solution between $(NEt_4)[Mo^{VI}NCl_4]$ and O_2 in CH_2Cl_2.

The chemical shifts and the coupling pattern are the same with that of the reaction solution of $(NEt_4)_2[Mo^{IV}O(bdt)_2]$ with excess oxygen gas. The results show that **1** readily reacts with oxygen gas in the both solution and solid states to produce the oxomolybdenum(IV) complex $[Mo^{IV}O(bdt)_2]^{2-}$. The observed oxomolybdenum(V) complex in the stoichiometric reaction is the reaction product of the oxomolybdenum(IV) complex with O_2 gas.

Reaction of $[Mo^{VI}NCl_4]$ with oxygen gas in the solution state. For the comparison of the reactivity of **1**, the reaction of $(NEt_4)[Mo^{VI}NCl_4]$ with oxygen gas was carried out. This nitrido complex is relatively stable to oxygen gas compared with **1**. Although Dehnicke et al. reported that $[Mo^{VI}NCl_4]^-$ reacts with dry O_2 in boiling CH_2Cl_2 to produce $[Mo^{V}OCl_4]^-$[32], absorption spectrum change of the CH_2Cl_2 reaction solution of the complex $(NEt_4)[Mo^{VI}NCl_4]$ with O_2 is almost

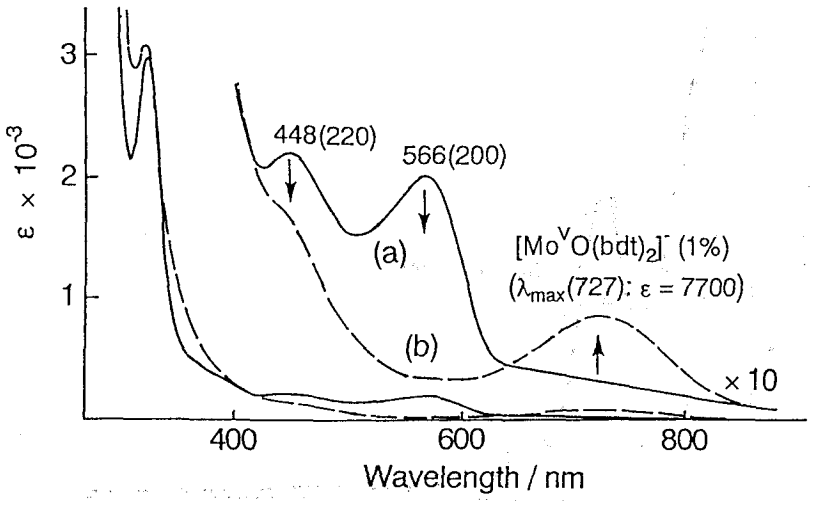

Figure 10. Absorption spectrum change of the reaction $(NEt_4)_2[Mo^{VI}N(bdt)_2Cl]$ (**1**) with 2 equimolar of H_2O (a, b) in MeCN solution. The oxygen gas bubbling to the (b) give the spectrum c.

negligible. (Figure 9) The results show that the thiolate ligand highly activates the reaction of the nitrido ligand with oxygen gas.

The reaction of 1 with H_2O. Generally, a Mo-nitride moiety is moisture sensitive. The reaction of **1** with H_2O was examined by absorption and IR spectrum. Addition of excess H_2O to the red purple MeCN solution of **1** rapidly gives a yellow solution. The absorption spectrum of the reaction mixture shows no characteristic peak. (Figure 10)

IR spectrum of the orange powder obtained from the reaction solution is the same with that of $[Mo^{IV}O(bdt)_2]^{2-}$. (Figure 11) The results clearly indicate that the reaction of **1** with H_2O gives the oxomolybdenum(IV) complex $[Mo^{IV}O(bdt)_2]^{2-}$ similar to the reaction with O_2 gas. Similarly, the reaction between the complex $(AsPh_4)[Mo^{VI}NCl_4]$ and moisture readily produce the oxomolybdenum(V) complex $(AsPh_4)[MoOCl_4]$.[32]

In order to understand the fate of nitride ligand in the reactions of **1** with O_2 or H_2O, attempts to identify the gas formed in the reaction solution using mass spectrum

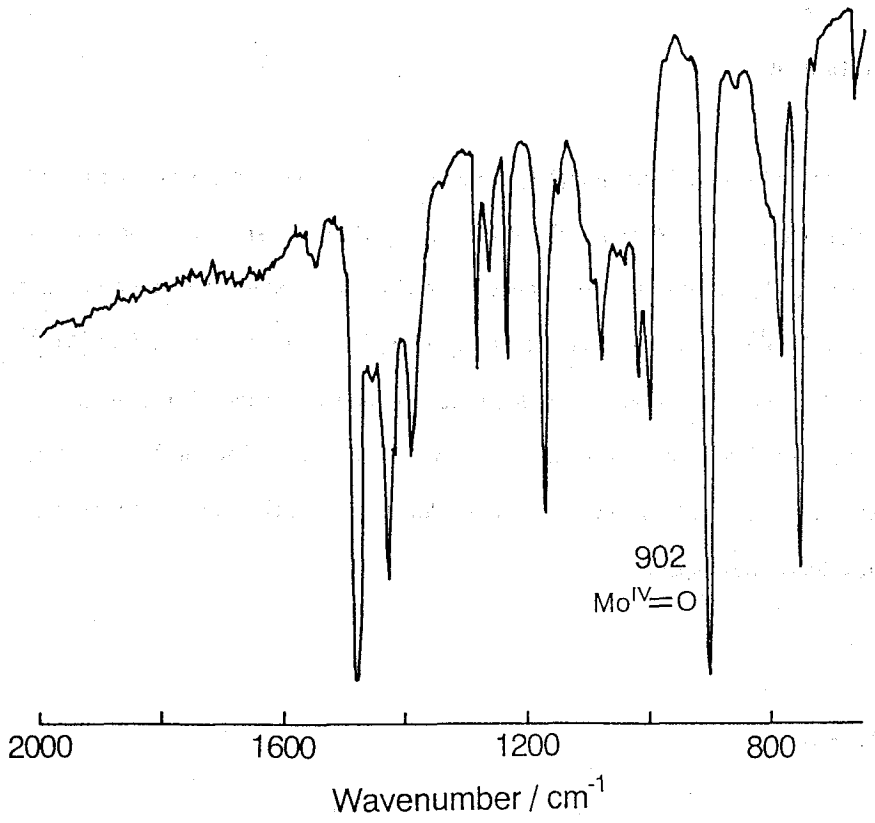

Figure 11. IR spectrum of the O_2-oxidized orange product.

were unsuccessful, which are expected to N_2, NH_3, or other N compounds, because of the hindrance of the intense back ground of nitrogen, water, and oxygen in atmosphere. Dehnicke et al. has proposed that the nitride ligand of $[Mo^{VI}NCl_4]^-$ changes to N_2 molecule in the reaction with O_2.[32]

Conclusion.

The nitridomolybdenum(VI) complex having two bdt ligands was synthesized, and characterized by Raman, IR, absorption, and NMR spectroscopic method. This complex readily reacts with oxygen gas or H_2O to produce the oxomolybdenum(IV) complex $[Mo^{IV}O(bdt)_2]^{2-}$. The reactivity is higher than that of $(AsPh_4)[Mo^{VI}NCl_4]$. The higher reactivity is due to the high electron density of the nitride ligand having the high nucleophillic reactivity to the H_2O, O_2 molecules. This activation effect of the thiolate ligand is due to the competitive $p\pi$-donation from S to $d\pi$ of Mo, as indicated by the results of these spectra.

References

(1) Hidai, M.; Tominari, K.; Uchida, Y. *J. Am. Chem. Soc.* **1972**, *94*, 110.

(2) Chatt, J.; Dilworth, J. R.; Richards, R. L. *Chem. Rev.* **1978**, *78*, 589.

(3) Ueyama, N.; Fukase, H.; Zaima, H.; Kishida, S.; Nakamura, A. *J. Mol. Catal.* **1987**, *43*, 141.

(4) Burgess, B. K. *Chem. Rev.* **1990**, *90*, 1377.

(5) Kim, J.; Rees, D. C. *Science* **1992**, *257*, 1677.

(6) Dehnicke, K.; Kolitsch, W. *Z. Naturforsch* **1977**, *B 32*, 1485-1486.

(7) Figuly, G. D.; Loop, C. K.; Martin, J. C. *J. Am. Chem. Soc.* **1989**, *111*, 654-658.

(8) Block, E.; Eswarakrishnan, V.; Gernon, M.; Lfori-Okai, G.; Saha, C.; Tang, K.; Zubieta, J. *J. Am. Chem. Soc.* **1989**, *111*, 658-665.

(9) Chatt, J.; Dilworth, J. R. *J. Chem. Soc., Dalton Trans.* **1974**, 517-518.

(10) Hursthouse, M. B.; Motevalli, M. *J. Chem. Soc., dalton Trns.* **1979**, 1362.

(11) Boyde, S.; Ellis, S. R.; Garner, C. D.; Clegg, W. *J. Chem. Soc., Chem. Commun.* **1986**, 1541.

(12) Yoshinaga, N.; Ueyama, N.; Okamura, T.; Nakamura, A. *Chem. Lett.* **1990**, 1655.

(13) Knopp, B.; Lörcher, K.-P.; Strähle, J. *Z. Naturforsch* **1977**, *B 32*, 1361-1364.

(14) Müller, U.; Schweda, E.; Strähle, J. *Z. Naturforsch* **1983**, *38b*, 1299-1300.

(15) Patt-Siebel, U.; Khabou, A.; Müller, U.; Dehnicke, K. *Z. Anorg. Allg. Chem.* **1989**, *569*, 91-96.

(16) Young, C. G.; Janos, F.; Bruck, M. A.; Wexler, P. A.; Enemark, J. A. *Aust. J. Chem.* **1990**, *43*, 1347-1355.

(17) Beck, J.; Schweda, E.; Strähle, J. *Z. Naturforsch* **1985**, *40b*, 1073-1076.

(18) Buth, S.; Wocadlo, S.; Neumüller, B.; Weller, F.; Dehnicke, K. *Z. Naturforsch* **1922**, *47b*, 706-712.

(19) Chan, D. M.-T.; Chisholm, M. H.; Folting, K.; Huffman, J. C.; Marchant, N. S. *Inorg. Chem.* **1986**, *25*, 4170-4174.

(20) Fenske, D.; Liebelt, W.; Dehnicke, K. *Z. Anorg. Allg. Chem.* **1980**, *467*, 83-88.

(21) Ueyama, N.; Kondo, M.; Oku, H.; Yoshinaga, N.; Okamura, T.; Nakamura, A. *to be submitted.*

(22) Dehnicke, K.; Strähle, J. *Angew. Chem. Int. Ed. Engl.* **1992**, *31*, 955-978.

(23) Dilworth, J. R.; Donovan-Mtunzi, S.; Kan, C. T.; Richards, R. L.; Mason, J. *Inorg. Chim. Acta.* **1981**, *53*, L161-L162.

(24) Donovan-Mtunzi, S.; Richards, R. L. *J. Chem. Soc., Dalton Trans.* **1984**, 1329-1332.

(25) Saika, A.; Slichter, C. P. *J. Chem. Phys.* **1954**, *22*, 26.

(26) Lamb, W. *Phys. Rev.* **1941**, *60*, 817.

(27) Jameson, C. J.; Gutowsky, H. S. *J. Chem. Phys.* **1964**, *40*, 1714.

(28) *Nitrogen NMR*; Witanowski, M.; Webb, G. A., Ed.; Plenun Prerss: London and New York, 1973.

(29) Nakamoto, K. *Infrared and Raman Spectra of Inorganic and Coordination Compounds*; John-Wiley: New York, 1986.

(30) Ueyama, N.; Yoshinaga, N.; Nakamura, A. *J. Chem. Soc., Dalton Trans.* **1990**, 387.

(31) Ueyama, N.; Yoshinaga, N.; Okamura, T.; Zaima, H.; Nakamura, A. *J. Mol. Catal.* **1991**, *64*, 247.

(32) Dehnicke, K.; Strähle, J. *Angew. Chem. Int. Ed. Engl* **1981**, *20*, 413-426.

(33) Seyferth, K.; Tauve, R. J. *J. Organomet. Chem.* **1982**, *229*, C19.

(34) Godemeyer, T.; Dehnicke, K.; Fluck, E. *Z. Anorg. Allg. Chem.* **1988**, *565*, 41-46.

Summary and Conclusion

The author investigated the specific chelating effect of the macromolecular ligands on the reactivity or the physical properties of oxomolybdenum ion. For this study the novel synthetic method of oxomolybdenum(IV) complexes having several alkanedithiolate chelating was developed. Thus, the ligand exchange method between $[Mo^{IV}O(p\text{-}ClC_6H_4S)_4]^{2-}$ and dithiols was found to give the novel oxomolybdenum(IV) complexes. By this novel synthetic method, $[Mo^{IV}O(dithiolato)_2]^{2-}$ (dithiolato = 1,2-ethanedithiolato, α,2-toluenedithiolato, 1,3-propanedithiolato, 1,2-propanedithiolato, 2,3-butanedithiolato) were successfully synthesized. These Mo(IV) complexes are not synthesized from the corresponding Mo(V) complex under the mild condition, because of the negative redox Mo(V)/Mo(IV) potential (*ca.* -0.8 ~ -1 V vs. SCE).

The X-ray crystallographic studies of these Mo(IV) complexes have shown the effect of the chelating size is caused by variation of the Mo-S-C bond angle. The chelating skeletons are regulated by the chelating size of the dithiolate ligands. Thus, 6-membered chelating of 1,3-propanedithiolate affords the larger Mo-S-C angle (*ca.* 115°) compared with that of the 5-membered chelating of 1,2-ethanedithiolate (*ca.* 105°). The oxomolybdenum(IV) complex having 1,3-propanedithiolate chelate *i.e.* larger Mo-S-C bond angle shows more negative Mo(V)/Mo(IV) redox potential (-1.01 V vs. SCE) through Mo-S d-π interaction.

On the other hand, the effect of the O-Mo-S-C torsion angle on the reactivity or the physical properties of oxomolybdenum(V and IV) complexes was discussed. The significant effect of the deviated O-Mo-S-C torsion angle from 90° on the properties of oxomolybdenum(V and IV) ion has been suggested by the theoretical calculation of the oxomolybdenum(V) complex having macromolecular peptide chelating. In Mo(IV) complexes synthesized, $[Mo^{IV}O(\alpha,2\text{-tdt})_2]^{2-}$ shows the most deviated O-Mo-S-C torsion angle from 90°, and shows the specific negative Mo(V)/Mo(IV) redox couple through Mo-S d-π interaction.

These studies have shown that the O-Mo-S-C torsion angle and the Mo-S-C bond angles largely affect to the properties of the oxomolybdenum(V and IV) complexes than that of the electronic effect from the substituents on the ligands. These are the macromolecular chelating effect observed in the several oxomolybdenum(V and IV) complexes. Enough specific O-Mo-S-C torsion angle and Mo-S-C bond angles for the occurrence of the specific reactivities are established in the more sterically regulated peptide chelation.

The oxo-transfer reactivity between oxo- and dioxomolybdenum(IV and VI) complexes were studied using complexes synthesized. The strong Mo-S bond of the alkanedithiolate chelating prevents the binucleation reaction of those complexes. This controlled reactivity is due to the inhibition of the cis-trans rearrangement of the intermediate complex produced during the reaction.

The effect of the dithiolate chelating on the nitridomolybdenum(VI) complex was also investigated. The 1,2-benzenedithiolate chelating affords the thermally stable nitridomolybdenum complex at room temperature. This nitride ligand is activated by the competitive electron donation from the $p\pi$ of S to $d\pi$ of Mo(VI) ion. This affords the significant activation mechanism for the intermediate of the dinitrogen reduction of nitrogenase.

List of Publications

1. Synthesis, Molecular Structure, and Physical Properties of an Oxomolybdenum(IV) Complex with *p*-Chlorobenzenethiolate, $[Mo^{IV}O(p\text{-}ClC_6H_4S)_4]^{2-}$, as a Model of Active Sites of Reduced Molybdo-Oxidases., Kondo, M.; Fukuyama, K.; Ueyama, N.; Nakamura, A. *Bull. Chem. Soc. Jpn.* **1993**, *66*, 1391-1396.

2. Structure and Properties of $(NEt_4)_2[Mo^{IV}O(\alpha,2\text{-toluenedithiolato})_2]$., Ueyama, N.; Kondo, M.; Oku, H.; Nakamura, A. *Bull. Chem. Soc. Jpn.* **1994**, *67*, 1840-1847.

3. Syntheses and Structures of Oxomolybdenum(IV) Complexes Having Alkanedithiolate Ligands. Effect of the Chelating Ring Size on the Physical Properties., Kondo, M.; Oku, H.; Ueyama, N.; Nakamura, A.; Waters, J. M.; Ainscough, E. W.; Brodie, A. M. to be published.

4. Binucleation Reactions between Oxomolybdenum(IV) and Dioxomolybdenum(VI) complexes Having Thiolate Ligands., Kondo, M.; Oku, H.; Ueyama, N.; Nakamura, A. to be published.

5. Synthesis and Properties of a Nitridomolybdenum(VI) Complex Having Benzenedithiolate Ligand. Effect of the Thiolate on the Activation of the Nitride Ligand., Kondo, M.; Oku, H.; Ueyama, N.; Nakamura, A. to be published.

6. Synthesis of an oxomolybdenum(V) complex Having a Tetradentate Peptide Chelating., Ueyama, N.; Kondo, M.; Sun, W.-Y.; Oku, H.; Nakamura, A. in preparation.

Other Papers

1. An Oxovanadium(IV) Complex Chelated by Bipyridyl Sulfide., Kondo, M.; Kawata, S.; Kitagawa, S.; Kiso, H.; Munakata, M. *Acta Cryst. C.* **1994** in press.

2. Oxygen Atom Transfer System in Which the (μ-Oxo)dimolybdenum(V) Complex Formation Does Not Occur: Synthesis, and Reactivities of Monooxomolybdenum(IV) Benzenedithiolato Complexes as Models of Molybdenum Oxidases., Oku, H.; Ueyama, N.; Kondo, M.; Nakamura, A. *Inorg. Chem.* **1994**, *33*, 209-216.

3. Synthesis and Structures of Infinite Sheet Copper(I) Complex Polymers with 2,6-dimethylpyrazine, $\{[Cu_2(C_6H_8N_2)_3](ClO_4)_2(C_3H_6O)_2\}_\infty$, and with 2-chloropyrazine, $\{[Cu_2(C_4H_3N_2Cl)_{4.5}](ClO_4)_2\}_\infty$., Kitagawa, S.; Kawata, S.; Kondo, M.; Nozaka, Y.; Munakata, M. *Bull Chem. Soc. Jpn.* **1993**, *66*, 3387-3392.

4. Fabrication of Infinite Two-Dimensional Sheets Built by Tetragonal Copper(II) Lattice. X-ray Crystal Structure and Magnetic Properties of $\{[Cu(C_6O_4Cl_2)(C_4H_4N_2)]\}_\infty$., Kawata, S.; Kitagawa, S.; Kondo, M.; Furuchi, I.; Munakata, M. Angew. Chem. **1994**, 106, 1851-1854.

5. Crystal Structure of a Binuclear Vanadium(III) Complex with a New Tripodal Ligand, $[V_2Cl_4(tped)(EtOH)_2]\cdot 2EtOH$., Kumagai, H.; Kawata, S.; Kondo, M.;Kitagawa, S.; Katada, M. *Inorg. Chim. Acta.* **1994**, *224*, 199-201.

6. Molecular Cavity for Tetrahedral and Y-shaped Anions. Synthetic and Structural Studies of Macrocyclic Dicopper(I) and Disilver(I) Compounds of 1,6-bis(diphenylphosphino)-hexane., Susumu Kitagawa, S.; Kondo, M.; Kawata. S. Wada. S.; Maekawa, M.; Munakata, M. *Inorg. Chem.* **1994** in press.